GUIDE TO THE
SPFRAC
SIMULATOR

Final Technical Report:

EVALUATING PERMEABILITY ENHANCEMENT USING ELECTRICAL TECHNIQUES

DOE Award Number DE-FG36-04GO14291

September 2008

Prepared by:
John W. Pritchett
Science Applications International Corporation
10260 Campus Point Drive
San Diego, California 92121
Tel: **(858) 826-1628**
E-mail: **john.w.pritchett@saic.com**

Submitted to:
Department of Energy
Golden Field Office
1617 Cole Blvd.
Golden, Colorado 80401

DISCLAIMER

This report is based upon research supported in part by the U. S. Department of Energy under Award No. DE-FG36-04GO14291.

Any findings, opinions, conclusions and/or recommendations expressed in this report are those of the author alone and do not necessarily reflect the views of the Department of Energy.

ACKNOWLEDGEMENTS

The author expresses his deep appreciation to Dr. Tsuneo Ishido of GSJ and to Dr. Sabodh Garg of SAIC for their helpful assistance and technical advice without which the SPFRAC simulator would never have been developed.

Financial support for this work was provided by the Geothermal Technologies Program of the U. S. Department of Energy (DOE-EERE), by the Geological Survey of Japan and the Japanese National Institute of Advanced Industrial Science and Technology (GSJ-AIST), and by Science Applications International Corporation (SAIC).

TABLE OF CONTENTS

LIST OF FIGURES

LIST OF TABLES

1. INTRODUCTION

Enhanced Geothermal Systems (EGS) development projects involve the artificial stimulation of relatively impermeable high-temperature underground regions (at depths of 2-4 kilometers or more) to create sufficient permeability to permit underground fluid circulation, so that hot water can be withdrawn from production wells and used to generate electric power. Several major research projects of this general type have been undertaken in the past in New Mexico (Fenton Hill), Europe, Japan and Australia. Recent U.S. activities along these lines focus mainly on stimulating peripheral areas of existing operating hydrothermal fields rather than on fresh "greenfield" sites, but the long-term objective of the Department of Energy's EGS program is the development of large-scale power projects based on EGS technology (*MIT*, 2006; *NREL*, 2008).

Usually, stimulation is accomplished by injecting water into a well at high pressure, enhancing permeability by the creation and propagation of fractures in the surrounding rock (a process known as "hydrofracturing"). Beyond just a *motivation*, low initial system permeability is also an essential *prerequisite* to hydrofracturing. If the formation permeability is too high, excessive fluid losses will preclude the buildup of sufficient pressure to fracture rock.

In practical situations, the actual result of injection is frequently to re-open pre-existing hydrothermally-mineralized fractures, rather than to create completely new fractures by rupturing intact rock. Pre-existing fractures can often be opened using injection pressures in the range 5 – 20 MPa. Creation of completely new fractures will usually require pressures that are several times higher. It is preferable to undertake development projects of this type in regions where tectonic conditions are conducive to shear failure, so that when pre-existing fractures are pressurized they will fail by shearing laterally. If this happens, the fracture will often stay open afterwards even if injection subsequently ceases.

The principal barrier to EGS utilization for electricity generation is project economics. Costs for geothermal electricity obtained from conventional hydrothermal systems are just marginally competitive. Unless and until the costs of routinely and reliably creating and exploiting artificial subterranean fracture networks that can deliver useful quantities of hot fluid to production wells for long periods of time (years) are reduced to levels comparable to those of a conventional geothermal development project, EGS will be of little interest to the electrical power industry.

A significant obstacle to progress in projects of this general type is the difficulty of appraising the properties (geometry, fluid transmissivity, *etc.*) of the fracture(s) created/re-opened by injection. Sustainability of power production is critically dependent upon reservoir thermal sweep efficiency, which depends in turn on the geometry of the fracture network and its interconnections with the various production and injection wells used to circulate fluid underground.

If no permeable connections are created between the wells, fluid flow will be too slow for practical utility. If the connections are too good, however (such as a production/injection well pair connected by a single very permeable fracture), production wellhead temperatures will decline rapidly. Unless the permeable fractures created by hydrofracturing can be accurately mapped, the cost of subsequent trial-and-error drilling to try to establish a suitable fluid circulation system is likely to dominate project economics and render EGS impractical.

Characterization of the underground fracture network presently relies virtually exclusively on microearthquake surveys (except at those points where fractures actually intersect boreholes and can be detected directly by downhole fluid-loss and televiewer logs). During the injection/hydrofracturing operation, as fractures are opened and extended, small seismic events will occur along the dislocation surface which can be detected by arrays of sensitive seismometers (usually buried at shallow depths and/or in neighboring shut-in observation wells). Ray-tracing analyses and similar techniques are then employed to estimate the spatial location of each seismic source. Once a sufficient number of such events have been documented, it is often possible to perceive patterns suggestive of fracture network geometry. This approach has limited spatial precision, however (uncertainties are usually worse than 100 meters), and can only discern fracture zones that actually produce detectable signals during pressurization. Moreover, microseismic surveys cannot discriminate among fractures of varying degrees of fluid transmissivity.

In recent years, techniques have been devised to calculate the effects of subterranean geothermal reservoir evolution upon surface geophysical surveys, based on the results of conventional numerical reservoir simulation calculations for hydrothermal reservoirs (*Pritchett et. al*, 2000). If repeated surveys exhibit systematic temporal changes from one survey to the next that can be correlated with events taking place in the reservoir, additional constraints are provided for history-matching studies, resulting in more robust and reliable reservoir models. Geophysical techniques considered to date include microgravity surveys, active seismic surveys, DC resistivity surveys (Schlumberger type), magnetotelluric (MT and CSAMT) surveys, and self-potential (SP) surveys. The computational postprocessors that carry out these calculations of changes in geophysical observables have been extensively tested and verified (*Pritchett,* 2003) and have been applied in various field studies, mainly in Japan (see, for example, *Nakanishi et al,* 2001; *Pritchett and Garg,* 2002; *Pritchett and Garg,* 2003).

Of these methods, the SP ("self-potential") technique appears to be most appropriate for monitoring the growth of underground fractures in EGS stimulation operations. Conventional earth-surface SP surveys will not be very helpful owing to the great depth and limited strength of the signals from hydrofracturing, but continuous downhole SP monitoring (using electrodes in nearby shut-in observation wells) could in principle sense the progress of the reservoir pressurization that results from stimulation operations (*Telford et. al,* 1990). If so, data of this type could be used to supplement microseismic data to more completely characterize the fracture system.

One essential question, of course, is whether SP changes of sufficient intensity for detection and interpretation (>10 millivolts or so) are likely to be generated by EGS hydrofracturing operations. Recent experiments in Japan using shallow wells have observed transient SP signals caused by relatively low-pressure injection into permeable formations (*Ishido and Pritchett,* 2003). EGS hydrofracturing in relatively impermeable rock will presumably produce electrical signals that are much more intense but also much deeper and that propagate more slowly through the earth.

A few years ago, a computational feasibility study using the STAR reservoir simulator (*Pritchett,* 1995) and the "SP postprocessor" (*Ishido and Pritchett,* 1999) demonstrated that the general concept is feasible (*Pritchett and Ishido,* 2005a). Pressurization of a fracture will cause the

propagation of intense SP signals through the reservoir, with amplitudes many times stronger than detection thresholds reaching distances of hundreds of meters from the fracture in just a few weeks. The present multi-year research effort (October 2004-December 2008) was designed to elaborate upon this original work and to develop practical techniques for the use of the "self-potential" method for monitoring fracture propagation and growth in an EGS reservoir.

During the first phase (October 2004-September 2005), primary emphasis was placed on two issues: *(1)* "free-field" SP signals to be expected from fracture pressurization operations (and how the signal characteristics depend upon the properties of the reservoir, of the fracture, and of the stimulation operation), and *(2)* the "near-field" effects that are likely to influence the signals (arising mainly from electrical currents flowing vertically within the injection and observation wells). In this part of the project, theoretical calculations to address these issues were carried out using the STAR simulator and the "SP Postprocessor" in a similar fashion to the work reported in the original *Pritchett and Ishido* (2005a) paper. Results of the first phase of the present project were presented in a comprehensive report by *Pritchett and Ishido* (2005b).

During the second phase (October 2005-September 2006), laboratory tests were performed at the Geological Survey of Japan in Tsukuba on rock samples taken from ~2430 meters depth in Well 34-9RD2 in the Coso Geothermal Field (which at the time DOE planned to use for testing EGS fracturing concepts) in order to obtain values for pertinent physical properties and how they change with temperature and fluid salinity. The properties of particular interest are porosity, permeability, electrical resistivity, electrical adsorption potential, and the streaming potential coefficient. Practical deployment issues (*e.g.* well completion techniques, required measurements, selection of instrumentation) were also addressed. This work was reported by *Pritchett et al.* (2006).

The final phase of the project involves the development of efficient computational tools for analysis and interpretation of downhole SP data, along with other pertinent information, to yield fracture characteristics. This work is now complete, and is presented in this report. A new mathematical simulator called "SPFRAC" has been developed, together with several graphical postprocessors for the presentation of computed results and comparisons between computations and field measurements. In SPFRAC (in contrast to the STAR system), a single simulator calculates both the hydraulic response and the resulting changes in subsurface electrical potential. Numerous simplifications (relative to the general-purpose formulation used in STAR) have been introduced, which have substantially reduced the computer time required to obtain useful results. These include restrictions to single-phase fluid flow, regarding temperature and fluid composition as functions of position only, certain geometric simplifications, and simplified constitutive relationships. But in addition, generalizations have been introduced to make SPFRAC better suited to address the hydrofracture/stimulation problem at hand, including more general treatment of the flow of fluid through fractured rock.

In Section 2, the mathematical foundations underlying SPFRAC are presented. Sections 3 and 4 amount to a "User's Manual" for SPFRAC which describe the procedures required for problem specification (Section 3) and the type of computed output that is available from the program (Section 4). Section 5 similarly describes the use of SPFRAC's graphical postprocessors. In Section 6, an illustrative example is described, and the input to and output from SPFRAC for that case are provided in the Appendices.

2. MATHEMATICAL BACKGROUND

Stable spatial distributions of electrical potential (voltage) are present naturally in the undisturbed earth, both at the ground surface and at depth. In geothermal areas, this "self-potential" (SP) can arise from as many as three different causes acting together: underground *temperature gradients* ("the earth as a thermocouple"), heterogeneities in subsurface formation *chemical composition* ("the earth as a battery"), and *electrokinetic effects* caused by fluid circulation through the rock ("the earth as a dynamo"). During geothermal field operation, however, temporal *changes* in the observed self-potential distribution will be dominated by electrokinetic effects, since the underground fluid flow pattern will change relatively rapidly with time as well flow rates change, compared to large-scale changes in system temperature or chemical composition (*Ishido and Pritchett,* 2000). Therefore, to interpret rapid changes in SP, it suffices to restrict our attention to electrokinetic phenomena.

2.1. Electrical Potential and Drag Current

It may easily be shown (*Ishido and Pritchett,* 1999) that the three-dimensional distribution of electrokinetic self-potential at an instant of time may be determined by solving a boundary-value problem given by Poisson's equation (derivable from Ohm's Law):

$$\nabla\cdot[\,\sigma\,\nabla V\,] \;=\; \nabla\cdot\boldsymbol{I}_{\mathbf{drag}} \qquad [2.1]$$

where V is electrical potential (volts), σ is electrical conductivity (siemens/meter), and $\boldsymbol{I}_{\mathbf{drag}}$ is the "drag current" density vector (amperes per square meter) induced by the flowing fluid. Therefore, if the distributions of electrical conductivity (resistivity $^{-1}$) and drag current density are known at a particular instant of time, equation [2.1] can be solved to obtain the simultaneous distribution of electrical potential (V) everywhere underground.

To model the "drag current density" ($\boldsymbol{I}_{\mathbf{drag}}$), the formulation devised by *Ishido and Mizutani* (1981) (which is based on extensive laboratory measurements on actual crustal rock samples of geothermal relevance) is adopted. Briefly, under single-phase fluid flow conditions this model expresses the drag current density as:

$$\boldsymbol{I}_{\mathbf{drag}} \;=\; -\,[(\varphi\varepsilon\zeta)/(\rho k\Theta^2)]\;\boldsymbol{M} \qquad [2.2]$$

where $\boldsymbol{M}$ is the local instantaneous liquid-phase mass flux vector (kilograms per second per square meter), ρ is the mass density of the liquid phase (kilograms per cubic meter), φ is the (dimensionless) system porosity, ε is the dielectric permittivity of the liquid phase (farads/meter), k is the absolute permeability of the rock (square meters), Θ is fluid-conduit tortuosity (dimensionless), and ζ is the adsorption potential or "zeta-potential" (volts). Calculation of these effects requires the functional dependence of various properties of the reservoir fluid upon quantities such as pressure, temperature and salinity.

The adsorption potential ζ in the above equation is a function of temperature, and also depends upon acidity (*pH*) and the concentrations of *1:1*- and *2:2*-valent electrolyte in the liquid brine; it is given by Equations 18, 20 and 21 of the above-cited paper by *Ishido and Mizutani,* assuming that the following empirical relationship holds for the distance (X_s) between the solid surface and the slipping plane in the electrical double layer:

$$X_s \text{ (meters)} = 3.4 \times 10^{-6}\, \mu \qquad [2.3]$$

where μ is the dynamic viscosity of the liquid phase in pascal-seconds. This formulation has been shown to yield good agreement with adsorption potential values measured in the laboratory for igneous and metamorphic rocks characteristic of geothermal systems (*Tosha et. al,* 2003). Values for ζ are ordinarily negative; the magnitude tends to increase with increasing temperature, and is usually of the order of –100 millivolts (mV) at temperatures near 200°C for brine salinities in the 1000 ppm ("part per million") range for a variety of rock types. The adsorption potential magnitude tends to decline with increasing brine salinity.

2.2. Darcy's Law

In the case of single-phase liquid flow in porous rock, the mass flux vector $\boldsymbol{M}$ is related to the fluid density (ρ), the rock permeability (k), the fluid dynamic viscosity (μ) and the gradient of "excess pressure" (p) by Darcy's Law:

$$\boldsymbol{M} = -(\rho k/\mu)\, \nabla p \qquad [2.4]$$

and p, the "excess pressure" or "overpressure" (a function of position and time) is the difference between the actual local instantaneous pressure (P) and the local hydrostatic pressure (P_{H}):

$$p = P - P_{\mathrm{H}} \qquad [2.5]$$

and the hydrostatic pressure is:

$$P_{\mathrm{H}} = P_{\mathrm{o}} + (d - d_{\mathrm{o}})\, \rho g \qquad [2.6]$$

where P_{o} represents a constant "average" pressure for the system (here taken as the undisturbed stable reservoir hydrostatic pressure at the fluid injection location), g is the acceleration of gravity (9.8 m/s^2), d is vertical depth, and d_{o} is the reference depth associated with P_{o} (*i.e.* the injection point depth).

2.3. The Streaming Potential Coefficient

In the special case of single-phase liquid flow through a system with uniform properties (conductivity, porosity, permeability, density, viscosity, salinity, temperature, tortuosity *etc.*), by incorporating Darcy's Law the above Poisson's equation [2.1] for the electrokinetic self-potential may be specialized to the following simple form:

$$\nabla^2 V = \xi\, \nabla^2 p \qquad [2.7]$$

where ξ, the so-called *"streaming potential coefficient",* is a correlation coefficient between pressure disturbance (p) and local electrical potential disturbance (V) given by:

$$\xi = (\varphi\, \varepsilon\, \zeta) / (\sigma\, \mu\, \Theta^2) \qquad [2.8]$$

As noted above, ζ is usually negative so $\xi < 0$ and regions of higher than average pressure (near a pressurized fracture, for example) will tend to be correlated with regions of negative electrokinetic potential anomaly. Although the uniformity assumptions implicit in equation [2.7] are too restrictive for the present purposes, the qualitative character of this correlation and the definition [equation 2.8] of the *"streaming potential coefficient"* ξ itself are key concepts behind the theoretical development underlying the SPFRAC simulator.

2.4. Fluid Mass Conservation

To establish the fluid mass flux vector $\boldsymbol{M}$ (which depends on both location and time), the distribution of the fluid pressure (also dependent upon position and time) is required. For this purpose, the principle of fluid mass conservation is invoked and can be written:

$$\partial(\varphi\rho) / \partial t \; + \; \nabla\cdot\boldsymbol{M} \; = \; source\ terms \qquad [2.9]$$

or, using Darcy's law,

$$\partial(\varphi\rho) / \partial t \; = \; \nabla\cdot \left[(\rho k / \mu) \, \nabla p \right] \; + \; source\ terms \qquad [2.10]$$

where, again, φ = porosity, ρ = fluid density, k = permeability, μ = fluid viscosity, and p = excess pressure or "overpressure". The *"source terms",* for the present application, represent the effects of the operation of wells (positive for injection and negative for production). The left-hand side of the above mass balance equation [2.10] may be decomposed to:

$$\partial(\varphi\rho) / \partial t \; = \; \varphi \times (\partial\rho / \partial t) \; + \; \rho \times (\partial\varphi / \partial t) \; = \; (\varphi\rho) \times (C_w \; + \; C_r) \times (\partial p / \partial t) \qquad [2.11]$$

where C_w and C_r are the isothermal "water compressibility" and "rock compressibility" respectively, and are given by:

$$C_w \; = \; (\partial\rho \,/\partial p) / \rho \qquad [2.12]$$

$$C_r \; = \; (\partial\varphi \,/\partial p) / \varphi \qquad [2.13]$$

and the partial derivatives are evaluated at constant temperature. The rock compressibility C_r will in general be a function of position. The fluid compressibility C_w may be regarded as a function of temperature and salinity for single-phase liquid flow, and since both temperature and salinity are regarded as functions of position only in the present case, the total compressibility:

$$C \; = \; C_w + C_r \qquad [2.14]$$

is also a function of position only (like ρ, μ and φ). Thus, we may finally write the above mass balance equation [2.10] as a diffusion equation for the fluid overpressure:

$$(\varphi\rho C) \times (\partial p / \partial t) \; = \; \nabla\cdot \left[(\rho k / \mu) \, \nabla p \right] \; + \; [source\ terms]_{\mathrm{m}} \qquad [2.15]$$

and the expression for the electrical potential V may now be written:

$$\nabla\cdot \left[\sigma \, \nabla V \right] \; = \; \nabla\cdot \left[\sigma \, \xi \, \nabla p \right] \; + \; [source\ terms]_{\mathrm{e}} \qquad [2.16]$$

2.5. Solution Technique

In the present application, in equations [2.15] and [2.16] the quantities φ (rock porosity), C (total compressibility), ρ (fluid density), μ (fluid viscosity), σ (electrical conductivity) and ξ (streaming potential coefficient) may be regarded as known functions of position only. The principal unknowns (functions of position and time) are the fluid overpressure (p) and the electrical potential (V). The rock permeability (k) is also a function of position and time which depends on the fluid overpressure p. The "source terms" in equations [2.15] and [2.16] arise from the presence of wells penetrating the region. In equation [2.15], "$[source\ terms]_{\mathrm{m}}$" represents the effects of fluid injection or withdrawal from the wells upon the distribution of fluid mass (and pressure). In equation [2.16], "$[source\ terms]_{\mathrm{e}}$" represents the electrical effects of buried highly-

conductive metallic well casings upon the distribution of electrical potential in the formation. These are discussed at length below.

The SPFRAC simulator uses a fully implicit finite-difference technique to solve the above system of equations ([2.15] and [2.16]) in a three-dimensional volume of space shaped like a rectangular prism subdivided into numerous "grid blocks". The computing volume is large, and extends far beyond the fractured region influenced by hydrofracturing. Usually, this fractured zone (and the feedzone of the injection well used to stimulate the system) will be centrally located within the computing volume. At large distances (*i.e.* at the outer perimeter of the computing volume), both the fluid overpressure p and the electrical potential V are taken to be equal to zero for all times t. The grid blocks adjacent to the grid boundaries will usually be much larger in size than those in the central region. The user assigns the dimensions of the various grid blocks; each block *(i, j, k)* will have a volume given by $\Delta v_{ijk} = \Delta x_i \times \Delta y_j \times \Delta z_k$.

Initially, both p and V are taken to be zero everywhere. Then, the solution is advanced in time by *(1)* solving [2.15] to find the distribution of fluid overpressure p after a short time interval (Δt), and then *(2)* solving [2.16] to determine the corresponding spatial distribution of electrical potential V at the same time. The process is then repeated to obtain pressures and potentials at a subsequent time level, and so on. In this way, the space/time distributions of p and V are calculated, step-by-step. Note that in equations [2.15] and [2.16] the distribution of electrical potential V depends on the pressure (p) distribution, but the pressure distribution itself is independent of V. This means that it is not necessary to recalculate the potential distribution (using equation [2.16]) each and every time that the pressure distribution is updated – electrical potential need only be recomputed when needed for comparisons with field measurements.

2.6. Modeling Fracture Permeability

Using SPFRAC, the rock permeability is regarded as the sum of *(1)* the "matrix" permeability k_m (which is small but nonzero in all of the blocks of the grid, is invariant with time and is user-specified), and *(2)* the "fracture" permeability k_f, which is non-zero in only a small fraction of the computational grid blocks, but which depends in general on time:

$$k\,(\boldsymbol{r},t) \;=\; k_m\,(\boldsymbol{r}) \;+\; k_f(\boldsymbol{r},t) \qquad [2.17]$$

The "matrix permeability" k_m is user-assigned, but the "fracture permeability" k_f is calculated within SPFRAC using an "equivalent hydraulic aperture" approach.

Consider a single planar smooth-walled rock fracture characterized by a particular value of "aperture" λ (the distance between the parallel rock faces bounding the fracture). It is easy to show that under conditions of steady laminar viscous liquid flow, the average fluid velocity in the fracture subject to a pressure gradient ∇p along the fracture will be given by:

$$u_{avg} \;=\; -\,(\,\nabla p\,/\,\mu\,)\;\times\;(\,\lambda^2\,/\,12\,) \qquad [2.18]$$

If we consider an element of such a fracture (of area a) embedded within a volume of rock of total volume v, it follows (invoking Darcy's Law) that the average additional "fracture permeability" contributed to the volume by the presence of the fracture will be given by:

$$\Delta k_f \;=\; (a\,/\,v)\;\times\;(\,\lambda^3\,/\,12\,) \qquad [2.19]$$

and the "fracture transmissivity" (or the *"kH product"*) is:

$$\text{"}kH\text{"} = \lambda^3 / 12 \qquad [2.20]$$

So, for a particular computational grid block (with $v = v_{ijk}$), the "fracture permeability" will simply be the total of the Δk_f's contributed by the various fractures that pass through the block.

Equation [2.19] describes how to calculate the "fracture permeability" due to a fracture of "equivalent hydraulic aperture" λ, but λ itself remains to be determined. For each fracture present, it is assumed that some initial aperture value λ_o prevails at $t = 0$ over the entire fracture. Thereafter, the aperture at each point in the fracture will change with time according to:

$$(\partial\lambda / \partial t) = B \times (\partial p / \partial t) \qquad [2.21]$$

where in general the coefficient B for any particular fracture may take on one of two values (B_i or B_d) at any particular time:

$$\begin{aligned} B &= B_i \quad \text{if } (\partial p / \partial t) > 0 \text{ and } p = p_{max} \\ B &= B_d \quad \text{if } (\partial p / \partial t) \le 0 \text{ or } p < p_{max} \end{aligned} \qquad [2.22]$$

where p_{max} means "the highest value of p experienced so far at this location," and where it is required that $B_d \le B_i$.

This model (equations [2.19] – [2.22]) provides substantial flexibility in prescribing the time-history of "fracture permeability" for a particular fracture. For example first consider the simplest case where $\lambda_o = 0$ and where $B_d = B_i$. Let us consider five temporally successive states (at $t = t_1$, t_2, t_3, t_4 and t_5), with the local fluid overpressure being zero, $p_{inj}/2$, p_{inj}, $p_{inj}/2$ and zero in that order (fracture pressurization followed by depressurization). The corresponding values of the fracture aperture and of the fracture transmissivity will be:

Time t	Overpressure p	Aperture λ	Transmissivity kH
t_1	0	0	0
t_2	$p_{inj} / 2$	$B_i \times p_{inj} / 2$	$(B_i \times p_{inj})^3 / 96$
t_3	p_{inj}	$B_i \times p_{inj}$	$(B_i \times p_{inj})^3 / 12$
t_4	$p_{inj} / 2$	$B_i \times p_{inj} / 2$	$(B_i \times p_{inj})^3 / 96$
t_5	0	0	0

Next, consider a similar situation but where $B_d = (B_i / 2)$. In that case, the corresponding results will be:

Time t	Overpressure p	Aperture λ	Transmissivity kH
t_1	0	0	0
t_2	$p_{inj} / 2$	$B_i \times p_{inj} / 2$	$(B_i \times p_{inj})^3 / 96$
t_3	p_{inj}	$B_i \times p_{inj}$	$(B_i \times p_{inj})^3 / 12$
t_4	$p_{inj} / 2$	$B_i \times p_{inj} \times (3/4)$	$(B_i \times p_{inj})^3 \times (9/256)$
t_5	0	$B_i \times p_{inj} / 2$	$(B_i \times p_{inj})^3 / 96$

which describes a fracture exhibiting permanent deformation, with finite residual transmissivity remaining even after pressurization is over. Finally, consider the effect of specifying non-zero values for the initial fracture aperture λ_o. If $\lambda_o > 0$, then the fracture will already be somewhat permeable before stimulation begins, and pressurization will have the effect of further increasing the fracture transmissivity. If on the other hand $\lambda_o < 0$ is specified, SPFRAC treats the fracture

permeability as zero for negative λ values, which means that the fracture will not actually begin to open physically until the local overpressure reaches a finite "threshold" given by:

$$p^* = -\lambda_o / B_i \qquad [2.23]$$

2.7. Representing the Injection Well

The effects of fluid injection are of central importance to the EGS reservoir stimulation problem, and are reflected in the SPFRAC simulator through the "$[source\ terms]_m$" in equation [2.15] above. For most of the blocks in the computational grid "$[source\ terms]_m$" will be zero, but at least one grid block will contain the "feedpoint" of the injection well where fluid mass is added to the grid volume as time goes on. SPFRAC also allows for a "feedzone" of finite vertical extent, involving multiple vertically-adjacent grid blocks and the simultaneous stimulation of multiple fracture systems. Also note that, although there is no particular requirement that the injection well feedzone intersects a fracture, calculations in which this is not the case are likely to be of little practical interest for EGS.

We consider the "feedzone" to consist of a vertical circular cylinder of finite height, with a diameter equal to the wellbore diameter (and ordinarily much smaller than the grid block dimensions). Injection may be specified by identifying the "feedblock(s)" involved and either prescribing a volumetric flow rate history or an injection pressure history (or a mixture, with pressure specified for part of the history and flow specified for the remainder). In either event, the objective is to uniquely establish the time-variation of the injection rate. The relationships in the feedblock(s) among the well radius r_{well}, the horizontal permeability in the feedblock k_h, the fluid viscosity in the feedblock μ_{ijk}, the vertical length of the open (*i.e.* uncased) section lying within the feedblock L_{ijk}, the well's "skin factor" s_{well}, the instantaneous overpressure within the injection well p_{well}, the instantaneous grid block pressure p_{ijk} and the volumetric flow rate of fluid from the well into the formation in the grid block R (*i.e.* cubic meters per second) are given by:

$$R = 2\,\pi\,L_{ijk}\,k_h\,(p_{well} - p_{ijk}) \,/\, \{\mu_{ijk} \times [\,\log_e(r_{eff}/r_{well}) + s_{well}\,]\,\} \qquad [2.24]$$

where r_{eff} is the so-called "effective well-block radius" which is proportional to the size of the feedblock itself. Rules for determining r_{eff} are well-established (see *Pritchett and Garg,* 1980; also see Appendix B of *Pritchett,* 2002). In the special case of a uniform grid with a square wellblock ($\Delta x = \Delta y$), the effective wellblock radius will be given by $r_{eff} = 0.1985 \times \Delta x$. Procedures for estimating r_{eff} automatically under more general circumstances are incorporated within the SPFRAC simulator.

2.8. Effects of Conductive Well Casings

As noted by *Pritchett and Ishido* (2005b), the presence of electrically conductive steel well casing pipe within the reservoir can perturb the electrical signals propagating outward from the pressurized fractures. To minimize such effects, *Pritchett et al.* (2006) recommended the use of nonmetallic casing materials for the observation wells, at least at depths comparable to the fracture system depth. But such recommendations may not be followed, and moreover material strength considerations will probably require the use of steel casing in the injection well, which means that the electrical potential distribution is likely to be perturbed near the well by electric currents flowing vertically in the pipe.

Since the electrical conductivity of steel (~10^7 siemens/meter, depending somewhat on alloy characteristics and temperature) exceeds the underground formation conductivity values typically measured in geothermal reservoirs by between eight and ten orders of magnitude, it suffices to regard these structures as infinitely conductive, so that at any instant of time the electrical potential along the pipe will be uniform, and the potential in the reservoir formation immediately adjacent to the pipe will be likewise the same everywhere along its surface. Currents will flow longitudinally in the metal pipe to equalize the potentials along its length, and the net electric current will be exactly zero, with electrons flowing outward from the pipe to the formation and inward from the formation to the pipe in equal numbers. Thus, for any particular continuous metallic conductor, the electrical potential will be at most a function of time.

SPFRAC considers two cases. In the first, the cylindrical conductor is very long and extends outward through the boundary of the computational volume (often all the way to the earth surface). In this case, it is assumed that the potential on the conductor is simply equal to zero (the imposed "distant" boundary value). If, however, the conductor is entirely contained within the study volume, it is assumed that the potential on the conductor, although uniform, will "float" and vary with time. Consequently, in the latter case a procedure for establishing the potential on the conductor at each instant of time is required.

The effects of electric currents flowing through these buried metal pipes and between the pipes and the surrounding geological formations are taken into account using the $[source\ terms]_e$ in equation [2.16]. For any particular computational grid block (*i, j, k*) containing a metal pipe, it is easy to show that the electric current (amperes) flowing from the pipe surface into the formation within the grid block volume is given by:

$$I_{ijk} = 2\,\pi\,L_{ijk}\,\sigma_{ijk}\,(V_{case} - V_{ijk}) \;/\; \log_e(r_{eff}/r_{case}) \qquad [2.25]$$

where as before L_{ijk} is the portion of the pipe length (in meters) that passes through grid block (*i,j,k*), σ_{ijk} is the electrical conductivity of the grid block (siemens/meter), V_{case} is the uniform instantaneous electrical potential along the pipe (volts), V_{ijk} is the instantaneous grid block potential (volts), r_{case} is the radius of the steel casing (*i.e.* the well radius, in meters) and r_{eff} (meters) is again the "effective well-block radius" calculated in exactly the same way as outlined above in Section 2.7.

If the conductor is "grounded" (that is, the pipe extends beyond the computational grid volume and is therefore at zero potential), then $V_{case} = 0$ and equation [2.25] may be summed over all of the grid blocks containing the pipe to establish the total electric current flowing through the outer boundary into the computing volume through this particular conductor:

$$I_{total}\ (\text{amperes}) = -2\,\pi \sum [L\,\sigma\,V / \log_e(r_{eff}/r_{case})]_{ijk} \qquad [2.26]$$

If on the other hand the conductor is "floating" (entirely contained within the computing volume), the electrical potential on the conductor at each instant of time may be established by the requirement that the net current in/out of the conductor as a whole must be zero, so:

$$V_{case} = \sum (W_{ijk} \times V_{ijk}) \;/\; \sum W_{ijk} \qquad [2.27]$$

where the grid block (*i,j,k*) weighting factor W_{ijk} is given by:

$$W_{ijk} = [\,L_{ijk} \times \sigma_{ijk}\,] \,/\, [\,\log_e(r_{eff}/r_{case})\,]_{ijk} \qquad [2.28]$$

2.9. Constitutive Relations

SPFRAC considers the native reservoir fluid to consist of liquid sodium chloride (NaCl) brine. The user specifies spatial distributions of temperature T and brine salinity S (mass fraction of dissolved NaCl in the fluid), and several pertinent properties are then automatically computed by the simulator using mathematical fits to handbook values for the properties of such brines. These quantities include the fluid density ρ, the fluid compressibility C_w, the fluid viscosity μ and the fluid electrical conductivity σ_w. These functional dependencies are illustrated graphically in Figures 2-1, 2-2, 2-3 and 2-4 respectively. The fluid's absolute dielectric permittivity (ε) is treated as a function of temperature; values are listed in Table 2-1.

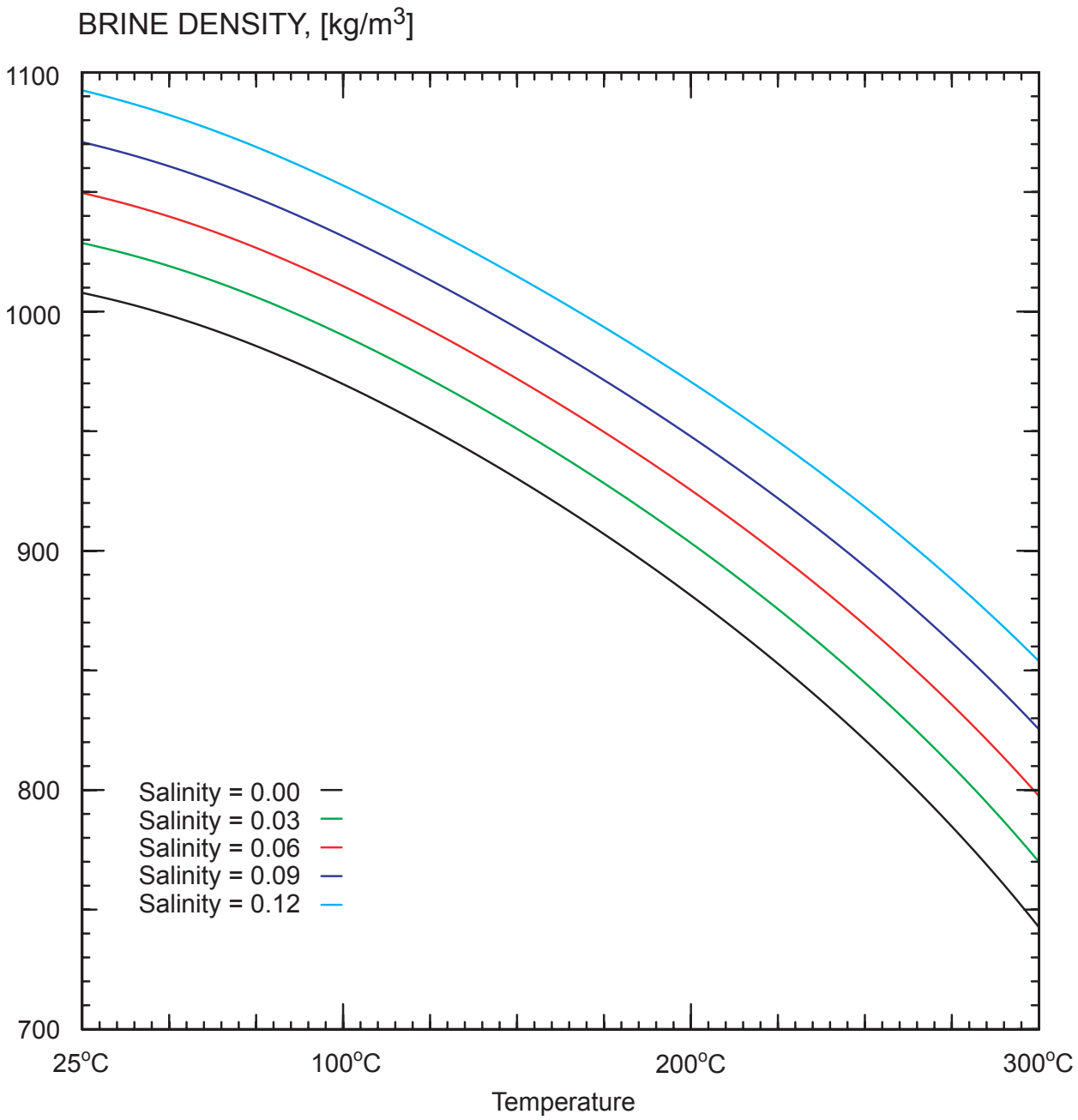

Figure 2-1: SPFRAC representation of native reservoir brine mass density (ρ) as a function of temperature and brine salinity.

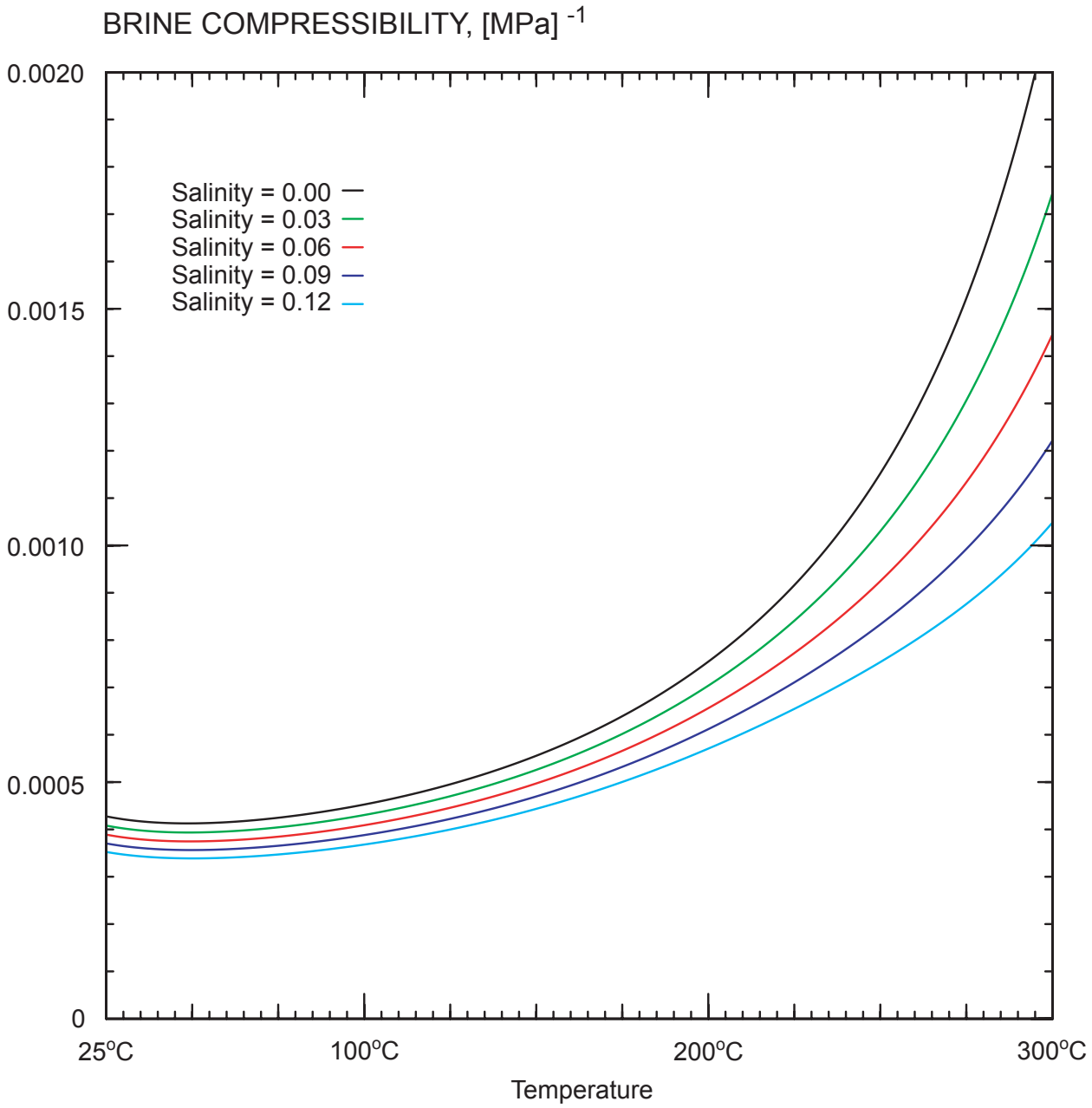

Figure 2-2: SPFRAC representation of native reservoir brine isothermal compressibility (C_w) as a function of temperature and brine salinity.

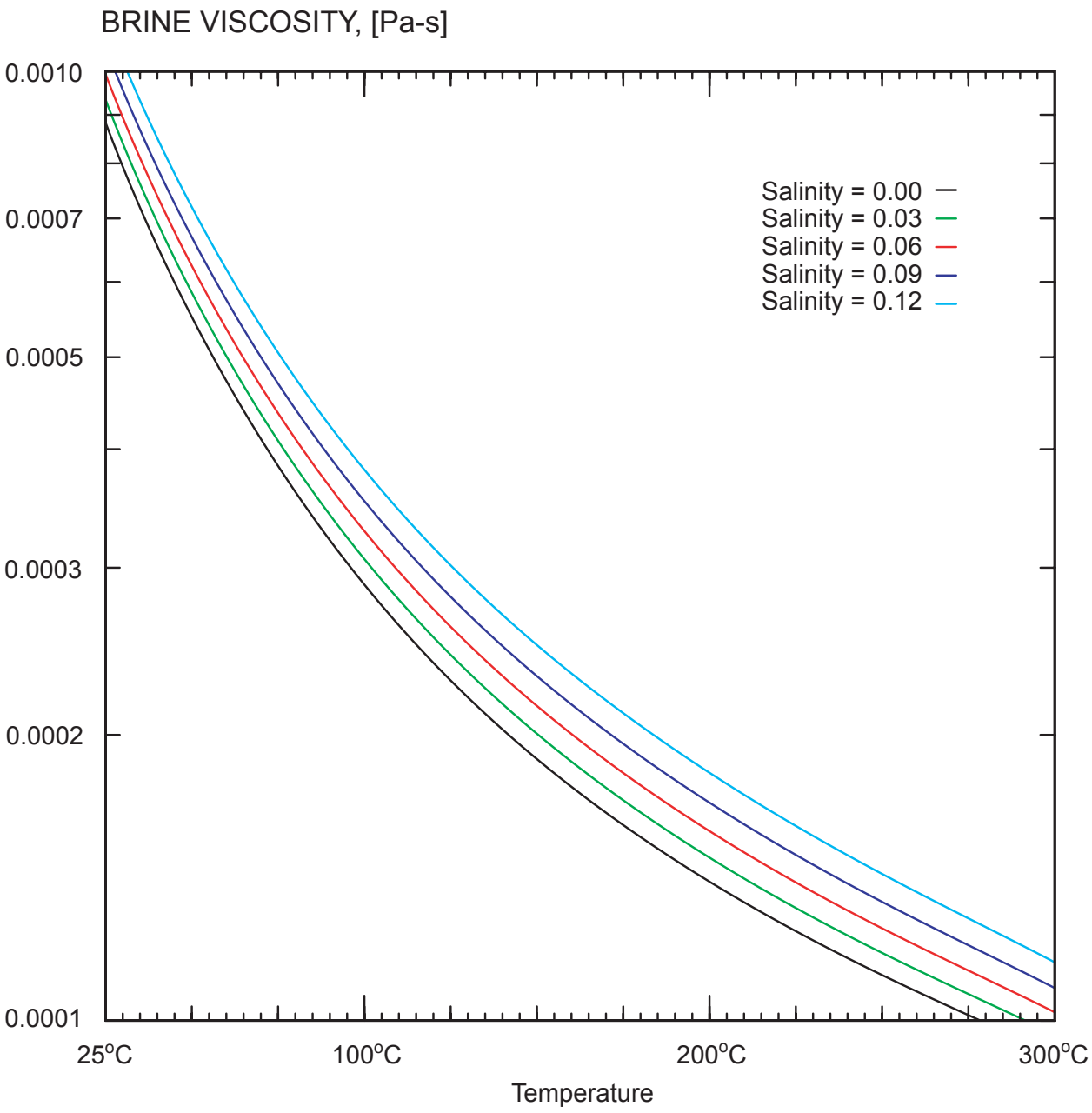

Figure 2-3: SPFRAC representation of native reservoir brine dynamic viscosity (μ) as a function of temperature and brine salinity.

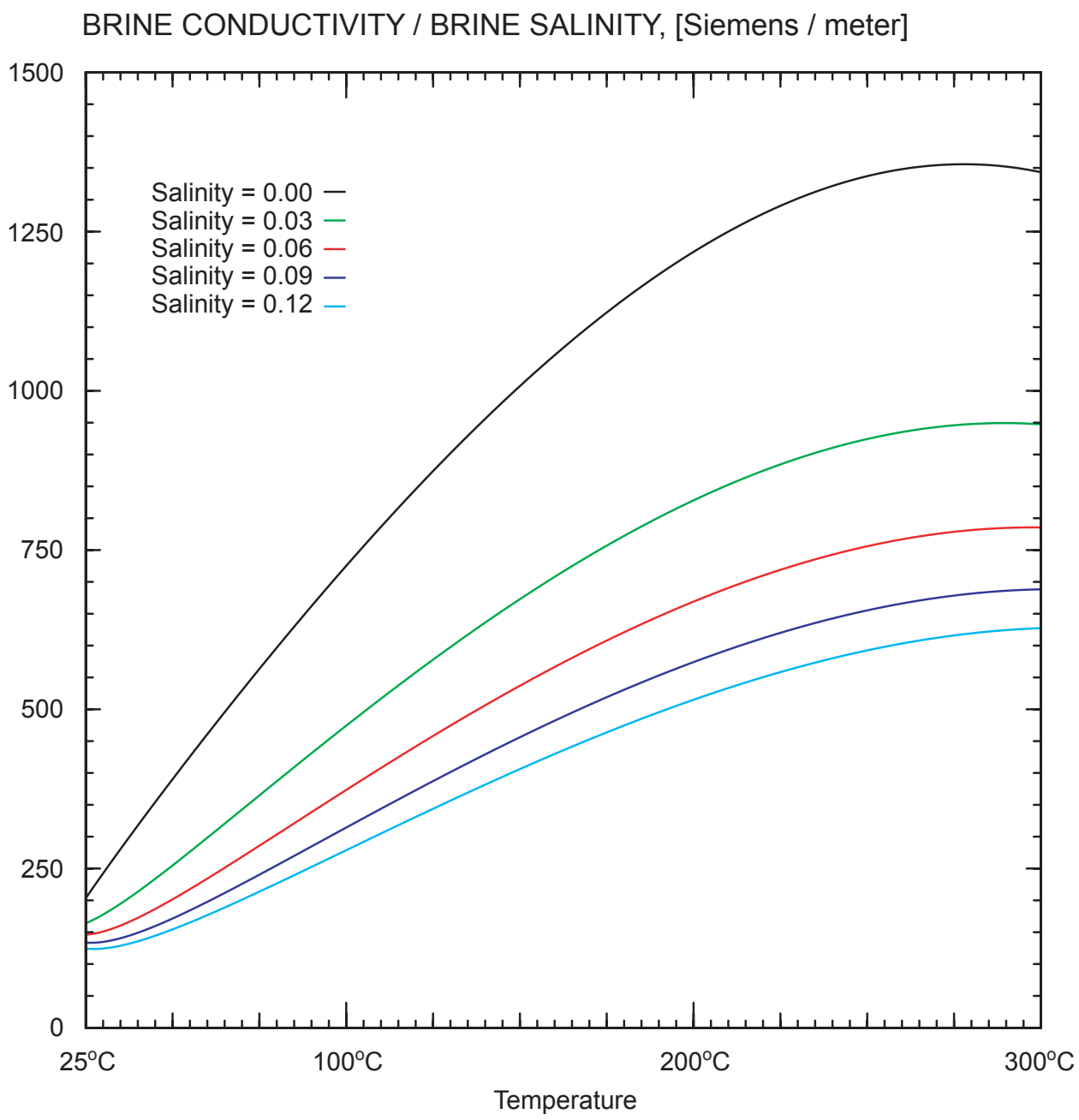

Figure 2-4: SPFRAC representation of native reservoir brine electrical conductivity σ_w as a function of temperature and brine salinity, expressed as the ratio of conductivity to salinity. Conductivity increases with increasing brine salinity, but the ratio [conductivity/salinity] declines slightly with increasing salinity. The SPFRAC description is valid for salinities from 10^{-6} up to about 0.3.

TABLE 2-1: SPFRAC representation of water absolute dielectric permittivity *(ε)* as a function of temperature *(T)*.

T	***ε***	***T***	***ε***
25°C	706 pF/m	165°C	369 pF/m
30°C	690 pF/m	170°C	360 pF/m
35°C	674 pF/m	175°C	352 pF/m
40°C	659 pF/m	180°C	344 pF/m
45°C	644 pF/m	185°C	337 pF/m
50°C	629 pF/m	190°C	329 pF/m
55°C	614 pF/m	195°C	322 pF/m
60°C	600 pF/m	200°C	314 pF/m
65°C	586 pF/m	205°C	307 pF/m
70°C	572 pF/m	210°C	300 pF/m
75°C	559 pF/m	215°C	293 pF/m
80°C	546 pF/m	220°C	287 pF/m
85°C	533 pF/m	225°C	280 pF/m
90°C	520 pF/m	230°C	273 pF/m
95°C	508 pF/m	235°C	267 pF/m
100°C	497 pF/m	240°C	261 pF/m
105°C	485 pF/m	245°C	254 pF/m
110°C	474 pF/m	250°C	248 pF/m
115°C	463 pF/m	255°C	242 pF/m
120°C	453 pF/m	260°C	236 pF/m
125°C	442 pF/m	265°C	230 pF/m
130°C	432 pF/m	270°C	224 pF/m
135°C	422 pF/m	275°C	218 pF/m
140°C	413 pF/m	280°C	212 pF/m
145°C	404 pF/m	285°C	206 pF/m
150°C	394 pF/m	290°C	201 pF/m
155°C	386 pF/m	295°C	195 pF/m
160°C	377 pF/m	300°C	189 pF/m

Note: 1 pF/m = 10^{-12} farads per meter

3. *SPFRAC* SIMULATOR OPERATING INSTRUCTIONS

The SPFRAC program system consists of several parts – a "simulator" (which actually solves the physics problem outlined in the preceding section) and six "graphical postprocessors" which can be used to create images illustrating the solutions obtained by the "simulator" and to compare them with field measurements. These programs were all written in the "Fortran 77" computing language (two small system-dependent "calendar" and "clock" utility routines are written in "C" for implementation on certain computer hardware/software configurations). SPFRAC consists of 25,754 lines of source code. The programs were written with portability in mind, and it is expected that transferring the software from one computing platform to another will be straightforward. Actual code development and testing was carried out using a PC with an AMD Opteron-64 processor operating under the Red Hat Linux operating system. Fortran and C compilations were accomplished using the Portland Group (PGI) "Workstation" toolkit.

3.1. General Procedure

The overall approach to be used to solve a particular problem is as follows. First, it is recommended that a new "directory" be created to contain all of the input and output files associated with the problem ("directory" is a Unix/Linux term – a "directory" is usually called a "folder" in Microsoft jargon). Then the user creates (or imports) the ASCII input files required to specify the problem in this directory. Preparation of these input files is the subject matter of this Section 3. Next, the "simulator" is executed on the computer, which creates a number of ASCII output text files (discussed in Section 4; examples are provided in Appendix B). Afterwards, some or all of the "graphical postprocessors" may be used to illustrate the results. This step may require the preparation of additional input data files by the user (as discussed in Section 5), but the principal data source for the plotting programs is the various "simulator" output text files. These postprocessors will produce additional ASCII "plot" files written in the "JPLOT" plotting language; these "plot" files may be supplied as input to the "JPLOT" graphics program (*Pritchett and Alexander,* 1986), which can either display images on the user's monitor or generate "encapsulated postscript" graphics files which may be manipulated using tools such as Adobe Illustrator. "JPLOT" is not a part of the SPFRAC program system, but is available separately for use with a variety of computing platforms and plotting equipment. Examples of SPFRAC graphic output created in this manner may be found in Appendix C of this report.

3.2. Reserved File Names

Particular "file names" are reserved for certain purposes in connection with SPFRAC. All of these reserved file names are twelve characters in length and consist of *(1)* an eight character label, followed by *(2)* a "period", followed by *(3)* a three-character suffix. All "executable" files have names of the form *"spf*****.exe"*. User-prepared input files used for specifying the problem and directing the postprocessors have names of the form *"in******.fil"*. User-supplied files containing measured field data for comparison with the computed results have names of the form *"dt******.fil"*. Output text files created by the "simulator" have names of the form *"rp******.fil"*. Graphical output ("plot") files created by the postprocessors for input to JPLOT have names of the form *"pl******.igf"*. Table 3-1 provides a list of all of these SPFRAC reserved file names.

TABLE 3-1: SPFRAC reserved file names.

Executable Files:

spfpltcp.exe	*spfpltcv.exe*	*spfpltin.exe*	*spfpltsp.exe*	*spfpltsv.exe*
spfpltwv.exe	*spfracsm.exe*			

User-Prepared Problem Specification Input Files:

incasing.fil	*incndavh.fil*	*incndaxy.fil*	*incndmdl.fil*	*incndrok.fil*
incndsrf.fil	*incomprs.fil*	*incontcr.fil*	*incontlb.fil*	*incontpl.fil*
incontsr.fil	*inconttm.fil*	*infrcgeo.fil*	*infrcmdl.fil*	*ingridor.fil*
ingridsx.fil	*ingridsy.fil*	*ingridsz.fil*	*ininjhis.fil*	*ininjwel.fil*
inpermis.fil	*inporost.fil*	*inprmavh.fil*	*inprmaxy.fil*	*inpsensr.fil*
insaltfr.fil	*instrmdl.fil*	*instrmpc.fil*	*intemper.fil*	*intimstp.fil*
intortuo.fil	*intwophs.fil*	*invsensr.fil*	*inzetapo.fil*	

User-Supplied Measurement Data Files:

dtinjcmi.fil	*dtinjflo.fil*	*dtinjprs.fil*	*dtspIIII.fil**	*dtsvIIII.fil**
*dtwvIIII.fil**				

Computer-Generated Output Data Text Files:

rpcasing.fil	*rpcndrok.fil*	*rpcndsrf.fil*	*rpcomprs.fil*	*rperform.fil*
rpflprop.fil	*rpfractr.fil*	*rpgdIIII.fil**	*rpgrgeom.fil*	*rphistry.fil*
rpinecho.fil	*rpinjhis.fil*	*rpinjwel.fil*	*rpperman.fil*	*rppermis.fil*
rpporost.fil	*rpprmavh.fil*	*rpprmaxy.fil*	*rppsensr.fil*	*rpresist.fil*
rpsaltfr.fil	*rpspIIII.fil**	*rpstrmpc.fil*	*rpstrzta.fil*	*rpsvIIII.fil**
rptemper.fil	*rptimstp.fil*	*rptortuo.fil*	*rptwophs.fil*	*rpvsensr.fil*
rpwellhs.fil	*rpwvIIII.fil**	*rpzetapo.fil*		

Computer-Generated Plot Files:

plinjcmi.igf	*plinjflo.igf*	*plinjprs.igf*	*plpcIIII.igf**	*plspIIII.igf**
*plsvIIII.igf**	*plvcIIII.igf**	*plwvIIII.igf**		

---

* *"IIII"* denotes a four-digit integer: *IIII = 0001, 0002, ... , 9999*.

3.3. Input File Syntax

The user-prepared input files (the *"in******.fil"* files and the *"dt******.fil"* files) each consist of a series of "lines" of data. Some of these lines will contain strings of alphabetic characters, while others will contain one or more numerical values (real numbers or integers) in a particular order to specify the desired input problem parameter values.

"Free-field" formatting may be used to specify the required numerical values on each input text line. Values may be separated by blanks, commas, colons, or any other desired delimiter character *except* any of the following:

0 1 2 3 4 5 6 7 8 9 + – d D e E . *(decimal point)* or **#**.

The "#" character plays a special role in SPFRAC input syntax. If a "#" appears in the *first column* of any input line, *that entire line will be disregarded* by SPFRAC. If the "#" character appears *anywhere else* in a line, the "#" character itself *and all characters appearing to the right of "#"* within that line will be disregarded. This convention was adopted to facilitate the inclusion of "comment" fields within input data files. Examples of input files prepared in this manner are provided in Appendix A of this report.

3.4. Input Files for *"spfracsm.exe"*

The input files used for problem specification for the SPFRAC simulator (executable file *"spfracsm.exe")* are as follows, listed alphabetically:

File Name	Type	Specifies/Describes	See Section
incasing.fil	optional	conductive well casings	3.16
incndavh.fil	optional	conductivity anisotropy	3.15
incndaxy.fil	optional	conductivity anisotropy	3.15
incndmdl.fil	optional	conductivity model	3.14
incndrok.fil	**required**	rock conductivity	3.14
incndsrf.fil	optional	surface conductivity	3.14
incomprs.fil	optional	rock compressibility	3.10
infrcgeo.fil	optional	fracture geometry	3.12
infrcmdl.fil	optional	fracture model	3.12
ingridor.fil	optional	grid orientation	3.7
ingridsx.fil	**required**	x-direction grid spacing	3.7
ingridsy.fil	**required**	y-direction grid spacing	3.7
ingridsz.fil	**required**	z-direction grid spacing	3.7

File Name	Type	Specifies/Describes	See Section
ininjhis.fil	**required**	fluid injection history	3.17
ininjwel.fil	**required**	injection well properties	3.17
inpermis.fil	**required**	isotropic rock permeability	3.11
inporost.fil	**required**	rock porosity	3.10
inprmavh.fil	optional	permeability anisotropy	3.11
inprmaxy.fil	optional	permeability anisotropy	3.11
inpsensr.fil	optional	pressure sensor locations	3.18
insaltfr.fil	**required**	native brine salinity	3.9
instrmdl.fil	**required**	streaming potential model	3.13
instrmpc.fil	optional	streaming potential	3.13
intemper.fil	**required**	temperature	3.9
intimstp.fil	**required**	time-step and output spacing	3.8
intortuo.fil	optional	tortuosity	3.13
intwophs.fil	optional	two-phase zone locations	3.7
invsensr.fil	optional	potential sensor locations	3.18
inzetapo.fil	optional	adsorption (zeta) potential	3.13

3.5. Coordinate Systems

Two overlapping spatial coordinate systems are employed by SPFRAC to describe the distributions of both input and output quantities. The relationship between these two coordinate systems is defined by input file *"ingridor.fil"* (see Section 3.7 below). The **"world"** coordinate system (signified by *X*, *Y*, *Z*) has its origin at the (North, East) position of some convenient local surveyed benchmark, at sea level elevation. The *X* coordinate measures distance East of the benchmark ("meters East"), the *Y* coordinate measures distance North of the benchmark ("meters North"), and the *Z* coordinate measures vertical elevation above sea level ("meters RSL").

The origin of the **"grid"** coordinate system (signified by *x, y, z*) is located at the geometrical center of the computational grid. The *z*-coordinate always measures distance upward and the *x*- and *y*-coordinates measure horizontal distance, but the grid may be rotated by an arbitrary angle θ around the *z*-axis relative to the "world" coordinate system, so that the *y*-coordinate represents distance θ degrees east of north and the *x*-coordinate measures distance θ degrees south of east, both relative to the grid center. As will be seen below, many of the input quantities to be provided by the user may be specified in either coordinate system.

3.6. The "Common Scalar Input Protocol" (CSIP)

Many of the input files listed above serve to specify the spatial distribution of a particular scalar quantity (such as porosity, permeability, temperature, salinity, electrical conductivity, *etc.*) throughout the various blocks in the computational grid, and the same basic input syntax is to be used for establishing all of them. In this section, this *"common scalar input protocol"* (CSIP for short) is described for a "dummy" scalar variable Γ. In subsequent sections, reference will often be made to this subsection to describe the input file structure needed to specify such variables.

First, consider the simplest possible situation – the value of the parameter Γ is to be uniform over the entire grid volume. In this case, the input file syntax is equally simple – the file consists of a single line containing a single numerical entry (the desired uniform Γ value). Examples of this syntax are to be found in Figure A-3 (Appendix A) for input files *"intemper.fil", "insaltfr.fil", "inporost.fil"* and *"incomprs.fil"*.

If the distribution of Γ is to be non-uniform the input file structure is more elaborate, and several options are possible. One example is to be found in the *"incndrok.fil"* file illustrated in Figure A-6 (Appendix A). The file will consist of a single "Default Line" followed by an arbitrary number of three-line "Clauses":

Default Line

Clause 1 Directive Line
Clause 1 Location Line
Clause 1 Parameter Line

Clause 2 Directive Line
Clause 2 Location Line
Clause 2 Parameter Line

↓

Clause N Directive Line
Clause N Location Line
Clause N Parameter Line

end-of-file

The "Default Line", as above, contains a single numerical value. Upon encountering the "Default Line", SPFRAC will first set the Γ parameter value equal to the value entered on that line for all blocks in the computational grid. Then, this initially uniform Γ distribution will be altered by the various "Clauses", in the order that the clauses are encountered in the input file.

The "Directive Line" in each "Clause" must contain one of the following six (case-insensitive) character strings:

CHANGE GRID	**CHANGE WORLD**
ADD GRID	**ADD WORLD**
MULTIPLY GRID	**MULTIPLY WORLD**

The "Location Line" contains six numerical values. If the "Directive Line" contains the text "GRID", the entries on the "Location Line" are (in the following order):

$$\boldsymbol{x_L} \qquad \boldsymbol{x_H} \qquad \boldsymbol{y_L} \qquad \boldsymbol{y_H} \qquad \boldsymbol{z_L} \qquad \boldsymbol{z_H}$$

which represent "grid coordinate" values (in meters) delineating the spatial region influenced by the "Clause" ($\boldsymbol{x_L} \le x \le \boldsymbol{x_H}$, $\boldsymbol{y_L} \le y \le \boldsymbol{y_H}$, $\boldsymbol{z_L} \le z \le \boldsymbol{z_H}$). If the "Directive Line" instead contains "WORLD", the "Location Line" entries are:

$$\boldsymbol{X_L} \qquad \boldsymbol{X_H} \qquad \boldsymbol{Y_L} \qquad \boldsymbol{Y_H} \qquad \boldsymbol{Z_L} \qquad \boldsymbol{Z_H}$$

and the region influenced by the "Clause" is ($\boldsymbol{X_L} \le X \le \boldsymbol{X_H}$, $\boldsymbol{Y_L} \le Y \le \boldsymbol{Y_H}$, $\boldsymbol{Z_L} \le Z \le \boldsymbol{Z_H}$) in "world coordinates" (meters East, meters North and meters RSL). In processing the "Clause", SPFRAC will examine each of the computational grid blocks and locate its geometric center in space. Only those blocks with central coordinates (x_i, y_j, z_k) or (X_{ijk}, Y_{ijk}, Z_{ijk}) within the above limits will be influenced by the "Clause".

The "Parameter Line" of each "Clause" must contain eight numerical values:

$$\boldsymbol{\Psi_{LLL}} \qquad \boldsymbol{\Psi_{HLL}} \qquad \boldsymbol{\Psi_{LHL}} \qquad \boldsymbol{\Psi_{HHL}} \qquad \boldsymbol{\Psi_{LLH}} \qquad \boldsymbol{\Psi_{HLH}} \qquad \boldsymbol{\Psi_{LHH}} \qquad \boldsymbol{\Psi_{HHH}}$$

For each grid block lying within the spatial range of the "Clause" as defined above, a value for Ψ is then obtained by tri-linear interpolation:

$$\begin{aligned}
\Psi_{ijk} \;=\; & \boldsymbol{\Psi_{LLL}} \times (1 - f_1) \times (1 - f_2) \times (1 - f_3) \\
& + \boldsymbol{\Psi_{HLL}} \times (\;\; f_1 \;\;) \times (1 - f_2) \times (1 - f_3) \\
& + \boldsymbol{\Psi_{LHL}} \times (1 - f_1) \times (\;\; f_2 \;\;) \times (1 - f_3) \\
& + \boldsymbol{\Psi_{HHL}} \times (\;\; f_1 \;\;) \times (\;\; f_2 \;\;) \times (1 - f_3) \\
& + \boldsymbol{\Psi_{LLH}} \times (1 - f_1) \times (1 - f_2) \times (\;\; f_3 \;\;) \\
& + \boldsymbol{\Psi_{HLH}} \times (\;\; f_1 \;\;) \times (1 - f_2) \times (\;\; f_3 \;\;) \\
& + \boldsymbol{\Psi_{LHH}} \times (1 - f_1) \times (\;\; f_2 \;\;) \times (\;\; f_3 \;\;) \\
& + \boldsymbol{\Psi_{HHH}} \times (\;\; f_1 \;\;) \times (\;\; f_2 \;\;) \times (\;\; f_3 \;\;)
\end{aligned} \qquad [3.1]$$

where, if the "Directive Line" contains "GRID":

$$f_1 \;=\; (x_i - \boldsymbol{x_L}) \,/\, (\boldsymbol{x_H} - \boldsymbol{x_L}) \qquad [3.2a]$$

$$f_2 \;=\; (y_j - \boldsymbol{y_L}) \,/\, (\boldsymbol{y_H} - \boldsymbol{y_L}) \qquad [3.2b]$$

$$f_3 \;=\; (z_k - \boldsymbol{z_L}) \,/\, (\boldsymbol{z_H} - \boldsymbol{z_L}) \qquad [3.2c]$$

or, if the "Directive Line" contains "WORLD":

$$f_1 \;=\; (X_{ijk} - \boldsymbol{X_L}) \,/\, (\boldsymbol{X_H} - \boldsymbol{X_L}) \qquad [3.3a]$$

$$f_2 \;=\; (Y_{ijk} - \boldsymbol{Y_L}) \,/\, (\boldsymbol{Y_H} - \boldsymbol{Y_L}) \qquad [3.3b]$$

$$f_3 \;=\; (Z_{ijk} - \boldsymbol{Z_L}) \,/\, (\boldsymbol{Z_H} - \boldsymbol{Z_L}) \qquad [3.3c]$$

The effect of the resulting value of Ψ_{ijk} on the previously-stored value of Γ_{ijk} depends on whether the "Directive Line" text string contains "CHANGE", "ADD" or "MULTIPLY":

$$\Gamma_{ijk}^{new} \;=\; \Psi_{ijk} \qquad \text{[for "CHANGE"]} \qquad [3.4]$$

$$\Gamma_{ijk}^{new} \;=\; \Psi_{ijk} \;+\; \Gamma_{ijk}^{old} \qquad \text{[for "ADD"]} \qquad [3.5]$$

$$\Gamma_{ijk}^{new} \;=\; \Psi_{ijk} \;\times\; \Gamma_{ijk}^{old} \qquad \text{[for "MULTIPLY"]} \qquad [3.6]$$

SPFRAC will continue to read the successive "Clauses" and alter the Γ distribution accordingly until an "end-of-file" is encountered.

3.7. Problem Geometry: Files *"ingridor.fil", "ingridsx.fil", "ingridsy.fil", "ingridsz.fil"* and *"intwophs.fil"*

File *"ingridor.fil"* specifies the relationship between the "grid" coordinate system (*x, y, z*) and the "world" coordinate system (*X, Y, Z*; meters East, meters North, and meters RSL; above sea level). If file *"ingridor.fil"* is not found in the local directory, the two coordinate systems will coincide. File *"ingridor.fil",* if present, will consist of a single line with four numerical entries:

$$\boldsymbol{X_o} \qquad \boldsymbol{Y_o} \qquad \boldsymbol{Z_o} \qquad \boldsymbol{\theta}$$

(Figure A-1 in Appendix A provides an example, also illustrated by Figure 6-1 in Section 6). The origin of coordinates in the "grid" coordinate system always lies at the center of the computational grid volume; the first three entries ($\boldsymbol{X_o}$, $\boldsymbol{Y_o}$ and $\boldsymbol{Z_o}$) describe this same location in "world" coordinates (meters East, meters North and meters RSL respectively). The final entry ($\boldsymbol{\theta}$) is the angle by which the grid's *y*-axis is rotated to the east relative to true north, and is to be provided in degrees of angle, with $-180° \le \boldsymbol{\theta} \le +180°$. The resulting coordinate transformations are:

$$x = (X - \boldsymbol{X_o}) \cos \boldsymbol{\theta} - (Y - \boldsymbol{Y_o}) \sin \boldsymbol{\theta} \qquad [3.7]$$

$$y = (X - \boldsymbol{X_o}) \sin \boldsymbol{\theta} + (Y - \boldsymbol{Y_o}) \cos \boldsymbol{\theta} \qquad [3.8]$$

$$z = (Z - \boldsymbol{Z_o}) \qquad [3.9]$$

and

$$X = \boldsymbol{X_o} + y \sin \boldsymbol{\theta} + x \cos \boldsymbol{\theta} \qquad [3.10]$$

$$Y = \boldsymbol{Y_o} + y \cos \boldsymbol{\theta} - x \sin \boldsymbol{\theta} \qquad [3.11]$$

$$Z = \boldsymbol{Z_o} + z \qquad [3.12]$$

Input file *"ingridsx.fil"* is required for program operation, and specifies the computational grid spacing in the *x*-direction by supplying the *x*-direction spatial extent of each grid block present in the order of increasing *x*. The various Δx values are all to be provided in meters, and all must be positive. The file consists of an arbitrary number of lines, and any desired number of grid block sizes may be specified on each line, for example:

Line 1: $\boldsymbol{\Delta x_1}$ $\boldsymbol{\Delta x_2}$ $\boldsymbol{\Delta x_3}$ $\boldsymbol{\Delta x_4}$ $\boldsymbol{\Delta x_5}$ $\boldsymbol{\Delta x_6}$

Line 2: $\boldsymbol{\Delta x_7}$ $\boldsymbol{\Delta x_8}$

Line 3: $\boldsymbol{\Delta x_9}$ $\boldsymbol{\Delta x_{10}}$ $\boldsymbol{\Delta x_{11}}$ $\boldsymbol{\Delta x_{12}}$

etc.

end-of-file

An example is provided in Appendix A, Figure A-1. The upper limit on the number of grid blocks in any coordinate direction is presently 75 (this limit can be increased, if needed, by program recompilation). The total grid extent in the *x*-direction is $-0.5 \sum \Delta x_i \le x \le +0.5 \sum \Delta x_i$.

Files *"ingridsy.fil"* and *"ingridsz.fil"* play the same role as *"ingridsx.fil"* and employ exactly the same structural syntax, but instead specify the grid block spacing in the *y*-direction (Δy_j) and in the *z*-direction (Δz_k) respectively.

As noted by *Pritchett and Ishido* (2005b), the presence of even a small amount of steam or gas within the pore space will constitute an impenetrable barrier to the propagation of either pressure or self-potential signals outward from the injection point, at least on time-scales of practical significance for monitoring hydrofracturing operations. Advantage was taken of this observation to simplify the SPFRAC formulation to consider only single-phase (liquid) fluid flow. Any regions within the volume of interest that contain two-phase mixtures of water and steam (or steam alone) may be regarded as maintained at both zero overpressure ($p = 0$) and zero potential ($V = 0$) for all t, and may therefore be excluded from the computing volume.

Ordinarily, the region influenced by two-phase flow will be relatively shallow and may often be described by a horizontal plane located at some elevation relative to sea level (Z_{boil}) below which the fluid is all-liquid and above which steam is present. Under most situations likely to be considered for EGS reservoir development, the reservoir will lie far deeper than Z_{boil}. But, as *Pritchett and Ishido* (2005b) showed, the presence of an overlying two-phase zone can have a perceptible effect on SP signals even if the stimulation operation takes place several hundred meters deeper.

Since the outer boundary conditions applied to the external surfaces of the SPFRAC computational grid volume are $p = V = 0$, so long as the two-phase interface is a horizontal plane it will suffice to employ a computational grid geometry with the upper grid surface coinciding with Z_{boil} vertical elevation to describe the situation. But if the boiling surface is not entirely planar and horizontal, input file *"intwophs.fil"* may be used to specify more complex boiling surface shapes, *i.e.* $Z_{boil}(X, Y)$ ("world" coordinates) or $z_{boil}(x, y)$ ("grid" coordinates).

Input file *"intwophs.fil",* if present, will consist of *(1)* a single "coordinate system" line, followed by *(2)* a "default" line, and then *(3)* as many "data" lines as are needed to specify the desired $Z_{boil}(X, Y)$ distribution:

Coordinate System Line
Default Line
First Data Line
Second Data Line
↓
Last Data Line
end-of-file

The "Coordinate System Line" will contain a character string: either **GRID** or **WORLD** (case-insensitive), to designate whether the input data are supplied using the "grid" or the "world" coordinate system. The "Default Line" will contain a single numerical entry: $z_{b\text{-}o}$ ("grid" coordinates) or $Z_{b\text{-}o}$ ("world" coordinates), which is the elevation of the boiling surface that will be first assigned over the entire area. Then, the various "Data Lines" will be processed, one after another, to alter this initially planar horizontal distribution. Each "Data Line" will contain eight numerical values:

X_L X_H Y_L Y_H Z_{LL} Z_{HL} Z_{LH} Z_{HH} ("world" coordinates)

or

x_L x_H y_L y_H z_{LL} z_{HL} z_{LH} z_{HH} ("grid" coordinates)

In the **WORLD** case, the effect of each "Data Line" will be to reset, over the rectangular region with $\boldsymbol{X_L} \le X \le \boldsymbol{X_H}$ and $\boldsymbol{Y_L} \le Y \le \boldsymbol{Y_H}$, the Z_{boil} distribution to:

$$\begin{aligned} Z_{boil} \;=\; & \boldsymbol{Z_{LL}} \times (1 - F_1) \times (1 - F_2) \\ & + \boldsymbol{Z_{HL}} \times (\quad F_1 \quad) \times (1 - F_2) \\ & + \boldsymbol{Z_{LH}} \times (1 - F_1) \times (\quad F_2 \quad) \\ & + \boldsymbol{Z_{HH}} \times (\quad F_1 \quad) \times (\quad F_2 \quad) \end{aligned} \qquad [3.13]$$

where

$$F_1 \;=\; (X - \boldsymbol{X_L}) \,/\, (\boldsymbol{X_H} - \boldsymbol{X_L}) \qquad [3.14]$$

$$F_2 \;=\; (Y - \boldsymbol{Y_L}) \,/\, (\boldsymbol{Y_H} - \boldsymbol{Y_L}) \qquad [3.15]$$

Similarly, in the **GRID** case each "Data Line" influences the region $\boldsymbol{x_L} \le x \le \boldsymbol{x_H}$, $\boldsymbol{y_L} \le y \le \boldsymbol{y_H}$:

$$\begin{aligned} z_{boil} \;=\; & \boldsymbol{z_{LL}} \times (1 - f_1) \times (1 - f_2) \\ & + \boldsymbol{z_{HL}} \times (\quad f_1 \quad) \times (1 - f_2) \\ & + \boldsymbol{z_{LH}} \times (1 - f_1) \times (\quad f_2 \quad) \\ & + \boldsymbol{z_{HH}} \times (\quad f_1 \quad) \times (\quad f_2 \quad) \end{aligned} \qquad [3.16]$$

where

$$f_1 \;=\; (x - \boldsymbol{x_L}) \,/\, (\boldsymbol{x_H} - \boldsymbol{x_L}) \qquad [3.17]$$

$$f_2 \;=\; (y - \boldsymbol{y_L}) \,/\, (\boldsymbol{y_H} - \boldsymbol{y_L}) \qquad [3.18]$$

All grid blocks for which the center of the grid block volume lies above the local "boiling level" Z_{boil} (or z_{boil}) will be flagged "two-phase", will be permanently assigned $p = V = 0$, and will not participate further in the calculation.

3.8. Time-Step, Duration, and Output Requirements: File *"intimstp.fil"*

Input file *"intimstp.fil"* is required for SPFRAC program operation. It is used to establish the temporal duration of the problem, the time-step size, and the output frequency requirements. An example is to be found in Figure A-2, Appendix A. The file consists of three lines: the first contains a case-insensitive alphabetic character string, the second contains a single positive number, and the third must contain at least two and not more than four numerical entries:

Line 1: **HOURS** *or* **SECONDS** *(character string)*

Line 2: $\boldsymbol{t_{max}}$

Line 3: $\boldsymbol{N_{recr}}$ $\boldsymbol{N_{dump}}$

or

$\boldsymbol{N_{recr}}$ $\boldsymbol{N_{dump}}$ $\boldsymbol{N_{hydro}}$

or

$\boldsymbol{N_{recr}}$ $\boldsymbol{N_{dump}}$ $\boldsymbol{N_{hydro}}$ $\boldsymbol{N_{limit}}$

end-of-file

If no value is provided for $\boldsymbol{N_{limit}}$ (Line 3), $\boldsymbol{N_{limit}}$ will be taken as infinity. If no $\boldsymbol{N_{hydro}}$ value is supplied, $\boldsymbol{N_{hydro}} = 1$ will be assigned. It is required that $\boldsymbol{t_{max}} > 0$; $\boldsymbol{N_{recr}}$, $\boldsymbol{N_{dump}}$, $\boldsymbol{N_{hydro}}$ and $\boldsymbol{N_{limit}}$ are all integers, and all must be positive.

Line 2 specifies the problem duration (t_{max}), and is to be provided either in hours or in seconds, according to the contents of Line 1 (one hour = 3600 seconds). N_{recr} designates the frequency with which the electrical potential distribution (V) will be recalculated using equation [2.16]; these recalculations will be carried out at intervals of (t_{max} / N_{recr}) and the total number of such recalculations will be equal to N_{recr}. At the time of each electrical potential recalculation, the local electrical potential value for each "potential sensor" and "metallic well casing" and the pressure value for each "pressure sensor" (see Sections 3.16 and 3.18 below) will be recorded for output from the program, creating potential *vs.* time and pressure *vs.* time records for comparison with field measurements on output files with names of the form *"rpsp****.fil", "rpsv****.fil"* and *"rpwv****.fil"*. Also, at these same times, the hydraulic conditions for the injection well (instantaneous pressure, instantaneous flow rate, and cumulative flow) will be recorded on an output file named *"rpwellhs.fil"* for purposes of pressure-transient analysis.

N_{dump} designates the frequency with which full "grid dump" output records will be created. Each "grid dump" will be written on a separate output file (with a name of the form *"rpgd****.fil"*), and will record the instantaneous values of overpressure (p) and electrical potential (V) for each block in the computational grid. These files can be quite large. "Dumps" will be performed every N_{dump} potential recalculations, so that the total number of output "dump" files created will be (N_{recr} / N_{dump}) and the time-interval between successive "dumps" is ($t_{max} \times N_{dump} / N_{recr}$).

N_{hydro} may be used to constrain the time-step size to be used for the temporal integration of the pressure equation (equation [2.15]), particularly for cases in which t_{max} is large and N_{recr} is small. The maximum value of the "hydrodynamic time step" will be given by t_{max} / ($N_{hydro} \times N_{recr}$). Smaller steps will be used by the simulator when necessary. If a value for N_{limit} is supplied, the simulation will be terminated if the total number of "hydrodynamic time steps" reaches N_{limit}.

3.9. Fluid Properties: Files *"intemper.fil"* and *"insaltfr.fil"*

As noted in Section 2.9, the native reservoir fluid is treated as a sodium chloride solution and many of its properties are regarded as functions of temperature T and salinity S (herein defined as the mass fraction of NaCl in the solution). These properties include fluid mass density (ρ), isothermal fluid compressibility (C_w), fluid viscosity (μ), fluid electrical conductivity (σ_w) and fluid dielectric permittivity (ε). SPFRAC neglects the effects of variations in pressure on these quantities. Therefore, to specify the distributions of these properties throughout the grid volume, it suffices to specify the spatial distributions of temperature and salinity.

Input file *"intemper.fil"* is required for program operation, and uses the *"Common Scalar Input Protocol"* (CSIP) to designate the temperature in each computational grid block (see Section 3.6 above for instructions). Temperatures are to be provided in degrees Celsius (°C). The range of permissible temperature values is constrained by the range of validity of the constitutive data fits discussed in Section 2.9. The recommended range is from 25°C to 300°C. Input temperatures lower than 0°C or greater than 350°C will be regarded as errors and will cause the program to terminate.

In a similar fashion, input file *"insaltfr.fil"* is used to specify the spatial distribution of salinity, again using the CSIP syntax (Section 3.6). Input values are to be specified as mass fractions of dissolved sodium chloride in the solution (*i.e.* kilograms of NaCl per kilogram of liquid). The

recommended range is from 10^{-5} to 0.3, and values less than 10^{-6} or greater than 0.5 will be treated as errors. In this connection, it should be noted that the finite solubility of NaCl in water means that salinity cannot exceed 0.265 at 25°C or 0.28 at 100°C. The salinity of the evaporatively concentrated brine in Utah's Great Salt Lake is about 0.1, and that of ordinary seawater is about 0.035. Waters with salinities of 10^{-4} or less are generally considered to be good quality drinking water. As noted by *Pritchett and Ishido* (2005b), if the reservoir salinity is much greater than that of seawater, SP signals from hydrofracturing operations will be significantly degraded in amplitude owing both to the high electrical conductivities of such brines and to the reduced magnitude of the adsorption potential ζ.

3.10. Formation Fluid Capacity: Files *"inporost.fil"* and *"incomprs.fil"*

Input file *"inporost.fil"* must be present in the local directory for SPFRAC operation; it specifies the spatial distribution of rock porosity (φ) using the CSIP input syntax (Section 3.6). It is recommended that $10^{-5} \le \varphi \le 0.5$. Porosity values $< 10^{-6}$ or > 0.9 will be treated as input errors. Optional input file *"incomprs.fil"* similarly uses CSIP to specify the spatial distribution of rock compressibility C_r (see discussion in Section 2.4). If file *"incomprs.fil"* is absent, it will be assumed that $C_r = 0$ everywhere. If the crystalline rock material is considered to be a linear-elastic solid, it may be shown that C_r will be given by:

$$C_r = [(1 - \varphi) / \varphi] \ / \ [M_{bulk} + (4\, M_{shear} / 3)] \qquad [3.19]$$

where φ is porosity, M_{bulk} is bulk modulus and M_{shear} is shear modulus. Values of C_r are to be provided in [pascals^{-1}]. The recommended range is $0 \le C_r \le 10^{-8}$ / Pa, and input values that exceed 10^{-6} / Pa will be treated as errors. For comparison, the fluid compressibility contribution (C_w) will be in the range 0.4×10^{-9} to 2.0×10^{-9} per pascal (see Figure 2-2).

3.11. Matrix Permeability: Files *"inpermis.fil"*, *"inprmavh.fil"* and *"inprmaxy.fil"*

Provision has been made in SPFRAC for the "country rock" or "matrix" permeability (that is, the reservoir permeability in the absence of fractures) to depend on location and possibly to differ in the various grid-coordinate directions (x, y, z). Ordinarily, of course, the matrix permeability (k_m) will be taken as isotropic, but SPFRAC permits the following formulation:

$$k_{mx} = k_m \times 6\,\beta_p / [(1 + \beta_p) \times (2 + \alpha_p)] \qquad [3.20]$$

$$k_{my} = k_m \times 6 / [(1 + \beta_p) \times (2 + \alpha_p)] \qquad [3.21]$$

$$k_{mz} = k_m \times 3\,\alpha_p / (2 + \alpha_p) \qquad [3.22]$$

This formulation has the following properties:

- If $\alpha_p = 1$ and $\beta_p = 1$, then $k_{mx} = k_{my} = k_{mz} = k_m$ (isotropic case).
- If $\alpha_p \ne 1$ and $\beta_p = 1$, then $(k_{mx} / k_{mz}) = (k_{my} / k_{mz}) = (1 / \alpha_p)$ and horizontal permeability ≠ vertical permeability.
- If $\alpha_p = 1$ and $\beta_p \ne 1$, then $k_{mz} = k_m = (k_{mx} + k_{my})/2$ but $(k_{mx} / k_{my}) = \beta_p$ and horizontal permeability depends on direction.

The spatial distribution of the "isotropic" matrix permeability k_m is provided by input file *"inpermis.fil",* using the CSIP input syntax (Section 3.6). Values are to be provided in square meters. The recommended range of values is from 10^{-19} m^2 (0.1 microdarcy) to 10^{-12} m^2 (one darcy). Input values less than 10^{-21} m^2 (one nanodarcy) or greater than 10^{-9} m^2 (one kilodarcy) will be treated as errors. Note that, as a practical matter, if the country rock permeability is greater than ten millidarcies or so (10^{-14} m^2), it will probably be impossible to build up enough pressure in the injection well to fracture the rock.

The "default" values for the anisotropy parameters α_p and β_p are $\alpha_p = \beta_p = 1$, so if an isotropic treatment is desired input files *"inprmavh.fil"* and *"inprmaxy.fil"* are redundant and may be eliminated. Otherwise, file *"inprmavh.fil"* uses the CSIP (Section 3.6) to specify the spatial distribution of α_p, and the data in *"inprmaxy.fil"* uses the same syntax to specify β_p. If either parameter is unity everywhere, the pertinent input file may be deleted. Recommended ranges of both α_p and β_p are from 0.1 to 10. Input values < 0.01 or > 100 will be treated as errors.

3.12. Fracture System Description: Files *"infrcmdl.fil"* and *"infrcgeo.fil"*

These two input files are used to specify the properties of the fracture system and how it is distributed spatially, so that the time-dependent "fracture permeability" k_f may be established. If no fractures are present, neither file should be present in the local directory. Otherwise, both will be required. Examples are provided in Appendix A, Figure A-4.

Input file *"infrcmdl.fil"* is used to create a "library" of fracture response models, and consists of from one to seven lines. Each of these lines will contain either two or three numerical values:

$$\boldsymbol{\lambda_o} \qquad \boldsymbol{B}$$

or

$$\boldsymbol{\lambda_o} \qquad \boldsymbol{B_i} \qquad \boldsymbol{B_d}$$

The significance of these quantities was discussed in Section 2.6; λ_o is the initial value of the "equivalent effective hydraulic aperture" λ (which will usually be zero, but may also be either positive or negative). The quantities B_i and B_d are values of $(\partial\lambda/\partial p)$; B_i is used if pressure is increasing and is not less than its historical maximum, and B_d is used otherwise. It is required that $B_i \geq B_d \geq 0$. If the two B values are the same, only one of them needs to be supplied. The B values are to be provided in meters per pascal and λ_o is provided in meters, so all of these values are small in magnitude; the B's will usually be of the order of 10^{-11} meters per pascal or so and the magnitude of λ_o, if nonzero, will usually be less than 10^{-4} meters. Each of the lines in input file *"infrcmdl.fil"* defines a different "fracture model" (*i.e.* a different relationship between "equivalent hydraulic fracture aperture" λ and overpressure p), and up to seven different models may be specified within a single computational case. In this fashion, different fractures within the reservoir may respond differently to changes in the local fluid pressure.

Input file *"infrcgeo.fil"* is used to specify the spatial distribution of the fractures. Although the illustrative example discussed in Section 6 has only a single fracture plane, SPFRAC can treat numerous overlapping/intersecting fracture planes. Each three-dimensional "fracture plane" is first subdivided by the user into a collection of triangular surfaces, each characterized by three "vertex locations", somewhat as indicated in Figure 3-1. Then, file *"infrcgeo.fil"* will consist of a series of "Clauses", each of which describes one of the triangular elements:

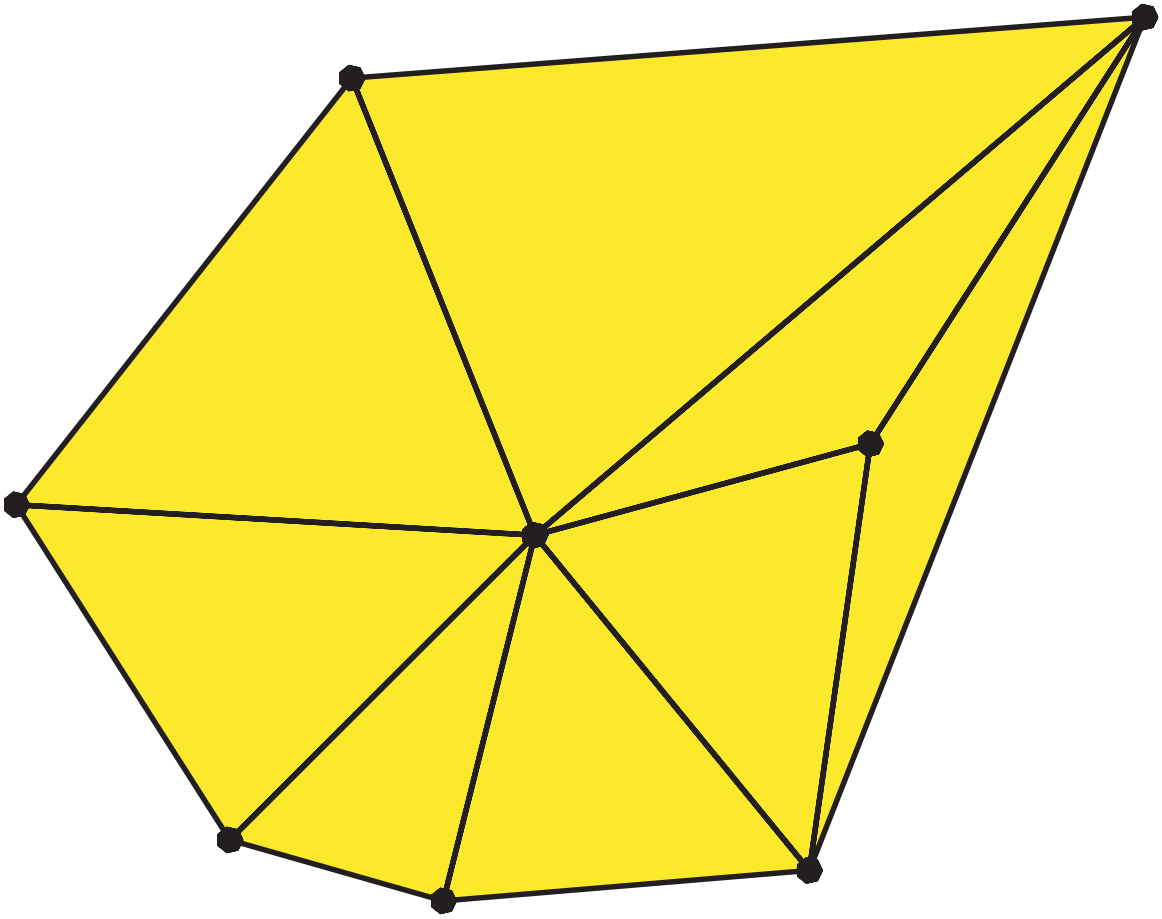

Figure 3-1: Representation of a “fracture plane” by connected triangular surface elements.

FIRST CLAUSE
SECOND CLAUSE
↓
LAST CLAUSE
end-of-file

Each of the "Clauses" representing one of the triangular elements will consist of five lines. Two forms are permissible, which differ only in whether the data are supplied in the "grid" or the "world" coordinate system:

Line 1: **GRID** *(case-insensitive character string)*
Line 2: N_{model} F_{rough}
Line 3: x_1 y_1 z_1
Line 4: x_2 y_2 z_2
Line 5: x_3 y_3 z_3

or

Line 1: **WORLD** *(case-insensitive character string)*
Line 2: N_{model} F_{rough}
Line 3: X_1 Y_1 Z_1
Line 4: X_2 Y_2 Z_2
Line 5: X_3 Y_3 Z_3

The spatial coordinates (*x, y, z*) or (*X, Y, Z*), to be provided in meters, locate the three vertices of the triangular element in "grid" or "world" coordinates as appropriate. Note that triangular elements specified in "world" and in "grid" coordinates may be mixed in a single *"infrcgeo.fil"* input file. N_{model} (an integer) designates which of the *"fracture response models"* specified by input file *"infrcmdl.fil"* (above) applies to this particular triangular element. If $N_{model} = 3$, for example, then the values of λ_o, B_i and B_d found on the third line of *"infrcmdl.fil"* will apply to the element.

Ordinarily, the dimensionless quantity F_{rough} should be set equal to unity. As discussed earlier, the effect of the presence of a fracture plane within a grid block (*i,j,k*) upon the fracture permeability k_f for that block is to contribute an increment Δk_f given by

$$\Delta k_f = (a / v_{ijk}) \times (\lambda^3 / 12) \qquad [3.23]$$

(for $\lambda > 0$; otherwise, the contribution is zero) where λ is the instantaneous aperture of the fracture at that point in space, v_{ijk} is the volume of the grid block, and a is the portion of the fracture surface area contained within the block, as discussed in Section 2.6. It should be noted in passing that "area" in this connection considers only one "side" of the fracture plane – the total "area" of the entire triangular element will be given by (base length) × (altitude/2), *not* twice that value. The value of a within a particular grid block (*i,j,k*) is calculated automatically by SPFRAC. The F_{rough} input quantity is provided to permit the user to modify this area, so that $a = a_{geometric} \times F_{rough}$. This might be done for a variety of reasons, such as representing the effects of partially-blocked fractures or of multiple parallel planar fractures with inter-fracture spacing less than the grid block size. It is of course required that F_{rough} be non-negative.

3.13. Streaming Potential: Files *"instrmdl.fil"*, *"inzetapo.fil"*, *"intortuo.fil"* and *"instrmpc.fil"*

SPFRAC makes provision for four different ways to specify the spatial distribution of the "streaming potential coefficient" ξ, formally defined by equation [2.8] of Section 2 and expressed in volts per pascal (and usually negative in sign). These are: *(1)* use the theoretical predictive model of *Ishido and Mizutani* (1981) to compute the adsorption potential ζ (volts) and specify the distribution of (dimensionless) tortuosity Θ using input file *"intortuo.fil", (2)* instead of using the Ishido/Mizutani model, supply suitable coefficients for an analytic fit to ζ as a function of fluid temperature T and salinity S (presumably based on laboratory measurements) and again use *"intortuo.fil"* to provide the distribution of tortuosity, *(3)* specify specific block-by-block values for ζ (volts) using input file *"inzetapo.fil"* and again specify tortuosity using *"intortuo.fil"*, or *(4)* specify block-by-block values of the streaming potential coefficient itself in volts per pascal using input file *"instrmpc.fil"* (in this case, *"intortuo.fil"* is not needed). These different options are discussed in the following subsections.

3.13.1. Ishido and Mizutani (1981) Model. In this case, input file *"instrmdl.fil"* will contain two lines, as follows:

Line 1: **ISHIDO** *(case-insensitive character string)*
Line 2: ΔpH

The theoretical formulation of *Ishido and Mizutani* (1981) contains a variable parameter ΔpH which influences the amplitude of the adsorption potential ζ somewhat; in the absence of data, using $\Delta pH = 5$ usually provides reasonable results. Figures 3-2 and 3-3 illustrate the values of ζ obtained from this model as functions of temperature and brine salinity for $\Delta pH = 4$, 5 and 6. The adsorption potential is always negative in sign; the magnitude increases with increasing temperature, increases slightly with increasing ΔpH, and decreases with increasing brine salinity. Using this model, SPFRAC will use the user-supplied spatial distributions of temperature and salinity and the above user-specified value for ΔpH to calculate the value of ζ for each grid block. Next, if input file *"intortuo.fil"* is present, it will be used to assign values for tortuosity Θ (≥ 1) to each block using the CSIP input file syntax discussed in Section 3.6. If file *"intortuo.fil"* is absent, SPFRAC will simply assign $\Theta = 1$ for all grid blocks.

The value of the streaming potential coefficient for each grid block will then be calculated from Equation [2.8]:

$$\xi = (\varphi \, \varepsilon \, \zeta) / (\sigma \, \mu \, \Theta^2) \qquad [3.24]$$

where φ is rock porosity (assigned by the user using input file *"inporost.fil"), ε* is the dielectric permittivity (a function of temperature; see Table 2-1), σ is total electrical conductivity (see Section 3.14 below), and μ is fluid dynamic viscosity (a function of temperature and salinity; see Figure 2-3). Using the "ISHIDO" option, input files *"inzetapo.fil"* and *"instrmpc.fil"* are unnecessary and if present they will be ignored.

3.13.2. Polynomial Model. This approach is similar to the above, but in this case the two-line contents of *"instrmdl.fil"* will be:

Line 1: **POLYNOMIAL** *(case-insensitive character string)*
Line 2: K_o K_T K_S

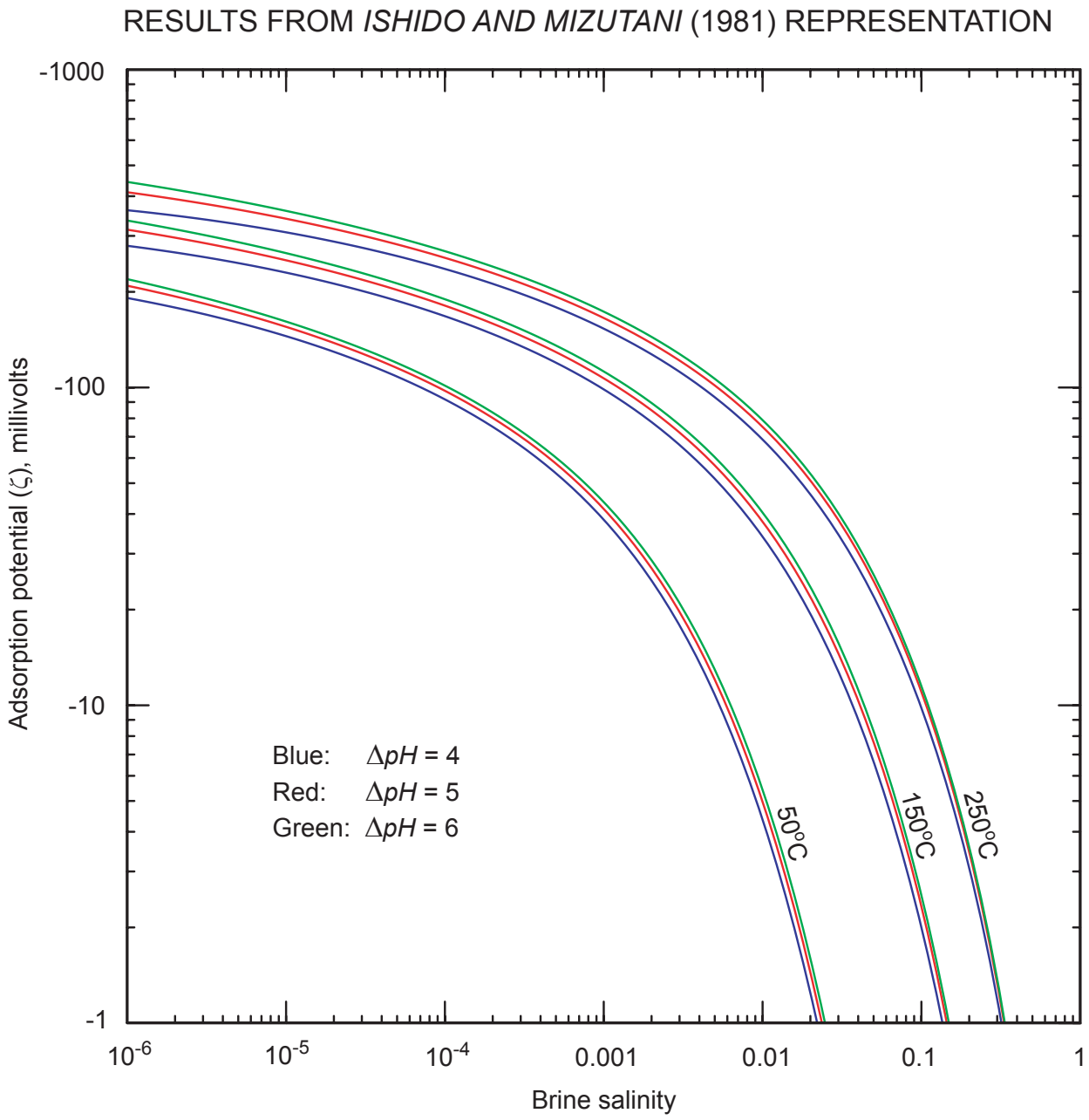

Figure 3-2: Adsorption potential or "zeta-potential" ζ as a function of brine salinity for 50°C, 150°C and 250°C temperature according to the model of *Ishido and Mizutani* (1981) as adopted for use in SPFRAC. The "Δ*pH*" parameter may be regarded as a data-fitting variable that may be used to reproduce laboratory test results on core samples. Note that ζ is negative, and that the magnitude of ζ increases with increasing temperature and decreases with increasing salinity.

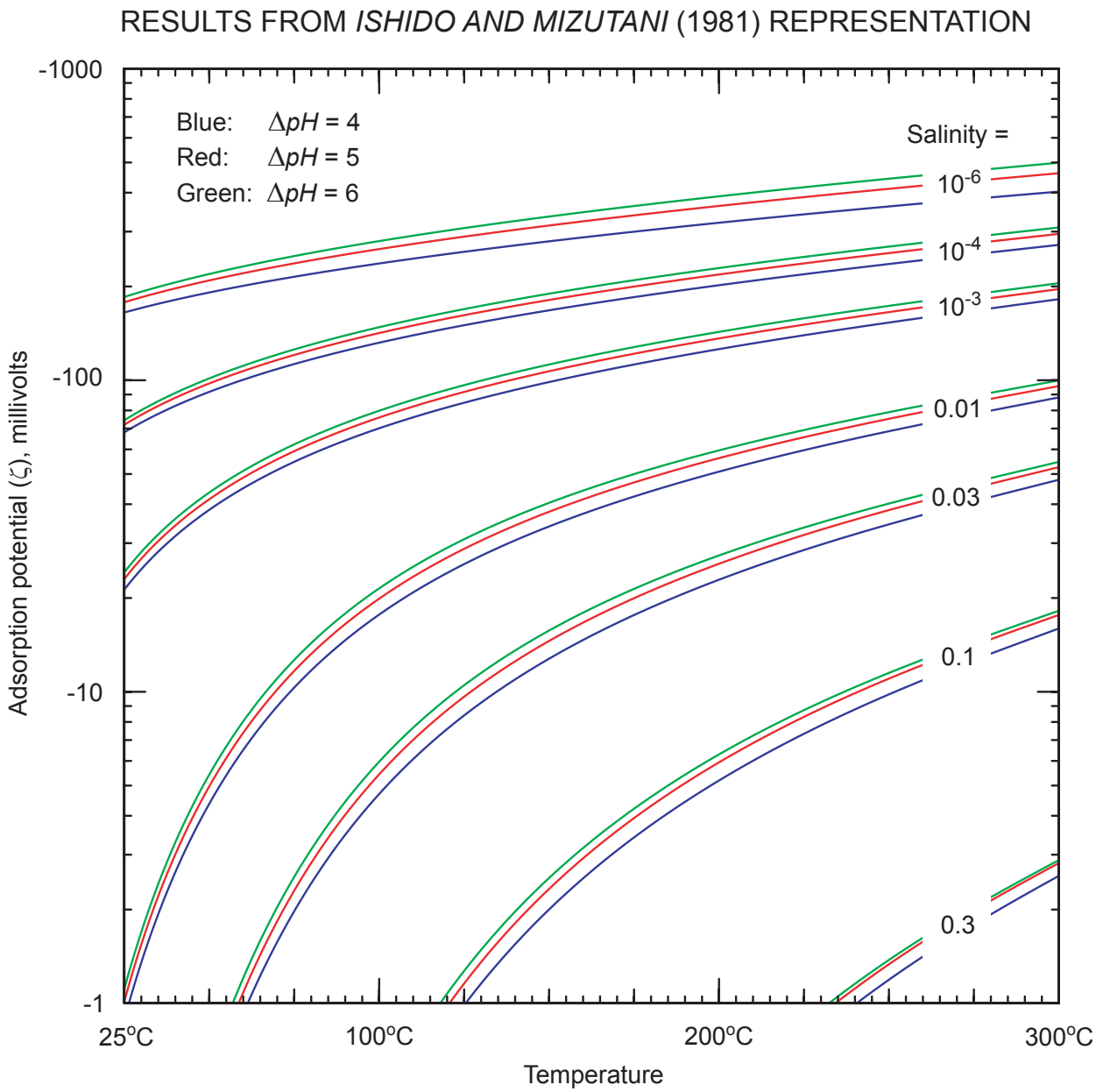

Figure 3-3: Adsorption potential or "zeta-potential" ζ as a function of temperature for brine salinities ranging from 10^{-6} to 0.3 according to the model of *Ishido and Mizutani* (1981) as adopted for use in SPFRAC. The "ΔpH" parameter may be regarded as a data-fitting variable that may be used to reproduce laboratory test results on core samples. Note that ζ is negative, and that the magnitude of ζ increases with increasing temperature and decreases with increasing salinity.

In this case, instead of invoking the Ishido/Mizutani formulation to obtain ζ as a function of temperature and salinity, the following algebraic form is used:

$$\zeta = (\boldsymbol{K_o} + \boldsymbol{K_T} \times T - \boldsymbol{K_S} \times S) \times \log_{10} S \qquad [3.25]$$

where ζ is in volts, T is temperature (°C) and S is brine salinity. These coefficients may be chosen so as to fit laboratory test data. Then, as above, file *"intortuo.fil"* is used to assign the distribution of tortuosity Θ, and the streaming potential coefficient ξ for each block is calculated using equation [3.24] above. Again, input files *"inzetapo.fil"* and *"instrmpc.fil"* are redundant and will be ignored if present.

3.13.3. Specifying Zeta-Potential. In the case, input file *"instrmdl.fil"* will contain only a single line:

Line 1: **ZETA POTENTIAL** *(case-insensitive character string)*

Using this option, input file *"inzetapo.fil"* must also be prepared by the user to provide the block-by-block spatial distribution of the adsorption potential ζ in volts, using the CSIP input file syntax described in Section 3.6. The user should keep in mind that ζ is ordinarily negative in sign. The tortuosity (Θ) distribution will also be required – again, this is accomplished using input file *"intortuo.fil"* as in the previous cases. Then, equation [3.24] is used to assign values of the streaming potential coefficient ξ to each grid block. Input file *"instrmpc.fil",* if present, will be ignored.

3.13.4. Specifying Streaming Potential Coefficient. The final case also involves a one-line *"instrmdl.fil"* input file:

Line 1: **STREAMING POTENTIAL COEFFICIENT** *(case-insensitive character string)*

In this case, neither file *"inzetapo.fil"* nor file *"intortuo.fil"* is needed. The user prepares an input file named *"instrmpc.fil"* according to the CSIP syntax (Section 3.6) to specify the spatial distribution of the streaming potential coefficient ξ itself, in volts per pascal. Again, recall that ξ is ordinarily negative in sign.

3.14. Electrical Conductivity: Files *"incndmdl.fil"*, *"incndrok.fil"* and *"incndsrf.fil"*

SPFRAC represents the local electrical conductivity (σ) as the sum of the "volumetric conductivity" σ_v and the "surface conductivity" σ_s:

$$\sigma = \sigma_v + \sigma_s \qquad [3.26]$$

and the distribution of "surface conductivity" σ_s is provided using CSIP syntax (Section 3.6) by optional input file *"incndsrf.fil"* in siemens/meter. If *"incndsrf.fil"* is absent, $\sigma_s = 0$ everywhere.

The "volumetric conductivity" σ_v depends on the separate electrical conductivities of the fluid (σ_w) and of the solid rock material (σ_r) and also on porosity φ according to some "mixing rule":

$$\sigma_v = \sigma_v (\varphi, \sigma_w, \sigma_r) \qquad [3.27]$$

The distribution of porosity φ is specified by input file *"inporost.fil"* (see Section 3.10 above) and the liquid phase conductivity σ_w is determined by the local temperature T and salinity S (see Figure 2.4, Section 2) which are in turn established by input files *"intemper.fil"* and *"insaltfr.fil"*

(Section 3.9 above). The spatial distribution of solid rock electrical conductivity σ_r remains to be determined; σ_r is specified in siemens per meter using input file *"incndrok.fil"* with CSIP input syntax (Section 3.6).

Six different electrical conductivity "mixing rules" (*i.e.,* mathematical representations for Equation [3.27]) for combining "fluid conductivity" σ_w with "rock conductivity" σ_r to create "volumetric conductivity" σ_v are available in SPFRAC. The user makes his choice among these six models using input file *"incndmdl.fil"*. The models are discussed in the following subsections.

3.14.1. Parallel Model. The "parallel model" is specified using a one-line *"incndmdl.fil"* input file which contains a single case-insensitive character string:

Line 1: **PARALLEL** *(case-insensitive character string)*

The "parallel model" mixes the conductivities in proportion to volume as follows:

$$\sigma_{v\text{-}parallel} = \varphi \times \sigma_w + (1 - \varphi) \times \sigma_r \qquad [3.28]$$

3.14.2. Series Model. This case will again entail a one-line *"incndmdl.fil"* input file containing a character string:

Line 1: **SERIES** *(case-insensitive character string)*

The "series model" mixes the conductivities using a harmonic mean:

$$\sigma_{v\text{-}series} = [\sigma_r \times \sigma_w] \; / \; [\varphi \times \sigma_r + (1 - \varphi) \times \sigma_w] \qquad [3.29]$$

and will produce smaller σ_v values than the "parallel" model.

3.14.3. Budiansky-Law Model. This approach is based on the mathematical analogy between electrical and thermal conductivity, and uses a formulation originally developed by *Budiansky* (1970). The single line in *"incndmdl.fil*" reads as follows for this case:

Line 1: **BUDIANSKY** *(case-insensitive character string)*

The resulting Budiansky model for σ_v is:

$$\sigma_{v\text{-}budiansky} = \text{smaller of } [\sigma_{v\text{-}parallel}, \text{ larger of } (\sigma_{v\text{-}series} \, , \sigma_B) \,] \qquad [3.30]$$

where σ_B is the real solution of:

$$2\sigma_B^{\,2} + \sigma_B \times [\sigma_w \, (1 - 3\varphi) + \sigma_r \, (3\varphi - 2)] - [\, \sigma_w \, \sigma_r \,] = 0 \qquad [3.31]$$

3.14.4. "No-Mixing" Model. This option may be employed if the user desires to simply specify the spatial distribution of σ_v directly, without using a mixing model. File *"incndmdl.fil"* will contain a single input line:

Line 1: **NOMIX** *(case-insensitive character string)*

and the effect will be simply to set:

$$\sigma_{v\text{-}nomix} = \sigma_r \qquad [3.32]$$

everywhere. In this case, the numerical values provided in input file *"incndrok.fil"* for σ_r will have a different physical significance than in the other cases.

3.14.5. Capillary-Tube Model. In this case, input file *"incndmdl.fil"* will consist of two lines:

Line 1: **CAPILLARY** *(case-insensitive character string)*

Line 2: $\boldsymbol{A_{cap}}$

The mixing model for σ_v is:

$$\sigma_{v\text{-}capillary} = \sigma_r + \boldsymbol{A_{cap}} \times \sigma_w \qquad [3.33]$$

It is required that $0 \leq \boldsymbol{A_{cap}} \leq 1$, and ordinarily $\boldsymbol{A_{cap}} << 1$.

3.14.6. Archie-Law Model. This option also involves a two-line *"incndmdl.fil"* file:

Line 1: **ARCHIE** *(case-insensitive character string)*

Line 2: $\boldsymbol{A_{archie}}$

The "Archie's Law" rule is as follows:

$$\sigma_{v\text{-}archie} = \boldsymbol{A_{archie}} \times \varphi^2 \times \sigma_w \qquad [3.34]$$

Note that $\boldsymbol{A_{archie}}$ must be positive and that the Archie's Law estimate for σ_v is independent of σ_r.

3.15. Conductivity Anisotropy: Files *"incndavh.fil"* and *"incndaxy.fil"*

Provision has been made in SPFRAC for the distribution of electrical conductivity to be anisotropic, in a manner similar to that for matrix permeability (see Section 3.11 above). The formulation is as follows:

$$\sigma_x = \sigma \times 6\,\beta_c / [(1 + \beta_c) \times (2 + \alpha_c)] \qquad [3.35]$$

$$\sigma_y = \sigma \times 6 / [(1 + \beta_c) \times (2 + \alpha_c)] \qquad [3.36]$$

$$\sigma_z = \sigma \times 3\,\alpha_c / (2 + \alpha_c) \qquad [3.37]$$

This formulation has the following properties:

- If $\alpha_c = 1$ and $\beta_c = 1$, then $\sigma_x = \sigma_y = \sigma_z = \sigma$ (isotropic case).
- If $\alpha_c \neq 1$ and $\beta_c = 1$, then $(\sigma_x / \sigma_z) = (\sigma_y / \sigma_z) = (1 / \alpha_c)$ and horizontal conductivity ≠ vertical conductivity.
- If $\alpha_c = 1$ and $\beta_c \neq 1$, then $\sigma_z = \sigma = (\sigma_x + \sigma_y)/2$ but $(\sigma_x / \sigma_y) = \beta_c$ and horizontal conductivity depends on direction.

As in the case of rock matrix permeability, the "default" values for the anisotropy parameters α_c and β_c are $\alpha_c = \beta_c = 1$, so if an isotropic treatment is desired input files *"incndavh.fil"* and *"incndaxy.fil"* are redundant and may be eliminated. Otherwise, file *"incndavh.fil"* uses the CSIP (Section 3.6) to specify the spatial distribution of α_c, and the data in *"incndaxy.fil"* uses the same syntax to specify β_c. If either parameter is unity everywhere, the pertinent input file may be deleted. Recommended ranges of both α_c and β_c are from 0.1 to 10. Input values of α_c or β_c that are < 0.01 or > 100 will be treated as errors.

3.16. Conductive Metallic Well Casings: File *"incasing.fil"*

As discussed previously in Section 2.8, provision has been made in SPFRAC for incorporating the effects of buried vertical cylindrical metallic conductors (well casings or casing sections) upon the distribution of electrical potential. These "casings" (if present) are specified by input file *"incasing.fil"*. An example may be found in Appendix A, Figure A-7.

Input file *"incasing.fil"* will consist of a series of from one to twenty "Clauses", each of which describes the geometry of a particular electrically-continuous conductive "casing". The limitation to a maximum of twenty such conductors may be increased, if needed, by recompiling the program. The *"incasing.fil"* file structure is:

CLAUSE DESCRIBING FIRST CONDUCTOR
CLAUSE DESCRIBING SECOND CONDUCTOR
↓
CLAUSE DESCRIBING LAST CONDUCTOR
end-of-file

Each "Clause" is to be structured as follows. Two forms are permissible, which differ only in whether the data are supplied in the "grid" or the "world" coordinate system:

Line 1:	**GRID** *(case-insensitive character string)*			
Line 2:	x_1	y_1	z_1	d_1
Line 3:	x_2	y_2	z_2	d_2
		↓		
Line N:	x_{N-1}	y_{N-1}	z_{N-1}	d_{N-1}
Line N+1:	x_N	y_N	z_N	
		or		
Line 1:	**WORLD** *(case-insensitive character string)*			
Line 2:	X_1	Y_1	Z_1	d_1
Line 3:	X_2	Y_2	Z_2	d_2
		↓		
Line N:	X_{N-1}	Y_{N-1}	Z_{N-1}	d_{N-1}
Line N+1:	X_N	Y_N	Z_N	

and both types of "Clause" (*"world"* and *"grid"*) may be freely intermixed within the same *"incasing.fil"* file. The upper bound on the number of lines in each clause is 1002. In both cases, Line 2 specifies the spatial location of the uppermost end of the casing pipe (x_1, y_1, z_1 or X_1, Y_1, Z_1). The last line (Line N+1) specifies the location of the deepest end of the pipe (x_N, y_N, z_N or X_N, Y_N, Z_N). These locations are all provided in meters. The lines must be entered in order of increasing depth (or decreasing elevation); $z_{n+1} < z_n$ or $Z_{n+1} < Z_n$. It is strongly recommended (but not absolutely required) that the conductors be considered to be vertical (*i.e.*, $x_{n+1} = x_n$, $y_{n+1} = y_n$ or $X_{n+1} = X_n$, $Y_{n+1} = Y_n$).

Note that the last line (Line N+1) contains only three numerical entries whereas lines $n = 2$ through N contain four. This is required; SPFRAC identifies the bottom of the assembly by the absence of a fourth entry in the last line. The fourth entry in the other lines provides the vertical distribution of "pipe diameter" ($= 2 \times r_{case}$), also in meters. The pipe diameter is taken to be uniform and equal to d_n for elevations between z_n and z_{n+1} (or Z_n and Z_{n+1}).

3.17. Injection Well: Files *"ininjwel.fil"* and *"ininjhis.fil"*

These files describe the injection well used to stimulate the reservoir and specify the injection time-history. File *"ininjwel.fil"* describes the geometry of the injection region, and consists of two lines (either "grid" coordinates or "world" coordinates may be used):

Line 1: **GRID** *(case-insensitive character string)*
Line 2: x_{inj} y_{inj} z_{top} z_{bot} s_{well} d_{well}

or

Line 1: **WORLD** *(case-insensitive character string)*
Line 2: X_{inj} Y_{inj} Z_{top} Z_{bot} s_{well} d_{well}

The spatial dimensions x_{inj}, y_{inj}, z_{top}, z_{bot} (or X_{inj}, Y_{inj}, Z_{top}, Z_{bot}) and d_{well} are to be provided in meters – s_{well} is the injection well's "skin factor" and is dimensionless. It is necessary that $Z_{top} > Z_{bot}$ (or $z_{top} > z_{bot}$). The "injection interval" (the pressurized "open" interval in the injection well through which injected fluid may enter the formation) is a vertical circular cylinder of diameter d_{well} meters (radius $r_{well} = d_{well}/2$) and the vertical axis of the cylinder extends between the point (x_{inj}, y_{inj}, z_{top}) and the point (x_{inj}, y_{inj}, z_{bot}), or between (X_{inj}, Y_{inj}, Z_{top}) and (X_{inj}, Y_{inj}, Z_{bot}). It is of course essential that these two points both lie within the grid volume, and desirable that they be centrally located.

File *"ininjhis.fil"* prescribes the time-history of fluid injection (either by prescribing pressure or volumetric flow rate, or a combination). An example will be found in Figure A-8, Appendix A. The first three lines designate the units in which data will be supplied (times in hours or in seconds; pressures in pascals or MPa; flow rates in liters/second, m^3/hour or m^3/second) using case-insensitive character strings:

Line 1: **HOURS** or **SECONDS**

Line 2: **MEGAPASCALS** or **PASCALS**

Line 3: **LITERS PER SECOND** or
CUBIC METERS PER HOUR or
CUBIC METERS PER SECOND

After the first three lines, at least one and no more than 1000 additional lines are to be provided which provide the injection history. There are four permissible forms for these lines, and the various forms may be intermixed within the same *"ininjhis.fil"* input file. The forms are:

Form 1: "**P**" t_{end} p_{begin} p_{end}
Form 2: "**P**" t_{end} p_{end}
Form 3: "**R**" t_{end} R_{begin} R_{end}
Form 4: "**R**" t_{end} R_{end}

Each line begins with a single alphabetic character (either *"p"* or *"r"*, case-insensitive), followed by either two or three numerical values. Values supplied for t_{end} will be in either seconds or hours, according to the contents of Line 1. Values for p_{begin} and p_{end} are to be provided in either pascals or MPa (according to Line 2) and values for flow rate (R_{begin} and R_{end})

will be supplied in liters/second, m^3/hour or m^3/second according to Line 3. The various lines must be supplied in order of increasing $\boldsymbol{t_{end}}$ and all $\boldsymbol{t_{end}}$ values must be positive, so:

$$0 < \boldsymbol{t_{end}}(1) < \boldsymbol{t_{end}}(2) < \boldsymbol{t_{end}}(3) < \ldots < \boldsymbol{t_{end}}(\text{last})$$

The $n^{\underline{th}}$ of these lines specifies the fluid injection rate (or the overpressure within the injection well) over a time interval extending from $\boldsymbol{t_{end}}(n–1)$ to $\boldsymbol{t_{end}}(n)$ – the first line describes the period $0 \le t \le \boldsymbol{t_{end}}(1)$. The first line in the sequence must be of either *"Form 1"* or *"Form 3"*. A *"Form 2"* line may only be used immediately following a *"Form 1"* line or another *"Form 2"* line. Similarly, a *"Form 4"* line may only appear immediately after a *"Form 3"* line or another *"Form 4"* line. If line n is of *"Form 1"*, the overpressure within the well between $t = \boldsymbol{t_{end}}(n–1)$ and $t = \boldsymbol{t_{end}}(n)$ will be given by:

$$p_{well}(t) = \boldsymbol{p_{begin}}(n) + [\boldsymbol{p_{end}}(n) - \boldsymbol{p_{begin}}(n)] \times [t - \boldsymbol{t_{end}}(n–1)] / [\boldsymbol{t_{end}}(n) - \boldsymbol{t_{end}}(n–1)] \qquad [3.38]$$

whereas the pressure variation specified by a *"Form 2"* line is:

$$p_{well}(t) = \boldsymbol{p_{end}}(n–1) + [\boldsymbol{p_{end}}(n) - \boldsymbol{p_{end}}(n–1)] \times [t - \boldsymbol{t_{end}}(n–1)] / [\boldsymbol{t_{end}}(n) - \boldsymbol{t_{end}}(n–1)] \qquad [3.39]$$

Note that if two *"Form 1"* lines (n and n+1) appear in sequence, the well pressure will change discontinuously at $t = \boldsymbol{t_{end}}(n)$ from $\boldsymbol{p_{end}}(n)$ to $\boldsymbol{p_{begin}}(n+1)$. Similarly, a *"Form 3"* line will specify the volumetric injection rate as:

$$R_{well}(t) = \boldsymbol{R_{begin}}(n) + [\boldsymbol{R_{end}}(n) - \boldsymbol{R_{begin}}(n)] \times [t - \boldsymbol{t_{end}}(n–1)] / [\boldsymbol{t_{end}}(n) - \boldsymbol{t_{end}}(n–1)] \qquad [3.40]$$

and a *"Form 4"* line will impose:

$$R_{well}(t) = \boldsymbol{R_{end}}(n–1) + [\boldsymbol{R_{end}}(n) - \boldsymbol{R_{end}}(n–1)] \times [t - \boldsymbol{t_{end}}(n–1)] / [\boldsymbol{t_{end}}(n) - \boldsymbol{t_{end}}(n–1)] \qquad [3.41]$$

3.18. Pressure and Potential Sensors: Files *"inpsensr.fil"* and *"invsensr.fil"*

"Sensors" for pressure and/or electrical potential may be specified by the user at particular spatial locations within the computational grid volume. After each recalculation of the electrical potential distribution (at intervals of $\boldsymbol{t_{max}} / \boldsymbol{N_{recr}}$; see discussion in Section 3.8 above), a value of electrical potential (or of fluid overpressure) will be interpolated among the nearest principal grid-block values and recorded on an output file. These temporal records of the potential (or pressure) at these specific locations may then be compared with measured histories from the field.

"Pressure Sensors" and "Potential Sensors" are specified using optional input files *"inpsensr.fil"* and *"invsensr.fil"* respectively. The input syntax for both files is the same, and is as follows:

Line 1: **GRID** *(case-insensitive character string)*
Line 2: $\boldsymbol{x_1}$ $\boldsymbol{y_1}$ $\boldsymbol{z_1}$
Line 3: $\boldsymbol{x_2}$ $\boldsymbol{y_2}$ $\boldsymbol{z_2}$
etc.
end-of-file

or

Line 1: **WORLD** *(case-insensitive character string)*
Line 2: X_1 Y_1 Z_1
Line 3: X_2 Y_2 Z_2
etc.
end-of-file

The (x_n, y_n, z_n) or (X_n, Y_n, Z_n) coordinates specify the spatial location of the n^{th} sensor. Up to 300 potential sensors (and 300 pressure sensors) may be identified for each simulator run. These limits may be increased, if needed, by recompiling the SPFRAC program.

4. *SPFRAC* SIMULATOR OUTPUT TEXT FILES

Each execution of the SPFRAC simulator will produce numerous ASCII ("text") output files reporting various aspects of the run. All of these files have names of the form "*rp******.fil"*, and all are human-readable. Some of them may also be used as input to the various graphical postprocessors. Examples of several of these files are provided in Appendix B.

At the beginning of each SPFRAC simulator run, the date and time of day corresponding to run initiation are determined, and this unique "datestamp" is then written on each of the output files produced by that particular run, to permit output files from different runs to be distinguished. In the "header" area of each output file, a text line similar to the following:

```
Output data file from the SPFRAC calculation initiated Tue Aug 26 14:21:05 2008.
```

will be written for this purpose. As noted above in Section 3.1, it is strongly recommended that a different directory be used for each execution of the simulator. If residual output files remain in the local directory from previous SPFRAC executions, ***they may be over-written by the current run!***

The output files generated by the SPFRAC simulator may be subdivided into three broad categories: *(a)* output files reporting on the general progress of the simulation from a computational point of view, *(b)* output files that acknowledge and elaborate upon the simulator's interpretation of the user's problem specifications, and *(c)* output files that report computed results for electrical potentials, pressures, flow rates, *etc.* and may be used subsequently as input to the graphical postprocessors. The following discussion will present the various output files in the above order.

4.1. Simulator Progress Reports

Three output files (*"rphistry.fil"*, *"rpinecho.fil"* and *"rperform.fil"*) fall into this category. Output file *"rphistry.fil"* will ordinarily be the first output file examined by the user, particularly if the run is terminated prematurely. An example may be found in Appendix B, Figure B-1. The file will contain a "chronology" of the run, briefly describing the input files encountered, the output files created, and similar matters. "Warnings" will be issued about questionable input specifications on the *"rphistry.fil"* file, and an explanation will be provided if an "error exit" occurs. SPFRAC does a considerable amount of "error checking" during the input phase, although the user is warned that these checking procedures are neither exhaustive nor foolproof.

Output file *"rpinecho.fil"* will contain an "echo-print" of all of the SPFRAC simulator input files found in the local directory at the time the calculation took place. Since this file will also contain the "datestamp" discussed above, this file provides an unambiguous record of the input specifications that resulted in the various output files that share the same "datestamp".

Finally, output file *"rperform.fil"* will ordinarily be of little interest to the practical user. It provides a chronological report on the number of recalculations of the pressure distribution (using equation [2.15]) and of the electrical potential distribution (equation [2.16]) carried out up to that point, and on the number of "iterations" required for each of the different aspects of the simulation.

4.2. Problem Specification Reports

As many as 25 files falling into this category may appear in the local directory. Most of them consist of block-by-block reports of the distribution of scalar quantities such as porosity, permeability, conductivity *etc.* as interpreted from the various *"in******.fil"* problem specification files discussed in Section 3. In this section, these files are described in essentially the same order as the corresponding input files were discussed in Section 3; in many cases, the file names are similar to those of the pertinent input files.

File *"rpgrgeom.fil"* displays the spatial orientation and grid spacing information provided by input files *"ingridor.fil"*, *"ingridsx.fil"*, *"ingridsy.fil"* and *"ingridsz.fil"* (see Section 3.7). The location of each grid-block center in "world" coordinates, the vertical thickness of the block, and its total volume are tabulated in the file. File *"rptwophs.fil"* lists all blocks flagged as "two-phase" by the input data found in file *"intwophs.fil"* (Section 3.7). If there are no two-phase blocks, this output file will not be created. File *"rptimstp.fil"* simply reports the information that was supplied by input file *"intimstp.fil"* (see Section 3.8).

File *"rptemper.fil"* provides a tabulation of the temperature T in each grid block as obtained from the data supplied by input file *"intemper.fil"* (Section 3.9). File *"rpsaltfr.fil"* similarly lists the block-by-block brine salinity S as specified by input file *"insaltfr.fil"* (Section 3.9). File *"rpflprop.fil"* provides a block-by-block tabulation of fluid density ρ, fluid dynamic viscosity μ, fluid compressibility C_w, fluid electrical conductivity σ_w and fluid dielectric permittivity ε as calculated using the SPFRAC internal constitutive representations (Section 2.9) based on the distributions of temperature and salinity found on input files *"intemper.fil"* and *"insaltfr.fil"* (Section 3.9).

File *"rpporost.fil"* tabulates the rock porosity (φ) specified for each grid block by input file *"inporost.fil"* (Section 3.10). File *"rpcomprs.fil"* similarly tabulates the block-by-block rock compressibility (C_r) specified by input file *"incomprs.fil"* (Section 3.10) and also lists the fluid compressibility (C_w) and the resulting total compressibility (C) for each grid block.

File *"rppermis.fil"* contains a block-by-block tabulation of the isotropic rock matrix permeability k_m as specified by input file *"inpermis.fil"* (Section 3.11). If permeability anisotropy is present, file *"rpperman.fil"* will list the permeability components k_{mx}, k_{my} and k_{mz} for each block and files *"rpprmavh.fil"* and *"rpprmaxy.fil"* will list block-by-block values of the anisotropy parameters α_p and β_p respectively, as obtained from the specifications that were found in files *"inprmavh.fil"* and *"inprmaxy.fil"*.

File *"rpfractr.fil"* reports the properties of each "fracture type" found in input file *"infrcmdl.fil"* and then goes on to report the description of each of the triangular "fracture elements" specified by input file *"infrcgeo.fil"* (Section 3.12). Then, a list of all grid blocks containing nonzero fracture surface area is prepared (along with the surface area within the block associated with each "fracture type"). Finally, a summary table is presented for each "fracture type", listing the total surface area and the number of grid blocks involved.

File *"rpstrzta.fil"* lists, for each block in the computational grid, the values of the adsorption potential (ζ) and the streaming potential coefficient (ξ) arising from the input specifications

discussed in Section 3.13. File *"rptortuo.fil"*:provides a block-by-block list of tortuosity (Θ) values as obtained from input file *"intortuo.fil"*. If input file *"inzetapo.fil"* was used to specify the distribution of adsorption potential ζ (see Section 3.13.3), output file *"rpzetapo.fil"* will provide the corresponding block-by-block output. Similarly, if the streaming potential coefficient ξ itself was supplied using input file *"instrmpc.fil"* as outlined in Section 3.13.4, the corresponding output will be found in file *"rpstrmpc.fil"*.

File *"rpcndsrf.fil"* provides a block-by-block tabulation of "surface conductivity" (σ_s) based on instructions found in file *"incndsrf.fil"* (if present), and file *"rpcndrok.fil"* provides a similar list of "rock conductivity" values (σ_r) obtained from file *"incndrok.fil"* (see discussion in Sections 3.14 and 3.15). File *"rpresist.fil"* summarizes the overall electrical conductivity distribution computed based on file *"incndmdl.fil"* including the effects of any anisotropy specified by files *"incndavh.fil"* and/or *"incndaxy.fil"*; this block-by-block tabulation lists the *x*-, *y*- and *z*-components of electrical resistivity (the reciprocal of conductivity), in ohm-meters.

File *"rpcasing.fil"* acknowledges the well-casing information that was supplied by input file *"incasing.fil"* (Section 3.16). File *"rpinjwel.fil"* similarly acknowledges the injection geometry information found in input file *"ininjwel.fil"* (Section 3.17) and also identifies the grid blocks into which fluid will be injected. File *"rpinjhis.fil"* summarizes the injection pressure/flowrate history that was prescribed by input file *"ininjhis.fil"* (Section 3.17). Finally, files *"rppsensr.fil"* and *"rpvsensr.fil"* provide lists of the locations of the "pressure sensors" and "potential sensors" respectively (in both "grid" and "world" coordinates) that were specified by input files *"inpsensr.fil"* and *"invsensr.fil"* (see Section 3.18).

4.3. Reports of Computed Results

Output file *"rpwellhs.fil"* contains a tabulated record of the performance of the injection well. At regular intervals ($\boldsymbol{t_{max}}$ /$\boldsymbol{N_{recr}}$; see Section 3.8), SPFRAC writes a line on the file which contains *(1)* the elapsed time t, in hours, *(2)* the instantaneous injection well overpressure p_{well}, in megapascals, *(3)* the instantaneous well injection rate R_{well}, expressed in liters per second, and *(4)* the cumulative volume of fluid injected up to time t, in cubic meters. Figure B-3 (in Appendix B) provides an example of file *"rpwellhs.fil"*. In addition, at the same times (t = an integer multiple of $\boldsymbol{t_{max}}$ /$\boldsymbol{N_{recr}}$), a line is written on each file present with a name of the form *"rpspIIII.fil"*, *"rpvpIIII.fil"* or *"rpwvIIII.fil"* (where *"IIII"* stands for a four-digit integer: *"IIII"* = *"0001"*, *"0002"*, *"0003"*, …, *"9999"*).

The *"rpsp****.fil"* output files report the pressure history recorded by the "pressure sensors" discussed in Section 3.18 and specified by input file *"inpsensr.fil"*; for example, output file *"rpsp0003.fil"* contains the pressure record for pressure sensor number 3 (of which the location is provided on line number 4 of file *"inpsensr.fil"*). The output file header lists the sensor location (in both the "grid" and "world" coordinate systems), and then, for each pertinent time, a line that contains the value of t (both in hours and in seconds) and the value of the overpressure p at the sensor location (both in kilopascals and in pascals).

Similarly, the *"rpsv****.fil"* output files report the voltage history recorded by the "electrical potential sensors" discussed in Section 3.18 and specified by input file *"invsensr.fil"*. The output file again lists the sensor location followed by a series of lines contain the values of t

(both in hours and in seconds) and the value of the local electrical potential V at the sensor location (both in millivolts and in volts). A sample *"rpsv****.fil"* file is shown in Figure B-5 of Appendix B.

The *"rpwv****.fil"* output files are very similar to the *"rpsv****.fil"* files, except that they are used to report the electrical potential histories of the conductive "well casings" specified by input file *"incasing.fil"* (see Section 3.16). File *"rpwv0001.fil"* provides the history for the first casing string, file *"rpwv0002.fil"* is for the second casing section, and so on. Figure B-4 in Appendix B provides an example of an *"rpwv****.fil"* output file.

Finally, bulky output files with names of the form *"rpgdIIII.fil"* (with *IIII* again representing a four-digit integer) are written every "dump time"; that is, at time intervals given by $\Delta t_{dump} = \boldsymbol{N_{dump}} \times \boldsymbol{t_{max}} / \boldsymbol{N_{recr}}$ (see Section 3.8). The first such "dump" record is written on output file *"rpgd0001.fil"*, the second on file *"rpgd0002.fil"*, and so forth. The "header" area of each *"rpgd****.fil"* file contains *(1)* the total number of hydrodynamic time-steps completed so far, *(2)* the elapsed time t, in both hours and seconds, *(3)* the minimum value of electrical potential V in the grid, *(4)* the maximum electrical potential value in the grid, *(5)* the minimum value of fluid overpressure p present, and *(6)* the maximum overpressure value. Then, for each grid block present, the location (in "world" coordinates; meters East, meters North and meters RSL) of the grid block center is provided, along with the corresponding value of the local instantaneous electrical potential V_{ijk} (millivolts) and of the fluid overpressure p_{ijk} (kilopascals). Figure B-6 in Appendix B provides a partial listing of an *"rpgd****.fil"* output "dump" file.

5. *SPFRAC* GRAPHICAL POSTPROCESSORS

Auxiliary programs have been developed to process several of the SPFRAC simulator output files, to compare these computed results with field information and to present the calculated results (and the comparisons with measured data) in graphical form. Output from these programs takes the form of graphics files with names of the form *"pl******.igf"*; these output files are written in the JPLOT graphics language (*Pritchett and Alexander,* 1986), and the JPLOT program (available separately) may be used to convert them to images on the screen and/or to create digital graphical representations suitable for inclusion in documents or slideshow presentations. Six graphics postprocessors are available, as follows:

Executable file name	**Makes plots of:**	**Computer-generated input files**	**User-created input files**	**Graphical output files**
spfpltin.exe	injection pressure, volumetric flow rate, cumulative injected volume as functions of time.	*rpwellhs.fil*	*dtinjprs.fil* *dtinjflo.fil* *dtinjcmi.fil*	*plinjprs.igf* *plinjflo.igf* *plinjcmi.igf*
spfpltsp.exe	pressure at pressure sensor locations as functions of time.	*rpspIIII.fil**	*dtspIIII.fil**	*plspIIII.igf**
spfpltsv.exe	voltage at potential sensor locations as functions of time.	*rpsvIIII.fil**	*dtsvIIII.fil**	*plsvIIII.igf**
spfpltwv.exe	voltage on metallic well casings as functions of time.	*rpwvIIII.fil**	*dtwvIIII.fil**	*plwvIIII.igf**
spfpltcp.exe†	pressure contours at specific times in user-specified planes.	*rpgdIIII.fil**	*incontpl.fil* *inconttm.fil* *incontcr.fil* *incontsr.fil* *incontlb.fil*	*plpcIIII.igf**
spfpltcv.exe†	voltage contours at specific times in user-specified planes.	*rpgdIIII.fil**	*incontpl.fil* *inconttm.fil* *incontcr.fil* *incontsr.fil* *incontlb.fil*	*plvcIIII.igf**

Notes: * *"IIII"* stands for a four-digit integer: *"0001", "0002", "0003", etc.*

† These programs also access simulator input files *"ingridor.fil", "ingridsx.fil", "ingridsy.fil"* and *"ingridsz.fil"* (see Section 3.7).

This section provides instructions to guide the user in the preparation of the pertinent input files (the *"dt******.fil"* files for the first four programs above and the *"incont**.fil"* files for the two contour-plotting programs).

5.1. Plotting Time-Histories

The first four programs in the above list (*"spfpltin.exe"*, *"spfpltsp.exe"*, *"spfpltsv.exe"* and *"spfpltwv.exe"*) all create plots of specific scalar quantities as functions of time. Examples may be found in Appendix C, Figures C-3 to C-5. Executing *"spfpltin.exe"* creates three images (on output graphics files *"plinjprs.igf"*, *"plinjflo.igf"* and *"plinjcmi.igf"*) showing *(a)* injection pressure *vs.* time, *(b)* volumetric injection rate *vs.* time, and *(c)* cumulative volume injected *vs.* time: see Figures C-3(a) – C-3(c). When *"spfpltsp.exe"* is executed, it first searches the local directory for files with names of the form *"rpspIIII.fil"*. For every such file that is found, it constructs a plot of pressure as a function of time on output file *"plspIIII.igf"*, which depicts the pressure history for pressure sensor number *"IIII"*. If there are no *"rpspIIII.fil"* files in the local directory, *"spfpltsp.exe"* will self-terminate immediately (with no damage done). Likewise, *"spfpltsv.exe"* seeks *"rpsvIIII.fil"* files and, if any are found, creates *"plsvIIII.igf"* plots showing sensor voltages as functions of time, and *"spfpltwv.exe"* also creates *"plwvIIII.igf"* images for any *"rpwvIIII.fil"* data files that are found (well casing voltages), except that plots are not created for "grounded" well casings (for which the electrical potential is always zero).

5.2. Representing Field Measurements

The *"spfpltin.exe"*, *"spfpltsp.exe"*, *"spfpltsv.exe"* and *"spfpltwv.exe"* programs all provide for the superposition of "measured data" on the plots for comparison with the calculated results. These "field data" are provided by the user by creating the *"dt******.fil"* input files. Examples of these files are to be found in Appendix A, Figures A-11 to A-13.

The *"dtinjprs.fil"*, *"dtinjflo.fil"* and *"dtinjcmi.fil"* input files provide *"spfpltin.exe"* with measured data for inclusion in plotting files *"plinjprs.igf"* (injection pressure *vs.* time), *"plinjflo.igf"* (injection volumetric flow rate *vs.* time) and *"plinjcmi.igf"* (cumulative volume injected *vs.* time) respectively. Using *"spfpltsp.exe",* the *"dtspIIII.fil"* files provide measured pressure sensor data for comparison with computed results from the *"rpspIIII.fil"* and the plot instructions will appear on the *"plspIIII.igf",* files. The situation is similar for the electrical potential sensors (*"spfpltsv.exe"*, *"dtsvIIII.fil"*, *"rpsvIIII.fil"* and *"plsvIIII.igf"*) and for the well-casing potential histories (*"spfpltwv.exe"*, *"dtwvIIII.fil"*, *"rpwvIIII.fil"* and *"plwvIIII.igf"*).

It should be noted in passing that there is no requirement that *"dt******.fil"* files be available for all (or any) of these plotting applications. If the postprocessors fail to find these files in the local directory, the resulting plots will show just the computed results alone (see Appendix C, Figure C-3(b), for an example).

The input syntax for all of the various *"dt******.fil"* input files is the same, as follows:

Line 1: C_{It} C_{0t} C_{Iy} C_{0y}

Line 2: τ_1 η_1 $(\delta\eta_1)$

Line 3: τ_2 η_2 $(\delta\eta_2)$

↓

Line N+1: τ_N η_N $(\delta\eta_N)$

end-of-file

The first line in the file contains four numerical values, and the remaining lines contain either two or three values (two-value and three-value lines may be intermixed in the same file). The first line contains coefficients to convert the input values (the τ_n, η_n and $\delta\eta_n$ values) into appropriate units for use by the plotting program. In all cases, the first column of data (τ) in the remaining lines represents "time". The coefficients $\boldsymbol{C_{1t}}$ and $\boldsymbol{C_{0t}}$ should be assigned values such that:

$$\boldsymbol{C_{0t}} + \boldsymbol{C_{1t}} \times \boldsymbol{\tau_n} = (\text{time in hours})_n \qquad [5.1]$$

In input files *"dtinjprs.fil"* (injection well overpressure) and *"dtspIIII.fil"* (overpressure at sensor *IIII*), the remaining coefficients should be set such that

$$\boldsymbol{C_{0y}} + \boldsymbol{C_{1y}} \times \boldsymbol{\eta_n} = (\text{overpressure in MPa})_n \qquad [5.2]$$

In input file *"dtinjflo.fil"*, $\boldsymbol{C_{0y}}$ and $\boldsymbol{C_{1y}}$ must instead be set so that:

$$\boldsymbol{C_{0y}} + \boldsymbol{C_{1y}} \times \boldsymbol{\eta_n} = (\text{injection flow rate in liters per second})_n \qquad [5.3]$$

In input file *"dtinjcmi.fil"*, the $\boldsymbol{C_{0y}}$ and $\boldsymbol{C_{1y}}$ values must assure that:

$$\boldsymbol{C_{0y}} + \boldsymbol{C_{1y}} \times \boldsymbol{\eta_n} = (\text{cumulative injection in cubic meters})_n \qquad [5.4]$$

In files *"dtsvIIII.fil"* and *"dtwvIIII.fil"*, $\boldsymbol{C_{0y}}$ and $\boldsymbol{C_{1y}}$ must be set to yield:

$$\boldsymbol{C_{0y}} + \boldsymbol{C_{1y}} \times \boldsymbol{\eta_n} = (\text{electrical potential in millivolts})_n \qquad [5.5]$$

Lines 2 through (N+1) in each *"dt******.fil"* file consist of either two or three numerical entries. The first is the time-like parameter τ, the second is the parameter of interest (η – pressure, volumetric flow rate, volume, or voltage) and the third, if present, represents the uncertainty in the measured value for η:

$$\eta\,(t_n) = \boldsymbol{\eta_n} \pm \boldsymbol{\delta\eta_n}$$

In Appendix C, Figure C-3(a) is an example of a typical plot made showing $\boldsymbol{\delta\eta_n}$ values and Figure C-3(c) is an example without them. Figure C-3(b) illustrates plotting results if the pertinent *"dt******.fil"* file is absent altogether. No more than 1000 (τ_n , η_n) data pairs may be included in any particular *"dt******.fil"* input file, but there is no requirement that the various (τ_n , η_n) data lines be entered in any particular order.

5.3. Contour Plotting

The *"spfpltcp.exe"* and *"spfpltcv.exe"* programs create two-dimensional "snapshot" contour plots of fluid overpressure *(p)* and of electrical potential *(V)* respectively, based on the data found in the *"rpgdIIII.fil"* simulator output "dump" files. Examples may be found in Appendix C, Figure C-1 (from *"spfpltcp.exe"*) and Figure C-2 (from *"spfpltcv.exe"*). In addition to the "dump" files themselves, both of these programs may read as many as five user-prepared *"incont**.fil"* input files that specify the detailed character of the images to be created. Both of the contour plotting programs treat these data files similarly – the only difference between them is that one plots fluid overpressure, whereas the other plots electrical potential. Usually, the same *"incont**.fil"* input files will suffice for both programs. Of the *"incont**.fil"* input files, only *"incontpl.fil"* is required. The other four are optional and, if absent, "defaults" are pre-defined in the plotting programs. The following discussion illustrates how to construct each of the *"incont**.fil"* files to create images with the desired properties.

5.3.1. Plotting Plane: file *"incontpl.fil".* This file specifies the square two-dimensional region which the contour plot(s) will represent. If plots in multiple planes are desired, multiple runs of the plotting programs may be made using different versions of this file. A sample *"incontpl.fil"* file is to be found in Appendix A, Figure A-10. The file consists of a single line with six numerical entries:

$$\boldsymbol{L_{box}} \quad \boldsymbol{X_{box}} \quad \boldsymbol{Y_{box}} \quad \boldsymbol{Z_{box}} \quad \boldsymbol{\alpha_{box}} \quad \boldsymbol{\delta_{box}}$$
end-of-file

The plotting region is a square of dimensions $\boldsymbol{L_{box}}$ meters by $\boldsymbol{L_{box}}$ meters, centered on the point $\boldsymbol{X_{box}}$ meters East, $\boldsymbol{Y_{box}}$ meters North and $\boldsymbol{Z_{box}}$ meters RSL in the "world" coordinate system. The plane is rotated $\boldsymbol{\alpha_{box}}$ degrees eastward in azimuth relative to the north-south axis, and is tipped $\boldsymbol{\delta_{box}}$ degrees in declination. It is required that the point ($\boldsymbol{X_{box}}$, $\boldsymbol{Y_{box}}$, $\boldsymbol{Z_{box}}$) lie within the volume of the computational grid, that $0 \le \boldsymbol{\alpha_{box}} \le 180°$, that $0 \le \boldsymbol{\delta_{box}} \le 180°$, and that $\boldsymbol{L_{box}} > 0$. The upper left-hand corner of the image corresponds to the point (X_{UL}, Y_{UL}, Z_{UL}) where:

$$X_{UL} \text{ (meters East)} = \boldsymbol{X_{box}} + [\boldsymbol{L_{box}}/2] \times [\cos \boldsymbol{\alpha_{box}} \times \cos \boldsymbol{\delta_{box}} - \sin \boldsymbol{\alpha_{box}}] \quad [5.6]$$

$$Y_{UL} \text{ (meters North)} = \boldsymbol{Y_{box}} + [\boldsymbol{L_{box}}/2] \times [\sin \boldsymbol{\alpha_{box}} \times \cos \boldsymbol{\delta_{box}} - \cos \boldsymbol{\alpha_{box}}] \quad [5.7]$$

$$Z_{UL} \text{ (meters RSL)} = \boldsymbol{Z_{box}} + [\boldsymbol{L_{box}}/2] \times \sin \boldsymbol{\delta_{box}} \quad [5.8]$$

The lower left-hand corner is located at:

$$X_{LL} \text{ (meters East)} = \boldsymbol{X_{box}} - [\boldsymbol{L_{box}}/2] \times [\cos \boldsymbol{\alpha_{box}} \times \cos \boldsymbol{\delta_{box}} + \sin \boldsymbol{\alpha_{box}}] \quad [5.9]$$

$$Y_{LL} \text{ (meters North)} = \boldsymbol{Y_{box}} - [\boldsymbol{L_{box}}/2] \times [\sin \boldsymbol{\alpha_{box}} \times \cos \boldsymbol{\delta_{box}} + \cos \boldsymbol{\alpha_{box}}] \quad [5.10]$$

$$Z_{LL} \text{ (meters RSL)} = \boldsymbol{Z_{box}} - [\boldsymbol{L_{box}}/2] \times \sin \boldsymbol{\delta_{box}} \quad [5.11]$$

The upper right-hand corner corresponds to:

$$X_{UR} \text{ (meters East)} = \boldsymbol{X_{box}} + [\boldsymbol{L_{box}}/2] \times [\cos \boldsymbol{\alpha_{box}} \times \cos \boldsymbol{\delta_{box}} + \sin \boldsymbol{\alpha_{box}}] \quad [5.12]$$

$$Y_{UR} \text{ (meters North)} = \boldsymbol{Y_{box}} + [\boldsymbol{L_{box}}/2] \times [\sin \boldsymbol{\alpha_{box}} \times \cos \boldsymbol{\delta_{box}} + \cos \boldsymbol{\alpha_{box}}] \quad [5.13]$$

$$Z_{UR} \text{ (meters RSL)} = \boldsymbol{Z_{box}} + [\boldsymbol{L_{box}}/2] \times \sin \boldsymbol{\delta_{box}} \quad [5.14]$$

and the location of the lower right hand corner is:

$$X_{LR} \text{ (meters East)} = \boldsymbol{X_{box}} - [\boldsymbol{L_{box}}/2] \times [\cos \boldsymbol{\alpha_{box}} \times \cos \boldsymbol{\delta_{box}} - \sin \boldsymbol{\alpha_{box}}] \quad [5.15]$$

$$Y_{LR} \text{ (meters North)} = \boldsymbol{Y_{box}} - [\boldsymbol{L_{box}}/2] \times [\sin \boldsymbol{\alpha_{box}} \times \cos \boldsymbol{\delta_{box}} - \cos \boldsymbol{\alpha_{box}}] \quad [5.16]$$

$$Z_{LR} \text{ (meters RSL)} = \boldsymbol{Z_{box}} - [\boldsymbol{L_{box}}/2] \times \sin \boldsymbol{\delta_{box}} \quad [5.17]$$

For example, if $\boldsymbol{\alpha_{box}} = \boldsymbol{\delta_{box}} = 0$ the plotting plane will be horizontal, with the *x*-axis measuring distance North and the *y*-axis measuring distance West. If $\boldsymbol{\alpha_{box}} = 90°$ and $\boldsymbol{\delta_{box}} = 0$, the plane will still be horizontal but the *x*-axis will measure distance East and the *y*-axis will measure distance North. If $\boldsymbol{\alpha_{box}} = \boldsymbol{\delta_{box}} = 90°$, the plot will represent a vertical plane oriented East-West.

5.3.2. Time Domain: file *"inconttm.fil".* This file is optional. If it is absent, the contour plotting programs will seek <u>all</u> "dump" files in the local directory with names of the form *"rpgdIIII.fil"* (each corresponding to a different time-level) and will create a contour plot for each one that they find. Input file *"inconttm.fil",* if present, consists of a single line containing either one or two integer entries. If it contains just a single entry (for example, *"7"*), then only the *"rpgd0007.fil"* dump file will be plotted (if it exists). If the *"inconttm.fil"* input line contains two entries (for example, *"3"* and *"6"*), then only the dump files with indices between these limits (*"rpgd0003.fil", "rpgd0004.fil"*, *"rpgd0005.fil"* and *"rpgd0006.fil"*) will be examined.

Both of the contour-plotting postprocessors choose their contour levels (and the appropriate contour-level spacing) based on the minimum and maximum values (of p or of V) encountered anywhere in the grid, considering all of the *"rpgd****.fil"* dump files that they examine for that run. All contour plots generated by a particular run of one of these postprocessors use the *same list* of contour levels. For example, the *"spfpltcv.exe"* run that created the images shown as Figures C-2(a) – C-2(f) in Appendix C was performed without an *"inconttm.fil"* present in the local directory. As a result, the postprocessor examined all the "dump" files present (files *"rpgd0001.fil"* – *"rpgd0006.fil"*), selected a contour level spacing of 50 mV, and used that value to construct all six plots. But subsequently, a new *"inconttm.fil"* file was created in the local directory containing a single line with the character "6" entered upon it. Re-running *"spfpltcv.exe"* produced the result shown in Appendix C, Figure C-2(g). This image illustrates the same potential distribution as Figure C-3(f), but this time (owing to the much reduced signal strength at late times), the program chose a contour level spacing of only 5 mV, resulting in a much better-resolved image. If the user desires to create a *time-sequence* of contour plots, it may be better to delete file *"inconttm.fil"* so that the contour levels will be consistent from one plot to the next. But if *high resolution* is desired for a particular "snapshot" contour plot, file *"inconttm.fil"* may be used to create the plots independently, each with its own custom selection of contour levels.

5.3.3. Contour Resolution: file *"incontcr.fil".* This optional file may also be used to influence the contour spacing and the number of contour levels that appear on the plots. Three levels of "contour resolution" are available: *"low"*, *"standard"* and *"high"*. The default level is *"standard"* and is used if the *"incontcr.fil"* file is absent. All of the contour plots displayed in Appendix C were made using *"standard"* contour resolution. Specifying *"low"* contour resolution will usually result in fewer contour lines appearing on each plot and in larger spacing between contours than in the *"standard"* case, and specifying *"high"* contour resolution will result in more contour levels (using smaller spacing). File *"incontcr.fil"* consists of a single line containing a case-insensitive character string:

LOW or ***STANDARD*** or ***HIGH*** (character string)
end-of-file

The user specifies his choice by entering *"low"*, *"standard"* or *"high"*. The same specification applies to all plots created by the postprocessor run.

5.3.4. Spatial Resolution: file *"incontsr.fil".* In order to construct the contour plots, the *"spfpltcp.exe"* and *"spfpltcv.exe"* postprocessors subdivide the square "plotting plane" (see Section 5.3.1 above) into a regular $M \times M$ array of M^2 individual equally-spaced points and then interpolate spatially among the computed grid-block values (of p or of V) to obtain values for constructing the plot. Again, three levels of spatial resolution (*"low", "standard"* and *"high"*) are available. If file *"incontsr.fil"* is absent, *"standard"* spatial resolution is the default. The syntax for input file *"incontsr.fil"* is exactly the same as for the *"incontcr.fil"* discussed above. The level of spatial resolution chosen determines the value used for M:

"LOW"	$M = 64$	(grid sampled 4,096 times per plot)
"STANDARD"	$M = 128$	(grid sampled 16,384 times per plot)
"HIGH"	$M = 256$	(grid sampled 65,536 times per plot)

Selecting higher resolution levels will usually improve plot clarity, but at the price of bulkier graphics files. The user is encouraged to experiment to optimize results for his application.

5.3.5. Contour Labels: file *"incontlb.fil".* As shown in Appendix C (Figures C-1 and C-2), the *"spfpltcp.exe"* and *"spfpltcv.exe"* contour-plotting postprocessors usually superimpose "labels" on at least some of the contour lines to aid the viewer in quantitative interpretation of the contour plots. These "labels" are written in a relatively small font to minimize their tendency to obscure plot detail. Sometimes, if the user intends to distribute the plots in a fashion that will require them to be reduced in size (such as publication in a journal that uses dual-column format or perhaps for a slideshow presentation), these labels may become illegible upon reduction. For such applications, a larger font size would be desirable. On the other hand, the user may wish to produce contour plots without these labels, so that tools such as "Adobe Illustrator" may instead be used to annotate the plot, or for other reasons. These options are available using input file *"incontlb.fil"*. This file consists of a single line which contains a case-insensitive text string:

NONE or ***STANDARD*** or ***LARGE*** (character string)
end-of-file

Choosing *"standard"* labeling (or deleting file *"incontlb.fil"*) will produce plots labeled in a manner similar to those displayed in Appendix C (Figures C-1 and C-2). Choosing *"none"* will result in contour plots with no contour labels. Choosing *"large"* labels will produce contour plots with labels that are 67% larger than those appearing on the contour plots in Appendix C.

6. AN ILLUSTRATIVE EXAMPLE

Consider a cubical region of space of total volume 27 cubic kilometers (3 km × 3 km × 3 km) extending vertically from –1500 m RSL (1500 meters below sea level) to –4500 m RSL (4500 meters below sea level). As indicated in Figure 6-1, the (*x,y,z*) "grid" coordinate system is rotated 30° to the east. A central injection well penetrates a single pre-existing horizontal fracture at the geometric center of the grid ($x = y = z = 0$; +1000 meters East, +2000 meters North, and –3000 meters RSL). The fracture is circular in shape with diameter 600 meters and is centered on the origin (and on the injection well). This geometry is similar to that examined by *Pritchett and Ishido* (2005a; 2005b). Two observation wells are present, displaced 400 meters and 600 meters 30° north of west from the injection well (at $x = –400$ and –600 meters, $y = 0$). As Figure 6-2 shows, each of the injection wells contains seven electrical sensors for measuring the electrical potential history, arrayed vertically in each well between –2890 m RSL and –3120 m RSL (at $z = –120$ m, –80 m, –40 m, 0, +40 m, +80 m and +120 m). A 43×43×43 computational grid (79,507 grid blocks total) is used with spacing ranging from 40 meters (centrally) to 400 meters (adjacent to the outer boundaries), as indicated.

For simplicity, most of the system properties are treated as uniform for this illustrative example. Temperature and brine salinity are uniform at 200°C and 0.001 (mass fraction NaCl) respectively; these yield a uniform native brine mass density (882 kg/m^3), dynamic viscosity (140 μPa-s), fluid compressibility (0.753/GPa) and fluid absolute dielectric permittivity (3.14×10^{-10} farad/m). The country rock porosity (0.01), compressibility (0.3/GPa), tortuosity (1.4) and permeability (10^{-17} m^2; 0.01 millidarcy) are likewise uniform throughout the volume, and the permeability is isotropic. The *Ishido/Mizutani* (1981) model was selected using a ΔpH value of 5, which yields a uniform adsorption potential or "zeta-potential" (ζ) of –136.2 millivolts (since both temperature and salinity are uniform). The system is subdivided into three layers as regards volumetric electrical conductivity:

Above –2900 m RSL	0.02500 siemens/m
–2900 to –3100 m RSL	0.01000 siemens/m
Below –3100 m RSL	0.00625 siemens/m

In addition, "surface conductivity" is added uniformly (0.001 S/m) throughout the grid volume. As a result, the electrical properties of the system are stratified as follows:

Vertical Layer	*Electrical Resistivity*	*Streaming Potential Coefficient*
–1500 m RSL to –2900 m RSL	38.46 Ω-m	59.9 mV/MPa
–2900 m RSL to –3100 m RSL	90.90 Ω-m	141.5 mV/MPa
–3100 m RSL to –4500 m RSL	137.93 Ω-m	214.8 mV/MPa

The two observation wells are considered to be completed with non-conductive casings (at least at the depths of interest), but the steel-cased injection well is uncased only between –2980 m RSL and –3020 m RSL (the 40-meter uncased section allows for fluid injection). The long upper portion of the steel injection well casing is assumed to remain at zero potential, but the lower 180-meter casing section is considered to "float", with a potential that is uniform along the pipe section but that is in general a function of time. All three wells are considered to be of 0.34-meter diameter (uniform with depth).

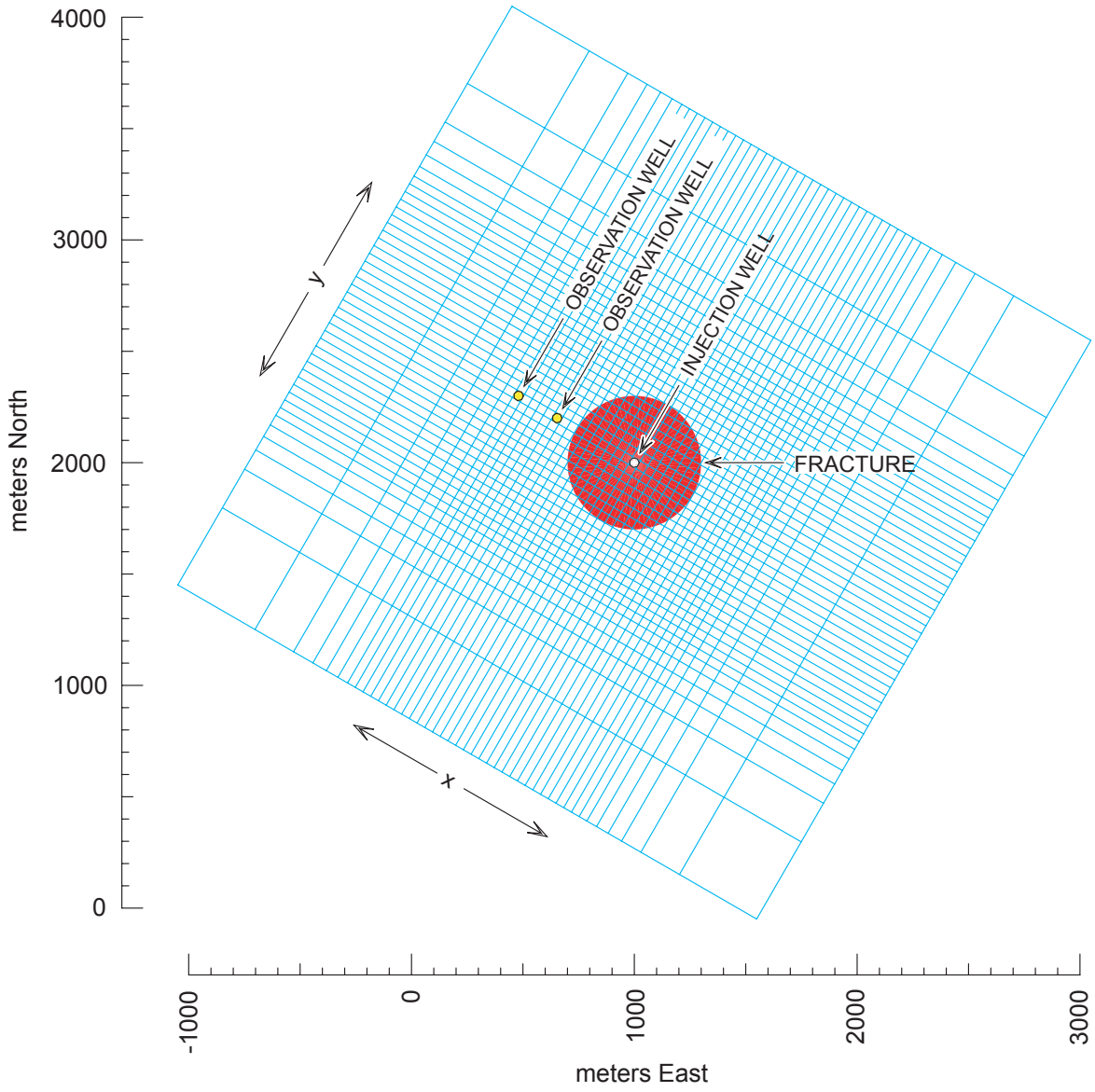

Figure 6-1: Horizontal plane through computational volume at –3000 meters RSL. *Cyan:* grid block boundaries. *Red:* circular 600-meter diameter horizontal fracture. Computational grid origin ($x = y = z = 0$) is located at 1000 meters East, 2000 meters North and –3000 meters RSL, which is also the location where fluid injection takes place through the central injection well to stimulate the fracture. The computational grid is rotated 30° around the z-axis. Two observation wells containing voltage sensors are present, 400 and 600 meters displaced from the injection well.

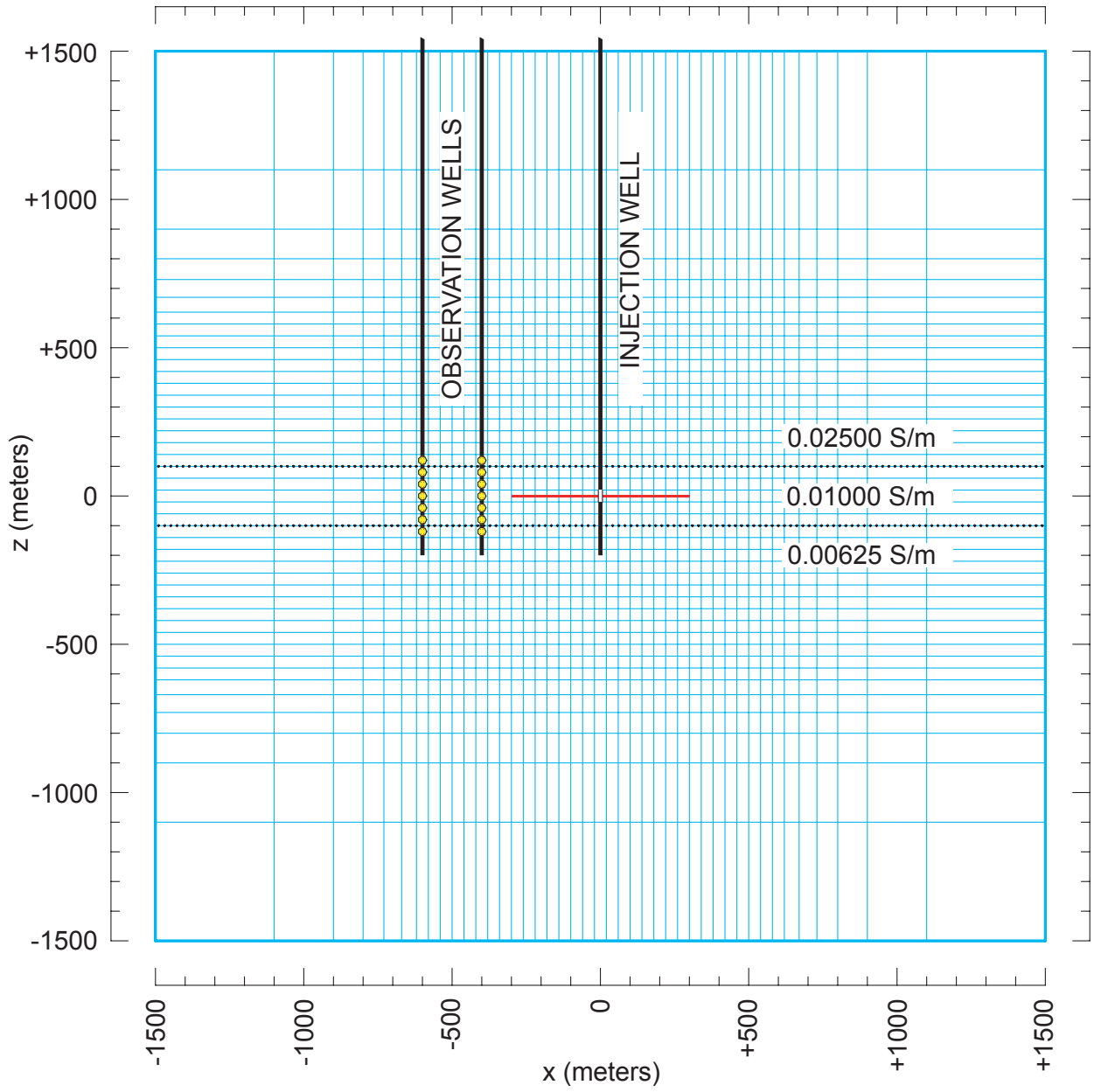

Figure 6-2: Vertical *x-z* plane through computational grid volume at $y = 0$ (through the injection and observation wells). *Red:* horizontal circular fracture (diameter = 600 m). Each observation well contains seven voltage sensors *(yellow)* spaced 40 meters apart centered upon the fracture plane at $z = 0$ (–3000 meters RSL). Volumetric electrical conductivity is 0.025 siemens/m above –2900 m RSL (z = +100 m) whereas below –3100 m RSL the value is only one-fourth as large. An intermediate value (0.01 S/m) prevails in a 200-meter thick layer surrounding the fracture. In addition, a "surface conductivity" of 0.001 S/m is imposed everywhere, so that the net electrical resistivities of the three layers are 38.46, 90.90 and 137.93 ohm-meters (in order of increasing depth). The observation wells have non-metallic casings, but the injection well has a steel casing extending upwards from –2980 m RSL ($z = +20$ m) and also metallic casing from –3020 m to –3200 m RSL ($z = –20$m to –200 m). The 40-meter injection interval is uncased. Fracture aperture and well diameters are grossly exaggerated in this illustration.

To stimulate the fracture, the overpressure within the injection well is first raised from zero to 10 MPa at $t = 0$ and maintained at that level for 16 days (384 hours). Then, the well overpressure is discontinuously changed back to zero and maintained at that value thereafter. The calculation describes a total time interval of 48 days (1152 hours); 16 days of stimulation followed by 32 days of recovery. The distribution of electrical potential is recomputed every eight hours.

The circular fracture is represented by 72 triangular elements, each with one of the vertices at the origin and with the other two vertices in the *x*-*y* plane at a radius of 300 meters and at 5° angular separation. All of these elements have the same representation for the relationships among fluid pressure, aperture, and transmissivity. Initially, the fracture aperture (λ) is equal to zero. As pressure increases, the aperture likewise increases with

$$B_i = [\partial\lambda/\partial p]_i = 18.171 \text{ millimeters / GPa}$$

But if pressure decreases, or if the local pressure is less than the maximum value attained so far, then

$$B_d = [\partial\lambda/\partial p]_d = 9.7369 \text{ millimeters / GPa}$$

The maximum injection pressure is 10 MPa (0.01 GPa). Thus, upon *(a)* pressurization followed by *(b)* depressurization, the transmissivity of the fracture (initially zero) will increase to a maximum value, and then drop back to a "residual" transmissivity value reflecting permanent fracture deformation. Both the "maximum" and "residual" transmissivity will depend upon the maximum overpressure experienced by that portion of the fracture. Since in the present case the maximum fracture overpressure ranges from 10 MPa at $r = 0$ to about 8.5 MPa at $r = 300$ m, these fracture transmissivity values range among the following (1 darcy-m = 10^{-12} m^2):

Maximum Overpressure	*Initial Transmissivity*	*Maximum Transmissivity*	*Residual Transmissivity*
8.5 MPa	0.0000 darcy-m	0.3071 darcy-m	0.0307 darcy-m
9.0 MPa	0.0000 darcy-m	0.3645 darcy-m	0.0365 darcy-m
9.5 MPa	0.0000 darcy-m	0.4287 darcy-m	0.0429 darcy-m
10.0 MPa	0.0000 darcy-m	0.5000 darcy-m	0.0500 darcy-m

For comparison, the total transmissivity of the entire three-kilometer thick section of unfractured country rock is only 0.03 darcy-meters, so that even after the fracture is completely depressurized the transmissivity of this single fracture will dominate the fluid-carrying capacity of the entire 27 km^3 study volume.

Input data files used to specify this illustrative problem for the SPFRAC simulator are shown in Appendix A of this report. Some of the simulator output files are listed (in part) in Appendix B, and the pictorial representations of the solution shown in Appendix C were obtained using the various graphical postprocessors available with the simulator. Using a 2006-vintage PC computer with an AMD Opteron-64 processor, Red Hat Linux and PGI Fortran, this calculation required about two hours (121 minutes) of computer time. Using a similarly configured but newer Dell T7400 machine (manufactured in 2008) with an Intel X5482 processor, the same calculation was completed in 59 minutes.

7. REFERENCES

Budiansky, B. (1970), Thermal and thermoelastic properties of isotropic composites, *J. Composite Materials 4*, pp. 286–295.

Ishido, T. and H. Mizutani (1981), Experimental and theoretical basis of electrokinetic phenomena in rock-water systems and its application to geophysics, *J. Geophys. Res. 86*, pp. 1763–1775.

Ishido, T., and J. W. Pritchett (1999), Numerical simulation of electrokinetic potentials associated with subsurface fluid flow, *J. Geophys. Res. 104*, pp. 15247–15259.

Ishido, T. and J. W. Pritchett (2000), Using numerical simulation of electrokinetic potentials in geothermal reservoir management, *Proc. World Geothermal Congress 2000,* Beppu-Morioka, Japan, pp. 2629–2634.

Ishido, T., and J. W. Pritchett (2003), Characterization of fractured reservoirs using continuous self-potential measurements, *Proc. 28th Workshop on Geothermal Reservoir Engineering,* Stanford University.

MIT (2005), *The Future of Geothermal Energy: Impact of Enhanced Geothermal Systems (EGS) on the United States in the 21st Century,* Massachusetts Institute of Technology, Cambridge, Massachusetts.

Nakanishi, S., J. W. Pritchett and T. Tosha (2001), Changes in ground surface geophysical signals induced by geothermal exploitation – computational studies based on a numerical reservoir model for the Oguni geothermal field, Japan, *GRC Transactions 25,* pp. 657–664.

NREL (2008), *An Evaluation of Enhanced Geothermal Systems Technology,* National Renewable Energy Laboratory, Department of Energy.

Pritchett, J. W. and S. K. Garg (1980), Determination of effective well-block radii for numerical reservoir simulations, *Water Resources Research 16(4)*, pp. 665-674.

Pritchett, J. W. and J. H. Alexander (1986), *JPLOT: A Postprocessing Automatic Graphics Package for Use with Fortran 77 Systems Capable of Hardcopy Vector Plotting*, Systems, Science and Software (S-Cubed) Report No. SSS-R-86-8180.

Pritchett, J. W. (1995), STAR: a geothermal reservoir simulation system, *Proc. World Geothermal Congress 1995,* Florence, Italy, pp. 2959–2963.

Pritchett, J. W., J. Stevens, P. Wannamaker, S. Nakanishi and S. Yamazawa (2000), Theoretical appraisal of surface geophysical survey methods for geothermal reservoir monitoring, *GRC Transactions 24,* pp. 617–622.

Pritchett, J. W. and S. K. Garg (2002), *Modeling and Numerical Simulation of the Sumikawa Geothermal Field*, Science Applications International Corp. Report SAIC-02/1013.

Pritchett, J. W. (2002), *STAR User's Manual, Version 9.0,* Science Applications International Corp. Report SAIC-02/1055.

Pritchett, J. W. and S. K. Garg (2003), *Coupling Techniques for Self-Potential Survey and Groundwater Analysis: Case Study of the Onikobe Geothermal Field*, Science Applications International Corp. Report SAIC-03/1013.

Pritchett, J. W. (2003), *Verification and Validation Calculations Using the STAR Geophysical Postprocessor Suite*, Science Applications International Corp. Report SAIC-03/1040.

Pritchett, J. W. and T. Ishido (2005a), Hydrofracture characterization using downhole electrical monitoring, *Proc. World Geothermal Congress 2005,* Antalya, Turkey.

Pritchett, J. W. and T. Ishido (2005b), *Evaluating Permeability Enhancement using Electrical Techniques – Final Report for Year 1,* Science Applications International Corp. Report to DOE, Award DE-FG36-04GO14291.

Pritchett, J. W., S. K. Garg, T. Ishido, N. Matsushima, H. Hase and B. J. Livesay (2006), *Evaluating Permeability Enhancement using Electrical Techniques – Final Report for Year 2,* Science Applications International Corp. Report to DOE, Award DE-FG36-04GO14291.

Telford, W. M., L. P. Geldart and R. E. Sheriff (1990), *Applied Geophysics Second Edition,* Cambridge Univ. Press.

Tosha, T., N. Matsushima and T. Ishido (2003), Zeta potential measured for an intact granite sample at temperatures to 200°C, *Geophys. Research Letters 30(6),* pp. 1295–1299.

APPENDIX A:
USER-PREPARED INPUT FILES UTILIZED TO SPECIFY ILLUSTRATIVE PROBLEM

Full contents of input file "ingridor.fil":

```
----*----|----*----|----*----|----*----|----*----|----*----|----*----|----*----|----*----|
# This file specifies the relationship between the "grid" coordinate
# system (x,y,z) and "world" coordinates (East, North and Elevation).
# Geometric center of computational grid is located at 1000 mE, 2000 mN,
# and -3000 mRSL.  Grid is rotated 30 degrees around the z-axis, so that
# y-axis points 30 degrees east of north.
#
1000 2000 -3000 30   # Origin E, N, RSL; rotation around z-axis
End-of-file --*----|----*----|----*----|----*----|----*----|----*----|----*----|----*----|
```

Contents of input file "ingridor.fil" with comments deleted:

```
----*----|----*----|----*----|----*----|----*----|----*----|----*----|----*----|----*----|
1000 2000 -3000 30
End-of-file --*----|----*----|----*----|----*----|----*----|----*----|----*----|----*----|
```

Full contents of input file "ingridsx.fil":

```
----*----|----*----|----*----|----*----|----*----|----*----|----*----|----*----|----*----|
# In the x-direction, the grid measures 3 km
# in size, with -1500m < x < +1500m.
# There are 43 discrete intervals, ranging in
# size between 40 and 400 meters / division.
#
400 200 100 70 60 50
40 40 40 40 40
40 40 40 40 40 40 40 40 40 40
40
40 40 40 40 40 40 40 40 40 40
40 40 40 40 40
50 60 70 100 200 400
End-of-file --*----|----*----|----*----|----*----|----*----|----*----|----*----|----*----|
```

Contents of input file "ingridsx.fil" with comments deleted:

```
----*----|----*----|----*----|----*----|----*----|----*----|----*----|----*----|----*----|
400 200 100 70 60 50
40 40 40 40 40
40 40 40 40 40 40 40 40 40 40
40
40 40 40 40 40 40 40 40 40 40
40 40 40 40 40
50 60 70 100 200 400
End-of-file --*----|----*----|----*----|----*----|----*----|----*----|----*----|----*----|
```

Figure A-1: Grid geometry input files *"ingridor.fil"*, *"ingridsx.fil", "ingridsy.fil"*, *"ingridsz.fil"* and *"intwophs.fil"* used to specify sample problem for *"spfracsm.exe"* run.

Full contents of input file "ingridsy.fil":

```
----*----|----*----|----*----|----*----|----*----|----*----|----*----|----*----|----*----|
# Grid spacing in the y-direction is the same as for the x-direction.
#
400 200 100 70 60 50
40 40 40 40 40
40 40 40 40 40 40 40 40 40 40
40
40 40 40 40 40 40 40 40 40 40
40 40 40 40 40
50 60 70 100 200 400
End-of-file --*----|----*----|----*----|----*----|----*----|----*----|----*----|----*----|
```

Contents of input file "ingridsy.fil" with comments deleted:

```
----*----|----*----|----*----|----*----|----*----|----*----|----*----|----*----|----*----|
400 200 100 70 60 50
40 40 40 40 40
40 40 40 40 40 40 40 40 40 40
40
40 40 40 40 40 40 40 40 40 40
40 40 40 40 40
50 60 70 100 200 400
End-of-file --*----|----*----|----*----|----*----|----*----|----*----|----*----|----*----|
```

Full contents of input file "ingridsz.fil":

```
----*----|----*----|----*----|----*----|----*----|----*----|----*----|----*----|----*----|
# Grid spacing in the z-direction is the same as for the x-direction.
#
400 200 100 70 60 50
40 40 40 40 40
40 40 40 40 40 40 40 40 40 40
40
40 40 40 40 40 40 40 40 40 40
40 40 40 40 40
50 60 70 100 200 400
End-of-file --*----|----*----|----*----|----*----|----*----|----*----|----*----|----*----|
```

Contents of input file "ingridsz.fil" with comments deleted:

```
----*----|----*----|----*----|----*----|----*----|----*----|----*----|----*----|----*----|
400 200 100 70 60 50
40 40 40 40 40
40 40 40 40 40 40 40 40 40 40
40
40 40 40 40 40 40 40 40 40 40
40 40 40 40 40
50 60 70 100 200 400
End-of-file --*----|----*----|----*----|----*----|----*----|----*----|----*----|----*----|
```

Input file "intwophs.fil" is absent.

Figure A-1: Grid geometry input files *(concl.)*

Full contents of input file "intimstp.fil":

```
----*----|----*----|----*----|----*----|----*----|----*----|----*----|----*----|----*----|
# The total problem duration is 1152 hours (48 days).  Electrical potential will
# be calculated 144 times during that period (every eight hours).  After every
# 24-th electrical potential calculation, the entire potential distribution
# will be dumped out on an output file (that is, every eight days;
# total number of "dumps" = 144 / 24 = 6).  A minimum of 2 hydraulic time-steps
# will be taken between each calculation of electrical potential (so maximum
# hydraulic time-step size is four hours).  The upper bound on the number
# of hydraulic time-steps is very large.
#
hours
1152
144 24 2 10000000
End-of-file --*----|----*----|----*----|----*----|----*----|----*----|----*----|----*----|
```

Contents of input file "intimstp.fil" with comments deleted:

```
----*----|----*----|----*----|----*----|----*----|----*----|----*----|----*----|----*----|
hours
1152
144 24 2 10000000
End-of-file --*----|----*----|----*----|----*----|----*----|----*----|----*----|----*----|
```

Figure A-2: Time-discretization input file *"intimstp.fil"* used to specify sample problem for *"spfracsm.exe"* run.

Full contents of input file "intemper.fil":

```
----*----|----*----|----*----|----*----|----*----|----*----|----*----|----*----|----*----|
# The system temperature is uniform and equal to 200 degrees Celsius.
#
200
End-of-file --*----|----*----|----*----|----*----|----*----|----*----|----*----|----*----|
```

Contents of input file "intemper.fil" with comments deleted:

```
----*----|----*----|----*----|----*----|----*----|----*----|----*----|----*----|----*----|
200
End-of-file --*----|----*----|----*----|----*----|----*----|----*----|----*----|----*----|
```

Full contents of input file "insaltfr.fil":

```
----*----|----*----|----*----|----*----|----*----|----*----|----*----|----*----|----*----|
# The dissolved NaCl mass fraction in the pore fluid is 1000 ppm (uniform).
#
.001
End-of-file --*----|----*----|----*----|----*----|----*----|----*----|----*----|----*----|
```

Contents of input file "insaltfr.fil" with comments deleted:

```
----*----|----*----|----*----|----*----|----*----|----*----|----*----|----*----|----*----|
.001
End-of-file --*----|----*----|----*----|----*----|----*----|----*----|----*----|----*----|
```

Full contents of input file "inporost.fil":

```
----*----|----*----|----*----|----*----|----*----|----*----|----*----|----*----|----*----|
# The rock porosity is uniform and equal to 1%.
#
.01
End-of-file --*----|----*----|----*----|----*----|----*----|----*----|----*----|----*----|
```

Contents of input file "inporost.fil" with comments deleted:

```
----*----|----*----|----*----|----*----|----*----|----*----|----*----|----*----|----*----|
.01
End-of-file --*----|----*----|----*----|----*----|----*----|----*----|----*----|----*----|
```

Full contents of input file "incomprs.fil":

```
----*----|----*----|----*----|----*----|----*----|----*----|----*----|----*----|----*----|
# Country rock is very stiff.  Compressibility = 3x10**-10/Pa corresponds
# to elastic modulus = 330 GPa for porosity = 0.01.  Rock compressibility is
# uniform throughout grid volume.
#
3.e-10
End-of-file --*----|----*----|----*----|----*----|----*----|----*----|----*----|----*----|
```

Contents of input file "incomprs.fil" with comments deleted:

```
----*----|----*----|----*----|----*----|----*----|----*----|----*----|----*----|----*----|
3.e-10
End-of-file --*----|----*----|----*----|----*----|----*----|----*----|----*----|----*----|
```

Figure A-3: Input files *"intemper.fil", "insaltfr.fil", "inporost.fil"* and *"incomprs.fil"* used to specify temperature, brine salinity, rock porosity and rock compressibility distributions for *"spfracsm.exe"* sample problem run.

Full contents of input file "inpermis.fil":

```
----*----|----*----|----*----|----*----|----*----|----*----|----*----|----*----|----*----|
# The country-rock (unfractured) permeability is 0.01 millidarcy everywhere.
#
1.e-17
End-of-file --*----|----*----|----*----|----*----|----*----|----*----|----*----|----*----|
```

Contents of input file "inpermis.fil" with comments deleted:

```
----*----|----*----|----*----|----*----|----*----|----*----|----*----|----*----|----*----|
1.e-17
End-of-file --*----|----*----|----*----|----*----|----*----|----*----|----*----|----*----|
```

Input file "inprmavh.fil" is absent.

Input file "inprmaxy.fil" is absent.

Full contents of input file "infrcmdl.fil":

```
----*----|----*----|----*----|----*----|----*----|----*----|----*----|----*----|----*----|
# The fracture aperture is zero initially.  Upon pressurization, the
# aperture increases with pressure at 1.81712e-11 meters per pascal.
# Upon depressurization, the slope is only 0.93769e-11 m/Pa, so if the fracture
# is first pressurized to 1.e+07 pascals (100 bars) and then completely
# depressurized, the final aperture will be > 0.  Since fracture transmissivity
# (kH) is given by (aperture**3)/12, this means that:
#
# Initial P = 0, aperture = 0,                  kH = 0
#  P = 100 bars, aperture = 1.81712e-04 meters, kH = 5.e-13 m**3 (0.50 darcy-m)
#   Final P = 0, aperture = 0.84343e-04 meters, kH = 5.e-14 m**3 (0.05 darcy-m)
#
0  1.81712e-11  0.97369e-11         # Initial aperture, d(aperture)/dP values
End-of-file --*----|----*----|----*----|----*----|----*----|----*----|----*----|----*----|
```

Contents of input file "infrcmdl.fil" with comments deleted:

```
----*----|----*----|----*----|----*----|----*----|----*----|----*----|----*----|----*----|
0  1.81712e-11  0.97369e-11
End-of-file --*----|----*----|----*----|----*----|----*----|----*----|----*----|----*----|
```

Figure A-4: Permeability input files *"inpermis.fil", "inprmavh.fil", "inprmaxy.fil", "infrcmdl.fil" and "infrcgeo.fil"* used to specify country rock native permeability, permeability anisotropy, fracture permeability/aperture representation, and fracture system geometry for *"spfracsm.exe"* sample problem run.

Full contents of input file "infrcgeo.fil":

```
----*----|----*----|----*----|----*----|----*----|----*----|----*----|----*----|----*----|
# An approximately circular horizontal fracture is centered on the injection
# point, and is of radius 300 meters.  It is represented by 72 triangular
# segments.
#
grid
 1 1
   300.00000     0.00000 0
   298.85841    26.14672 0
 0 0 0
grid
 1 1
   298.85841    26.14672 0
   295.44233    52.09445 0
 0 0 0
                          [345 lines skipped here]
grid
 1 1
   298.85841   -26.14672 0
   300.00000     0.00000 0
 0 0 0
End-of-file --*----|----*----|----*----|----*----|----*----|----*----|----*----|----*----|
```

Contents of input file "infrcgeo.fil" with comments deleted:

```
----*----|----*----|----*----|----*----|----*----|----*----|----*----|----*----|----*----|
grid
 1 1
   300.00000     0.00000 0
   298.85841    26.14672 0
 0 0 0
grid
 1 1
   298.85841    26.14672 0
   295.44233    52.09445 0
 0 0 0
                          [345 lines skipped here]
grid
 1 1
   298.85841   -26.14672 0
   300.00000     0.00000 0
 0 0 0
End-of-file --*----|----*----|----*----|----*----|----*----|----*----|----*----|----*----|
```

Figure A-4: Permeability input files *(concl.)*

Full contents of input file "instrmdl.fil":

```
----*----|----*----|----*----|----*----|----*----|----*----|----*----|----*----|----*----|
# To calculate the zeta-potential, the model of Ishido and Mizutani is used,
# with a delta-pH value of 5.
#
ishido
5
End-of-file --*----|----*----|----*----|----*----|----*----|----*----|----*----|----*----|
```

Contents of input file "instrmdl.fil" with comments deleted:

```
----*----|----*----|----*----|----*----|----*----|----*----|----*----|----*----|----*----|
ishido
5
End-of-file --*----|----*----|----*----|----*----|----*----|----*----|----*----|----*----|
```

Input file "inzetapo.fil" is absent.

Input file "instrmpc.fil" is absent.

Full contents of input file "intortuo.fil":

```
----*----|----*----|----*----|----*----|----*----|----*----|----*----|----*----|----*----|
# Country rock tortuosity is uniform.
#
1.4
End-of-file --*----|----*----|----*----|----*----|----*----|----*----|----*----|----*----|
```

Contents of input file "intortuo.fil" with comments deleted:

```
----*----|----*----|----*----|----*----|----*----|----*----|----*----|----*----|----*----|
1.4
End-of-file --*----|----*----|----*----|----*----|----*----|----*----|----*----|----*----|
```

Figure A-5: Input files *"instrmdl.fil", "inzetapo.fil", "instrmpc.fil"* and *"intortuo.fil"* used to establish the distribution of the streaming potential coefficient for *"spfracsm.exe"* sample problem run.

Full contents of input file "incndmdl.fil":

```
----*----|----*----|----*----|----*----|----*----|----*----|----*----|----*----|----*----|
# Text string specifies which "mixing model" to use to combine rock and fluid
# electrical conductivities to obtain total volumetric conductivity.  "Nomix"
# means just regard the input "rock" conductivity as the total conductivity.
nomix
End-of-file --*----|----*----|----*----|----*----|----*----|----*----|----*----|----*----|
```

Contents of input file "incndmdl.fil" with comments deleted:

```
----*----|----*----|----*----|----*----|----*----|----*----|----*----|----*----|----*----|
nomix
End-of-file --*----|----*----|----*----|----*----|----*----|----*----|----*----|----*----|
```

Full contents of input file "incndrok.fil":

```
----*----|----*----|----*----|----*----|----*----|----*----|----*----|----*----|----*----|
# Default conductivity is 0.01 siemen/m (100 ohm-m resistivity)
.01
# Above -2900 mRSL, conductivity is 0.025 S/m (40 ohm-m)
change world
-15000 +15000 -15000 +15000 -2900 0
.025 .025 .025 .025 .025 .025 .025 .025
# Below -3100 mRSL, conductivity is 0.00625 S/m (160 ohm-m)
change world
-15000 +15000 -15000 +15000 -9000 -3100
.00625 .00625 .00625 .00625 .00625 .00625 .00625 .00625
End-of-file --*----|----*----|----*----|----*----|----*----|----*----|----*----|----*----|
```

Contents of input file "incndrok.fil" with comments deleted:

```
----*----|----*----|----*----|----*----|----*----|----*----|----*----|----*----|----*----|
.01
change world
-15000 +15000 -15000 +15000 -2900 0
.025 .025 .025 .025 .025 .025 .025 .025
change world
-15000 +15000 -15000 +15000 -9000 -3100
.00625 .00625 .00625 .00625 .00625 .00625 .00625 .00625
End-of-file --*----|----*----|----*----|----*----|----*----|----*----|----*----|----*----|
```

Full contents of input file "incndsrf.fil":

```
----*----|----*----|----*----|----*----|----*----|----*----|----*----|----*----|----*----|
# "Surface conductivity" is small and uniform at 0.001 siemen/meter.
.001
End-of-file --*----|----*----|----*----|----*----|----*----|----*----|----*----|----*----|
```

Contents of input file "incndsrf.fil" with comments deleted:

```
----*----|----*----|----*----|----*----|----*----|----*----|----*----|----*----|----*----|
.001
End-of-file --*----|----*----|----*----|----*----|----*----|----*----|----*----|----*----|
```

Input file "incndavh.fil" is absent.

Input file "incndaxy.fil" is absent.

Figure A-6: Input files *"incndmdl.fil", "incndrok.fil", "incndsrf.fil", "incndavh.fil"* and *"incndaxy.fil"* used to establish the distribution of the electrical conductivity (resistivity) for *"spfracsm.exe"* sample problem run.

Full contents of input file "incasing.fil":

```
----*----|----*----|----*----|----*----|----*----|----*----|----*----|----*----|----*----|
#
# Casing 1 is the upper part of the injection well casing.
# It reaches beyond the grid boundary, so will always have zero potential.
#
world
1000 2000     0 .34  # Location (mE, mN, mRSL) of top, and diameter (meters)
1000 2000 -2980      # Location of bottom of section
#
# Casing 2 is the lower part of the injection well casing, below the stimulation
# section.  The potential "floats", and is calculated as a function of time.
#
world
1000 2000 -3020 .34  # Location (mE, mN, mRSL) of top, and diameter (meters)
1000 2000 -3200      # Location of bottom of section
End-of-file --*----|----*----|----*----|----*----|----*----|----*----|----*----|----*----|
```

Contents of input file "incasing.fil" with comments deleted:

```
----*----|----*----|----*----|----*----|----*----|----*----|----*----|----*----|----*----|
world
1000 2000     0 .34
1000 2000 -2980
world
1000 2000 -3020 .34
1000 2000 -3200
End-of-file --*----|----*----|----*----|----*----|----*----|----*----|----*----|----*----|
```

Figure A-7: Input file *"incasing.fil"* used to specify the locations of electrically conductive well casings for *"spfracsm.exe"* sample problem run.

Full contents of input file "ininjwel.fil":

```
----*----|----*----|----*----|----*----|----*----|----*----|----*----|----*----|----*----|
# The injection well is located at 1000 mE and 2000 mN (the center of the grid)
# and the "open" stimulation section is centered around midplane at -3000 mRSL,
# with one grid layer vertical thickness (40 m).  The hole diameter is 0.34 m,
# and the skin factor is zero.
#
world
1000 2000 -2980 -3020 .34 0
End-of-file --*----|----*----|----*----|----*----|----*----|----*----|----*----|----*----|
```

Contents of input file "ininjwel.fil" with comments deleted:

```
----*----|----*----|----*----|----*----|----*----|----*----|----*----|----*----|----*----|
world
1000 2000 -2980 -3020 .34 0
End-of-file --*----|----*----|----*----|----*----|----*----|----*----|----*----|----*----|
```

Full contents of input file "ininjhis.fil":

```
----*----|----*----|----*----|----*----|----*----|----*----|----*----|----*----|----*----|
# Between t = 0 and t = 384 hours, injection well overpressure is maintained at
# 100 bars (10**7 pascals).  After that time, it is maintained at zero.
#
hours
pascals
liters per second
p  384.0000000001 100.e+05 100.e+05
p 1152 0 0
End-of-file --*----|----*----|----*----|----*----|----*----|----*----|----*----|----*----|
```

Contents of input file "ininjhis.fil" with comments deleted:

```
----*----|----*----|----*----|----*----|----*----|----*----|----*----|----*----|----*----|
hours
pascals
liters per second
p  384.0000000001 100.e+05 100.e+05
p 1152 0 0
End-of-file --*----|----*----|----*----|----*----|----*----|----*----|----*----|----*----|
```

Figure A-8: Input files *"ininjwel.fil"* and *"ininjhis.fil"* used to specify the location, geometry, and injection pressure (or flow-rate) history of the injection well stimulating the fracture system for *"spfracsm.exe"* sample problem run.

Full contents of input file "invsensr.fil":

```
----*----|----*----|----*----|----*----|----*----|----*----|----*----|----*----|----*----|
# All electrical sensors are located symmetrically in x-z plane at y=0.
# Two observation wells are present at x = -600 m and -400 m. In each well,
# seven sensors are located, elevated vertically at -120m, -80m, -40m, 0m,
# +40m, +80m and +120m relative to the grid midplane (and to fracture plane).
#
grid
-600 0 -120  #--------------------
-600 0 -80   #
-600 0 -40   #   First
-600 0 0     #   Observation
-600 0 +40   #   Well
-600 0 +80   #
-600 0 +120  #--------------------
-400 0 -120  #--------------------
-400 0 -80   #
-400 0 -40   #   Second
-400 0 0     #   Observation
-400 0 +40   #   Well
-400 0 +80   #
-400 0 +120  #--------------------
End-of-file --*----|----*----|----*----|----*----|----*----|----*----|----*----|----*----|
```

Contents of input file "invsensr.fil" with comments deleted:

```
----*----|----*----|----*----|----*----|----*----|----*----|----*----|----*----|----*----|
grid
-600 0 -120
-600 0 -80
-600 0 -40
-600 0 0
-600 0 +40
-600 0 +80
-600 0 +120
-400 0 -120
-400 0 -80
-400 0 -40
-400 0 0
-400 0 +40
-400 0 +80
-400 0 +120
End-of-file --*----|----*----|----*----|----*----|----*----|----*----|----*----|----*----|
```

Input file "inpsensr.fil" is absent.

Figure A-9: Input files *"inpsensr.fil"* and *"invsensr.fil"* used to specify the locations or pressure sensors and electrical potential sensors (respectively) for *"spfracsm.exe"* sample problem run.

Full contents of input file "incontpl.fil":

```
----*----|----*----|----*----|----*----|----*----|----*----|----*----|----*----|----*----|
2000 1000 2000 -3000 120 90
#
# This file specifies size, location and orientation of
# the plotting plane for contour plot programs.
# In this case, the size of the region to be plotted
# is 2000 meters by 2000 meters (first entry).
# The center of the square plotting region is located
# at 1000 meters East (second entry), 2000 meters North
# (third entry), and 3000 meters below sea level
# (-3000m RSL; fourth entry).  The plotting plane is
# rotated to 120 degrees Azimuth (fifth entry; parallel
# to the grid x-axis, which measures distance 30 degrees
# south of true East), and to (sixth entry) 90 degrees
# Declination (i.e., the plot plane is vertical, parallel
# to the grid x-axis, and centered on the geometric
# center of the computational grid).
End-of-file --*----|----*----|----*----|----*----|----*----|----*----|----*----|----*----|
```

Contents of input file "incontpl.fil" with comments deleted:

```
----*----|----*----|----*----|----*----|----*----|----*----|----*----|----*----|----*----|
2000 1000 2000 -3000 120 90
End-of-file --*----|----*----|----*----|----*----|----*----|----*----|----*----|----*----|
```

Input file "inconttm.fil" is absent.

Input file "incontsr.fil" is absent.

Input file "incontcr.fil" is absent.

Input file "incontlb.fil" is absent.

Figure A-10: Input files *"incontpl.fil", "inconttm.fil", "incontsr.fil". "incontcr.fil"* and *"incontlb.fil"* used to direct the creation of contour plots of pressure and of electrical potential using the *"spfpltcp.exe"* and *"spfpltcv.exe"* plotting postprocessors (respectively) for the sample problem run. The resulting plots are shown in Appendix C, Figures C-1 and C-2. These programs also require the "*ingridor.fil", "ingridsx.fil", "ingridsy.fil"* and *"ingridsz.fil"* input files (see Figure A-1, above) from the original *"spfracsm.exe"* run, and obtain the pressure and potential spatial distribution data from the various *"rpgd00**.fil"* output files (see Appendix B, Figure B-6).

Full contents of input file "dtinjprs.fil":

```
----*----|----*----|----*----|----*----|----*----|----*----|----*----|----*----|----*----|
# Conversion factor data on following line.  Data are in psia;
# 1MPa = 145 psi; 1 psi = 0.006897 MPa.  Initial undisturbed
# pressure at stimulation depth = 4300 psia (29.6571 MPa).
#
  1   0   0.006897   -29.6571
#
# In this input file, times are in hours (first column) and "measured"
# pressures are in psia (second column).  Uncertainty in measurements
# is plus or minus 25 psi for all measurements (third column).
#
  -1  4300 25
   0  4300 25
   0  5730 25
 100  5750 25
 200  5740 25
 300  5760 25
 380  5700 25
 390  4400 25
 400  4340 25
 500  4260 25
 600  4280 25
 700  4330 25
 800  4310 25
 900  4300 25
1000  4300 25
1100  4300 25
End-of-file --*----|----*----|----*----|----*----|----*----|----*----|----*----|----*----|
```

Contents of input file "dtinjprs" with comments deleted:

```
----*----|----*----|----*----|----*----|----*----|----*----|----*----|----*----|----*----|
  1   0   0.006897   -29.6571
  -1  4300 25
   0  4300 25
   0  5730 25
 100  5750 25
 200  5740 25
 300  5760 25
 380  5700 25
 390  4400 25
 400  4340 25
 500  4260 25
 600  4280 25
 700  4330 25
 800  4310 25
 900  4300 25
1000  4300 25
1100  4300 25
End-of-file --*----|----*----|----*----|----*----|----*----|----*----|----*----|----*----|
```

Figure A-11: Injection-well pressure-transient data files *"dtinjprs.fil", "dtinjflo.fil"* and *"dtinjcmi.fil"* used to provide "measured" data for comparison with calculations as plotted by *"spfpltin.exe",* which creates plots of injection well pressure, flow rate and cumulative flow as functions of time (see Appendix C, Figure C-3). Computed data are obtained from *"spfracsm.exe"* output file *"rpwellhs.fil"* (see Appendix B, Figure B-3).

Full contents of input file "dtinjcmi.fil":

```
----*----|----*----|----*----|----*----|----*----|----*----|----*----|----*----|----*----|
# "Measured" input data are provided in hours and in
# cubic meters cumulative injection.  Note that data may be
# entered in any order.
1 0 1 0
 384 7500
   0    0
 120 3300
 360 7200
 240 5400
 480 6500
 600 6100
 840 5700
 720 5800
 960 5500
1080 5400
End-of-file --*----|----*----|----*----|----*----|----*----|----*----|----*----|----*----|
```

Contents of input file "dtinjcmi" with comments deleted:

```
----*----|----*----|----*----|----*----|----*----|----*----|----*----|----*----|----*----|
1 0 1 0
 384 7500
   0    0
 120 3300
 360 7200
 240 5400
 480 6500
 600 6100
 840 5700
 720 5800
 960 5500
1080 5400
End-of-file --*----|----*----|----*----|----*----|----*----|----*----|----*----|----*----|
```

Input file "dtinjflo.fil" is absent.

Figure A-11: Injection-well pressure-transient data files *(concl.)*

Full contents of input file "dtsv0008.fil":

```
----*----|----*----|----*----|----*----|----*----|----*----|----*----|----*----|----*----|
1 0 1 0
152 15
304 -15
456 -65
608 -100
760 -100
912 -90
End-of-file --*----|----*----|----*----|----*----|----*----|----*----|----*----|----*----|
```

Full contents of input file "dtsv0011.fil":

```
----*----|----*----|----*----|----*----|----*----|----*----|----*----|----*----|----*----|
1 0 1 0
152 -45
304 -110
456 -155
608 -135
760 -115
912 -95
End-of-file --*----|----*----|----*----|----*----|----*----|----*----|----*----|----*----|
```

Full contents of input file "dtsv0014.fil":

```
----*----|----*----|----*----|----*----|----*----|----*----|----*----|----*----|----*----|
1 0 1 0
152 -10
304 -45
456 -75
608 -80
760 -70
912 -65
End-of-file --*----|----*----|----*----|----*----|----*----|----*----|----*----|----*----|
```

Other "dtsv00**.fil" files are similar.

Figure A-12: Potential-sensor time-history data files *"dtsv00**.fil"* used to provide "measured" data for comparison with calculations as plotted by *"spfpltsv.exe",* which creates plots of sensor electrical potential as functions of time (such as shown in Appendix C, Figure C-4). Computed data are obtained from *"spfracsm.exe"* output files *"rpsv00**.fil"* (see Appendix B, Figure B-5).

Full contents of input file "dtwv0002.fil":

```
----*----|----*----|----*----|----*----|----*----|----*----|----*----|----*----|----*----|
1 0 1000 0
20  -0.1  .05
40  -0.1  .05
60  -0.2  .05
80  -0.2  .05
100 -0.2  .05
120 -0.3  .05
140 -0.3  .05
160 -0.3  .05
180 -0.3  .05
200 -0.4  .05
220 -0.4  .05
240 -0.4  .05
260 -0.4  .05
280 -0.4  .05
300 -0.4  .05
320 -0.5  .05
340 -0.5  .05
360 -0.5  .05
380 -0.5  .05
400 -0.5  .05
420 -0.4  .05
440 -0.4  .05
460 -0.4  .05
480 -0.4  .05
500 -0.4  .05
520 -0.3  .05
540 -0.3  .05
560 -0.3  .05
580 -0.3  .05
600 -0.3  .05
620 -0.3  .05
640 -0.3  .05
660 -0.3  .05
680 -0.2  .05
700 -0.2  .05
720 -0.2  .05
740 -0.2  .05
760 -0.2  .05
780 -0.2  .05
800 -0.2  .05
820 -0.2  .05
840 -0.2  .05
860 -0.2  .05
880 -0.2  .05
900 -0.2  .05
920 -0.2  .05
940 -0.2  .05
960 -0.2  .05
End-of-file --*----|----*----|----*----|----*----|----*----|----*----|----*----|----*----|
```

Figure A-13: Well-casing electrical potential time-history data file *"dtwv0002.fil"* used to provide "measured" data for comparison with calculations as plotted by *"spfpltwv.exe",* which creates plots of the potential on the metallic casing pipe as a function of time (see Appendix C, Figure C-5). Note that "measured" potential values are in volts, which are converted to millivolts for plotting by the "1000" conversion factor found on the first line. Computed data are obtained from *"spfracsm.exe"* output file *"rpwv0002.fil"* (see Appendix B, Figure B-4).

APPENDIX B:
SELECTED OUTPUT FILES CREATED BY ILLUSTRATIVE PROBLEM CALCULATION

Contents of SPFRAC output file "rphistry.fil":

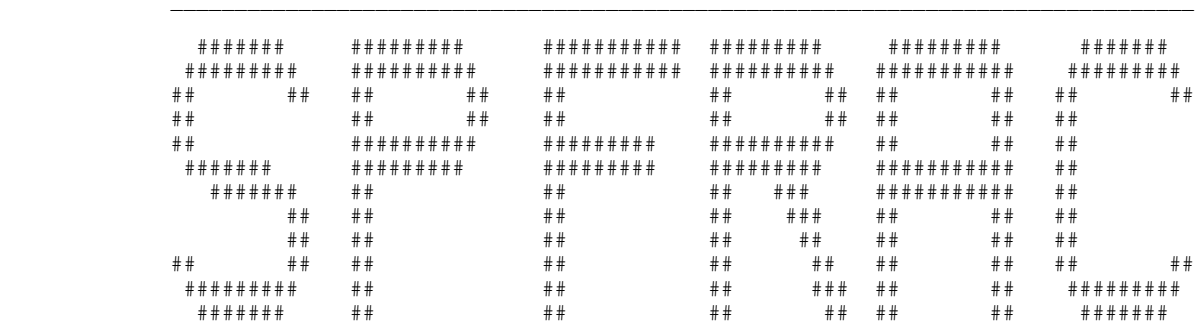

```
Output data file from the SPFRAC calculation initiated Tue Aug 12 11:51:55 2008.

PROBLEM SPECIFICATION PHASE BEGINS

Echo-prints of all input files found in local directory were written on
  output file "rpinecho.fil".
Reading input file "intimstp.fil" to obtain calculation duration, output
  frequencies, and time-step information.
Detailed report on specifications of problem duration, etc. was written
  on output file "rptimstp.fil".
Reading input file "ingridsx.fil" to obtain grid spacing in x-direction.
Number of grid blocks is 43 representing 3000.0000 meters.
Smallest interval: 40.000000 meters.
Average interval:  69.767442 meters.
Largest interval:  400.00000 meters.
Reading input file "ingridsy.fil" to obtain grid spacing in y-direction.
Number of grid blocks is 43 representing 3000.0000 meters.
Smallest interval: 40.000000 meters.
Average interval:  69.767442 meters.
Largest interval:  400.00000 meters.
Reading input file "ingridsz.fil" to obtain grid spacing in z-direction.
Number of grid blocks is 43 representing 3000.0000 meters.
Smallest interval: 40.000000 meters.
Average interval:  69.767442 meters.
Largest interval:  400.00000 meters.
Reading input file "ingridor.fil" to obtain grid orientation.
Location of geometric center of computational grid:
 1000.0000 meters East, 2000.0000 meters North, -3000.000 meters RSL.
The x-coordinate measures distance 30.000000 degrees South of East.
The y-coordinate measures distance 30.000000 degrees East of North.
The z-coordinate measures distance upward.
Detailed grid geometry report was written on output file "rpgrgeom.fil".
Initial values of all overpressures and potentials set to zero.
Reading input file "intemper.fil" to obtain spatial temperature distribution.
Detailed distribution report for temperature
  was written on output file "rptemper.fil".
Reading input file "insaltfr.fil" to obtain spatial distribution of salinity
  (the mass fraction of dissolved NaCl in the pore liquid).
Detailed distribution report for fluid salinity (dissolved NaCl mass fraction)
  was written on output file "rpsaltfr.fil".
Detailed report on spatial distribution of native brine properties
  was written on output file "rpflprop.fil".
Reading input file "inporost.fil" to obtain rock porosity distribution.
Detailed distribution report for country rock porosity
  was written on output file "rpporost.fil".
Reading input file "incomprs.fil" to obtain rock compressibility distribution.
Detailed report on spatial compressibility distribution
  was written on output file "rpcomprs.fil".
```

Figure B-1: Output *"rphistry.fil"* file generated by sample problem *"spfracsm.exe"* run.

```
Reading input file "intortuo.fil" to obtain pore tortuosity distribution.
Detailed distribution report for country rock tortuosity
  was written on output file "rptortuo.fil".
Reading input file "inpermis.fil" to obtain
  rock isotropic permeability distribution.
Detailed distribution report for isotropic rock permeability
  was written on output file "rppermis.fil".
Input file "inprmavh.fil" not found.
No vertical/horizontal permeability anisotropy present.
Input file "inprmaxy.fil" not found.
No x/y horizontal permeability anisotropy present.
Reading input file "infrcmdl.fil" to obtain fracture model parameters.
Reading input file "infrcgeo.fil" to obtain fracture system geometry.
Detailed report describing fracture system was written on
  output file "rpfractr.fil".
Reading input file "incndrok.fil" to obtain
  rock isotropic conductivity distribution.
Detailed distribution report for isotropic solid rock electrical conductivity
  was written on output file "rpcndrok.fil".
Reading input file "incndmdl.fil" to identify
  model for combining conductivities.
Total conductivity = rock conductivity.
Reading input file "incndsrf.fil" to obtain
  surface conductivity data.
Detailed distribution report for surface electrical conductivity
  was written on output file "rpcndsrf.fil".
Input file "incndavh.fil" not found.
No vertical/horizontal conductivity anisotropy present.
Input file "incndaxy.fil" not found.
No x/y horizontal conductivity anisotropy present.
Detailed report on spatial distribution of electrical
  resistivity was written on output file "rpresist.fil".
Reading input file "instrmdl.fil" to choose model for
  zeta-potential and streaming potential coefficient.
Ishido/Mizutani model selected
  with delta-pH = 5.00000.
Detailed report on the spatial distributions of adsorption (zeta) potential
  and streaming potential coefficient was written on output file "rpstrzta.fil".
Reading input file "intwophs.fil" to locate two-phase region.
Input file "intwophs.fil" absent.  No two-phase region present.
Reading input file "incasing.fil"to obtain descriptions
  of metallic well casings.
Reading input data for well casing number 1.
Reading input data for well casing number 2.
Detailed well casing report was written on output file "rpcasing.fil".
Reading input file "ininjwel.fil" to obtain injection well description.
Detailed report on injection well geometry was written
  on output file "rpinjwel.fil".
Reading input file "ininjhis.fil" to obtain
  specified injection flowrate/pressure history.
Detailed report on injection history specification was written
  on output file "rpinjhis.fil".
Reading input file "invsensr.fil" to locate potential sensors.
Detailed report on potential sensor locations was
  written on output file "rpvsensr.fil".
Reading input file "inpsensr.fil" to locate pressure sensors.
Input file "inpsensr.fil" absent.  No pressure sensors present.

PROBLEM SPECIFICATION PHASE COMPLETED

COMPUTATIONAL PHASE BEGINS

History record created for step 8 (28800.000000000 seconds).
History record created for step 10 (57600.000000000 seconds).
History record created for step 12 (86400.000000000 seconds).
```

Figure B-1: Output *"rphistry.fil"* file *(cont.)*.

```
History record created for step 14 (115200.00000000 seconds).
History record created for step 16 (144000.00000000 seconds).
History record created for step 18 (172800.00000000 seconds).
History record created for step 20 (201600.00000000 seconds).
History record created for step 22 (230400.00000000 seconds).
History record created for step 24 (259200.00000000 seconds).
History record created for step 26 (288000.00000000 seconds).
History record created for step 28 (316800.00000000 seconds).
History record created for step 30 (345600.00000000 seconds).
History record created for step 32 (374400.00000000 seconds).
History record created for step 34 (403200.00000000 seconds).
History record created for step 36 (432000.00000000 seconds).
History record created for step 38 (460800.00000000 seconds).
History record created for step 40 (489600.00000000 seconds).
History record created for step 42 (518400.00000000 seconds).
History record created for step 44 (547200.00000000 seconds).
History record created for step 46 (576000.00000000 seconds).
History record created for step 48 (604800.00000000 seconds).
History record created for step 50 (633600.00000000 seconds).
History record created for step 52 (662400.00000000 seconds).
History record created for step 54 (691200.00000000 seconds).
Full-grid dump record created on file "rpgd0001.fil"
  for step 54 (691200.00000000 seconds; 192.00000000000 hours).
History record created for step 56 (720000.00000000 seconds).
History record created for step 58 (748800.00000000 seconds).
History record created for step 60 (777600.00000000 seconds).

                  [120 lines skipped here]

History record created for step 288 (4060800.0000000 seconds).
History record created for step 290 (4089600.0000000 seconds).
History record created for step 292 (4118400.0000000 seconds).
History record created for step 294 (4147200.0000000 seconds).
Full-grid dump record created on file "rpgd0006.fil"
  for step 294 (4147200.0000000 seconds; 1152.0000000000 hours).

COMPUTATIONAL PHASE COMPLETED

PREPARING TEMPORAL HISTORY REPORTS

Voltage record from sensor 1 written on output file "rpsv0001.fil".
Voltage record from sensor 2 written on output file "rpsv0002.fil".
Voltage record from sensor 3 written on output file "rpsv0003.fil".
Voltage record from sensor 4 written on output file "rpsv0004.fil".
Voltage record from sensor 5 written on output file "rpsv0005.fil".
Voltage record from sensor 6 written on output file "rpsv0006.fil".
Voltage record from sensor 7 written on output file "rpsv0007.fil".
Voltage record from sensor 8 written on output file "rpsv0008.fil".
Voltage record from sensor 9 written on output file "rpsv0009.fil".
Voltage record from sensor 10 written on output file "rpsv0010.fil".
Voltage record from sensor 11 written on output file "rpsv0011.fil".
Voltage record from sensor 12 written on output file "rpsv0012.fil".
Voltage record from sensor 13 written on output file "rpsv0013.fil".
Voltage record from sensor 14 written on output file "rpsv0014.fil".
Voltage record for well casing 1 written on output file "rpwv0001.fil".
Voltage record for well casing 2 written on output file "rpwv0002.fil".
Injection well pressure/volume history written on output file "rpwellhs.fil".
Simulator performance report written on output file "rperform.fil".

TEMPORAL HISTORY REPORTS COMPLETE

JOB FINISHED

Execution completed Tue Aug 12 13:54:59 2008.
Total CPU time used = 2.0101778 hours.
```

Figure B-1: Output *"rphistry.fil"* file *(concl.).*

Contents of SPFRAC output file "rperform.fil":

```
  #######     #########      ############  #########     #########      #######
 #########    ##########     ############  ##########   ############    #########
##       ##   ##       ##    ##            ##       ##  ##        ##    ##       ##
##            ##       ##    ##            ##       ##  ##        ##    ##
##            ##########     #########     ##########  ##        ##    ##
 #######      #########      #########     #########   ############    ##
   #######    ##             ##            ##   ###    ############    ##
         ##   ##             ##            ##    ###   ##        ##    ##
         ##   ##             ##            ##     ##   ##        ##    ##
##       ##   ##             ##            ##      ##  ##        ##    ##       ##
 #########    ##             ##            ##      ### ##        ##     #########
  #######     ##             ##            ##       ## ##        ##      #######
```

Output data file from the SPFRAC calculation initiated Tue Aug 12 11:51:55 2008.

Summary of SPFRAC simulator performance during the calculation:

	Fluid Pressure Solution		Self-Potential Solution	
	cumulative time steps	cumulative iterations	cumulative time steps	cumulative iterations
8.0000000 hours elapsed	8	906	1	2748
16.000000 hours elapsed	10	1290	2	3120
24.000000 hours elapsed	12	1767	3	3480
32.000000 hours elapsed	14	2373	4	3840
40.000000 hours elapsed	16	3102	5	4200
[110 lines skipped here]				
928.00000 hours elapsed	238	70296	116	37260
936.00000 hours elapsed	240	70566	117	37536
944.00000 hours elapsed	242	70830	118	37812
952.00000 hours elapsed	244	71088	119	38088
960.00000 hours elapsed	246	71346	120	38364
968.00000 hours elapsed	248	71604	121	38856
976.00000 hours elapsed	250	71862	122	39132
984.00000 hours elapsed	252	72120	123	39408
992.00000 hours elapsed	254	72378	124	39684
1000.0000 hours elapsed	256	72636	125	39960
1008.0000 hours elapsed	258	72888	126	40236
1016.0000 hours elapsed	260	73140	127	40512
1024.0000 hours elapsed	262	73392	128	40788
1032.0000 hours elapsed	264	73644	129	41064
1040.0000 hours elapsed	266	73896	130	41340
1048.0000 hours elapsed	268	74148	131	41616
1056.0000 hours elapsed	270	74400	132	41892
1064.0000 hours elapsed	272	74652	133	42168
1072.0000 hours elapsed	274	74904	134	42444
1080.0000 hours elapsed	276	75150	135	42720
1088.0000 hours elapsed	278	75396	136	43212
1096.0000 hours elapsed	280	75642	137	43488
1104.0000 hours elapsed	282	75888	138	43764
1112.0000 hours elapsed	284	76134	139	44040
1120.0000 hours elapsed	286	76380	140	44316
1128.0000 hours elapsed	288	76626	141	44592
1136.0000 hours elapsed	290	76872	142	44868
1144.0000 hours elapsed	292	77118	143	45144
1152.0000 hours elapsed	294	77364	144	45420

Figure B-2: Output *"rperform.fil"* file generated by sample problem *"spfracsm.exe"* run.

Contents of SPFRAC output file "rpwellhs.fil":

```
  #######     #########      ###########  #########     #########      #######
 #########    ##########     ###########  ##########   ###########    #########
##       ##   ##       ##    ##           ##       ##  ##       ##    ##       ##
##            ##       ##    ##           ##       ##  ##       ##    ##
##            ##########     #########    ##########  ##       ##    ##
 #######      #########      #########    #########   ###########    ##
   #######    ##             ##           ##   ###    ###########    ##
         ##   ##             ##           ##    ###   ##       ##    ##
         ##   ##             ##           ##     ##   ##       ##    ##
##       ##   ##             ##           ##      ##  ##       ##    ##       ##
 #########    ##             ##           ##      ### ##       ##     #########
  #######     ##             ##           ##       ## ##       ##      #######
```

Output data file from the SPFRAC calculation initiated Tue Aug 12 11:51:55 2008.

Computed pressure / injection-volume history for the injection well:

Elapsed time	Well overpressure	Well injection rate	Cumulative injection
8.0000000 hr	10.000000000000 MPa	10.439452475900 l/s	335.80800863125 cu.m.
16.000000 hr	10.000000000000 MPa	9.8763913648000 l/s	623.69126264306 cu.m.
24.000000 hr	10.000000000000 MPa	9.4295256311000 l/s	898.56339906614 cu.m.
32.000000 hr	10.000000000000 MPa	8.9123992120000 l/s	1159.0779757050 cu.m.

[40 lines skipped here]

360.00000 hr	10.000000000000 MPa	3.8794754011000 l/s	7182.0107168954 cu.m.
368.00000 hr	10.000000000000 MPa	3.8537773936000 l/s	7293.1829927706 cu.m.
376.00000 hr	10.000000000000 MPa	3.8289124768000 l/s	7403.6332423483 cu.m.
384.00000 hr	10.000000000000 MPa	3.8048373479000 l/s	7513.3845086770 cu.m.
392.00000 hr	0.0000000000000 MPa	-6.960239347000 l/s	7276.0599353926 cu.m.
400.00000 hr	0.0000000000000 MPa	-4.637724041000 l/s	7129.2152564727 cu.m.
408.00000 hr	0.0000000000000 MPa	-3.515084344000 l/s	7021.1385512781 cu.m.
416.00000 hr	0.0000000000000 MPa	-2.870844906000 l/s	6934.3834306400 cu.m.
424.00000 hr	0.0000000000000 MPa	-2.456703901000 l/s	6860.9408322560 cu.m.

[80 lines skipped here]

1072.0000 hr	0.0000000000000 MPa	-0.234060347000 l/s	5426.4699949101 cu.m.
1080.0000 hr	0.0000000000000 MPa	-0.231125941000 l/s	5419.7925559628 cu.m.
1088.0000 hr	0.0000000000000 MPa	-0.228254905000 l/s	5413.1982554938 cu.m.
1096.0000 hr	0.0000000000000 MPa	-0.225445267000 l/s	5406.6853112031 cu.m.
1104.0000 hr	0.0000000000000 MPa	-0.222695133000 l/s	5400.2519958609 cu.m.
1112.0000 hr	0.0000000000000 MPa	-0.220002688000 l/s	5393.8966350800 cu.m.
1120.0000 hr	0.0000000000000 MPa	-0.217366190000 l/s	5387.6176051962 cu.m.
1128.0000 hr	0.0000000000000 MPa	-0.214783963000 l/s	5381.4133312514 cu.m.
1136.0000 hr	0.0000000000000 MPa	-0.212254399000 l/s	5375.2822850770 cu.m.
1144.0000 hr	0.0000000000000 MPa	-0.209775953000 l/s	5369.2229834696 cu.m.
1152.0000 hr	0.0000000000000 MPa	-0.207347138000 l/s	5363.2339864552 cu.m.

Figure B-3: Output *"rpwellhs.fil"* file generated by sample problem *"spfracsm.exe"* run.

Contents of SPFRAC output file "rpwv0002.fil":

```
_____________________________________________________________________________

  #######     #########      ###########  #########     #########      #######
 #########    ##########     ###########  ##########   ###########    #########
##       ##   ##       ##    ##           ##       ##  ##        ##   ##       ##
##            ##       ##    ##           ##       ##  ##        ##   ##
##            ##########     #########    ##########   ##        ##   ##
 #######      #########      #########    #########    ###########   ##
   #######    ##             ##           ##   ###     ###########   ##
         ##   ##             ##           ##    ###    ##        ##   ##
         ##   ##             ##           ##     ##    ##        ##   ##
##       ##   ##             ##           ##      ##   ##        ##   ##       ##
 #########    ##             ##           ##      ###  ##        ##    #########
  #######     ##             ##           ##       ##  ##        ##     #######

_____________________________________________________________________________

Output data file from the SPFRAC calculation initiated Tue Aug 12 11:51:55 2008.

Electrical potential history for well casing number 2
Time                                          Electrical Potential
8.0000000 hours (28800.000000000 seconds)    -33.65154 mV (-0.033651543681 volt)
16.000000 hours (57600.000000000 seconds)    -62.00340 mV (-0.062003397926 volt)
24.000000 hours (86400.000000000 seconds)    -86.68724 mV (-0.086687236563 volt)
32.000000 hours (115200.00000000 seconds)    -108.6201 mV (-0.108620119107 volt)

                              [40 lines skipped here]

360.00000 hours (1296000.0000000 seconds)    -496.7298 mV (-0.496729827925 volt)
368.00000 hours (1324800.0000000 seconds)    -501.7650 mV (-0.501765007524 volt)
376.00000 hours (1353600.0000000 seconds)    -506.6887 mV (-0.506688693455 volt)
384.00000 hours (1382400.0000000 seconds)    -511.5040 mV (-0.511504027833 volt)
392.00000 hours (1411200.0000000 seconds)    -497.3745 mV (-0.497374537702 volt)
400.00000 hours (1440000.0000000 seconds)    -482.8557 mV (-0.482855664731 volt)
408.00000 hours (1468800.0000000 seconds)    -468.9656 mV (-0.468965598309 volt)
416.00000 hours (1497600.0000000 seconds)    -455.9435 mV (-0.455943521836 volt)
424.00000 hours (1526400.0000000 seconds)    -443.8192 mV (-0.443819218169 volt)

                              [80 lines skipped here]

1072.0000 hours (3859200.0000000 seconds)    -129.9741 mV (-0.129974059971 volt)
1080.0000 hours (3888000.0000000 seconds)    -128.5451 mV (-0.128545120245 volt)
1088.0000 hours (3916800.0000000 seconds)    -127.1401 mV (-0.127140132161 volt)
1096.0000 hours (3945600.0000000 seconds)    -125.7586 mV (-0.125758566613 volt)
1104.0000 hours (3974400.0000000 seconds)    -124.3999 mV (-0.124399908741 volt)
1112.0000 hours (4003200.0000000 seconds)    -123.0637 mV (-0.123063657352 volt)
1120.0000 hours (4032000.0000000 seconds)    -121.7493 mV (-0.121749324580 volt)
1128.0000 hours (4060800.0000000 seconds)    -120.4564 mV (-0.120456435469 volt)
1136.0000 hours (4089600.0000000 seconds)    -119.1845 mV (-0.119184527579 volt)
1144.0000 hours (4118400.0000000 seconds)    -117.9332 mV (-0.117933150611 volt)
1152.0000 hours (4147200.0000000 seconds)    -116.7019 mV (-0.116701866040 volt)
```

Figure B-4: Output *"rpwv0002.fil"* file generated by sample problem *"spfracsm.exe"* run.

Contents of SPFRAC output file "rpsv0011.fil":

```
_____________________________________________________________________________

  #######     #########      ###########  #########     #########      #######
 #########    ##########     ###########  ##########   ###########    #########
##       ##   ##       ##    ##           ##       ##  ##        ##   ##       ##
##            ##       ##    ##           ##       ##  ##        ##   ##
##            ##########     #########    ##########  ##        ##   ##
 #######      #########      #########    #########   ###########   ##
   #######    ##             ##           ##   ###    ###########   ##
         ##   ##             ##           ##    ###    ##        ##   ##
         ##   ##             ##           ##     ##    ##        ##   ##
##       ##   ##             ##           ##      ##   ##        ##   ##       ##
 #########    ##             ##           ##      ###  ##        ##    #########
  #######     ##             ##           ##       ##  ##        ##     #######
_____________________________________________________________________________

Output data file from the SPFRAC calculation initiated Tue Aug 12 11:51:55 2008.

Electrical potential signal recorded by sensor number 11

Sensor location:                In grid coordinates:
     653.58984 meters East,     x = -400.0000 meters,
     2200.0000 meters North,    y = 0.0000000 meters,
     -3000.000 meters RSL.      z = 0.0000000 meters.

Time                                        Electrical Potential
8.0000000 hours (28800.000000000 seconds)    0.2963246 mV (2.963245786E-04 volt)
16.000000 hours (57600.000000000 seconds)    0.5588550 mV (5.588549856E-04 volt)
24.000000 hours (86400.000000000 seconds)    0.5856808 mV (5.856807584E-04 volt)
32.000000 hours (115200.00000000 seconds)    0.2339656 mV (2.339655527E-04 volt)
40.000000 hours (144000.00000000 seconds)    -0.561149 mV (-5.61148908E-04 volt)

                          [50 lines skipped here]

448.00000 hours (1612800.0000000 seconds)    -154.6310 mV (-0.154630984359 volt)
456.00000 hours (1641600.0000000 seconds)    -154.8504 mV (-0.154850385193 volt)
464.00000 hours (1670400.0000000 seconds)    -154.8267 mV (-0.154826709758 volt)
472.00000 hours (1699200.0000000 seconds)    -154.5898 mV (-0.154589805969 volt)
480.00000 hours (1728000.0000000 seconds)    -154.1672 mV (-0.154167173805 volt)
488.00000 hours (1756800.0000000 seconds)    -153.5838 mV (-0.153583817791 volt)
496.00000 hours (1785600.0000000 seconds)    -152.8623 mV (-0.152862253480 volt)
504.00000 hours (1814400.0000000 seconds)    -152.0226 mV (-0.152022601587 volt)
512.00000 hours (1843200.0000000 seconds)    -151.0827 mV (-0.151082728523 volt)
520.00000 hours (1872000.0000000 seconds)    -150.0584 mV (-0.150058414686 volt)
528.00000 hours (1900800.0000000 seconds)    -148.9635 mV (-0.148963533682 volt)
536.00000 hours (1929600.0000000 seconds)    -147.8102 mV (-0.147810236685 volt)
544.00000 hours (1958400.0000000 seconds)    -146.6091 mV (-0.146609129899 volt)
552.00000 hours (1987200.0000000 seconds)    -145.3694 mV (-0.145369444683 volt)
560.00000 hours (2016000.0000000 seconds)    -144.0992 mV (-0.144099195778 volt)

                          [70 lines skipped here]

1128.0000 hours (4060800.0000000 seconds)    -75.74803 mV (-0.075748031963 volt)
1136.0000 hours (4089600.0000000 seconds)    -75.17524 mV (-0.075175238039 volt)
1144.0000 hours (4118400.0000000 seconds)    -74.60967 mV (-0.074609667927 volt)
1152.0000 hours (4147200.0000000 seconds)    -74.05120 mV (-0.074051195593 volt)
```

Figure B-5: Output *"rpsv0011.fil"* file generated by sample problem *"spfracsm.exe"* run.

Contents of SPFRAC output file "rpgd0003.fil":

```
  #######     #########      ###########  #########     #########      #######
 #########    ##########     ###########  ##########   ###########    #########
##       ##   ##       ##    ##           ##       ##  ##        ##   ##       ##
##            ##       ##    ##           ##       ##  ##        ##   ##
##            ##########     #########    ##########  ##        ##   ##
 #######      #########      #########    #########   ###########   ##
   #######    ##             ##           ##   ###    ###########   ##
         ##   ##             ##           ##    ###   ##        ##   ##
         ##   ##             ##           ##     ##   ##        ##   ##
##       ##   ##             ##           ##      ##  ##        ##   ##       ##
 #########    ##             ##           ##      ### ##        ##    #########
  #######     ##             ##           ##       ## ##        ##     #######
```

Output data file from the SPFRAC calculation initiated Tue Aug 12 11:51:55 2008.

Total number of hydrodynamic time-steps completed: 150
Elapsed time = 2073600.0000000 seconds = 576.00000000000 hours
Minimum grid electrical potential = -360.8100136067 millivolts
Maximum grid electrical potential = 61.572202377623 millivolts
Minimum grid fluid overpressure = 0.0000000000000 kilopascals
Maximum grid fluid overpressure = 2836.3243171067 kilopascals

Grid Block			Location meters			Electrical Potential	Fluid Overpressure
i	j	k	East	North	RSL	(millivolts)	(kilopascals)
			[45546 lines skipped here]				
6	22	22	441.41361	2322.5000	-3000.000	4.8434973775249	51.146778645667
7	22	22	480.38476	2300.0000	-3000.000	-0.224972628404	108.09126648972
8	22	22	515.02577	2280.0000	-3000.000	-9.376979627377	196.42189821702
9	22	22	549.66679	2260.0000	-3000.000	-25.90339230309	342.57950159929
10	22	22	584.30781	2240.0000	-3000.000	-52.71733224561	567.69840492730
11	22	22	618.94882	2220.0000	-3000.000	-91.73774988572	885.30803701969
12	22	22	653.58984	2200.0000	-3000.000	-141.4938396041	1284.1422678881
13	22	22	688.23085	2180.0000	-3000.000	-193.8515282812	1704.9360995144
14	22	22	722.87187	2160.0000	-3000.000	-230.4160763470	2015.2863996862
15	22	22	757.51289	2140.0000	-3000.000	-215.5496584042	1960.9401030296
16	22	22	792.15390	2120.0000	-3000.000	-207.6508839621	1952.6472703282
17	22	22	826.79492	2100.0000	-3000.000	-198.7662830430	1933.2624977249
18	22	22	861.43594	2080.0000	-3000.000	-188.2272121186	1898.1007156611
19	22	22	896.07695	2060.0000	-3000.000	-174.7879975284	1839.4636921684
20	22	22	930.71797	2040.0000	-3000.000	-155.7685095315	1740.7030551074
21	22	22	965.35898	2020.0000	-3000.000	-124.1833975814	1555.5674511504
22	22	22	1000.0000	2000.0000	-3000.000	-57.63996783135	1122.8066526209
23	22	22	1034.6410	1980.0000	-3000.000	-124.1833975772	1555.5674511504
24	22	22	1069.2820	1960.0000	-3000.000	-155.7685095257	1740.7030551074
25	22	22	1103.9230	1940.0000	-3000.000	-174.7879975185	1839.4636921684
26	22	22	1138.5641	1920.0000	-3000.000	-188.2272121045	1898.1007156611
27	22	22	1173.2051	1900.0000	-3000.000	-198.7662830258	1933.2624977249
28	22	22	1207.8461	1880.0000	-3000.000	-207.6508839414	1952.6472703282
29	22	22	1242.4871	1860.0000	-3000.000	-215.5496583812	1960.9401030296
30	22	22	1277.1281	1840.0000	-3000.000	-230.4160763217	2015.2863996862
31	22	22	1311.7691	1820.0000	-3000.000	-193.8515282537	1704.9360995144
32	22	22	1346.4102	1800.0000	-3000.000	-141.4938395748	1284.1422678881
33	22	22	1381.0512	1780.0000	-3000.000	-91.73774985457	885.30803701969
34	22	22	1415.6922	1760.0000	-3000.000	-52.71733221318	567.69840492730
35	22	22	1450.3332	1740.0000	-3000.000	-25.90339226987	342.57950159929
36	22	22	1484.9742	1720.0000	-3000.000	-9.376979593056	196.42189821702
37	22	22	1519.6152	1700.0000	-3000.000	-0.224972592667	108.09126648972
38	22	22	1558.5864	1677.5000	-3000.000	4.8434974142364	51.146778645667
			[45546 lines skipped here]				

Figure B-6: Output *"rpgd0003.fil"* file generated by sample problem *"spfracsm.exe"* run.

APPENDIX C:
GRAPHICS POSTPROCESSOR OUTPUT FROM ILLUSTRATIVE PROBLEM CALCULATION

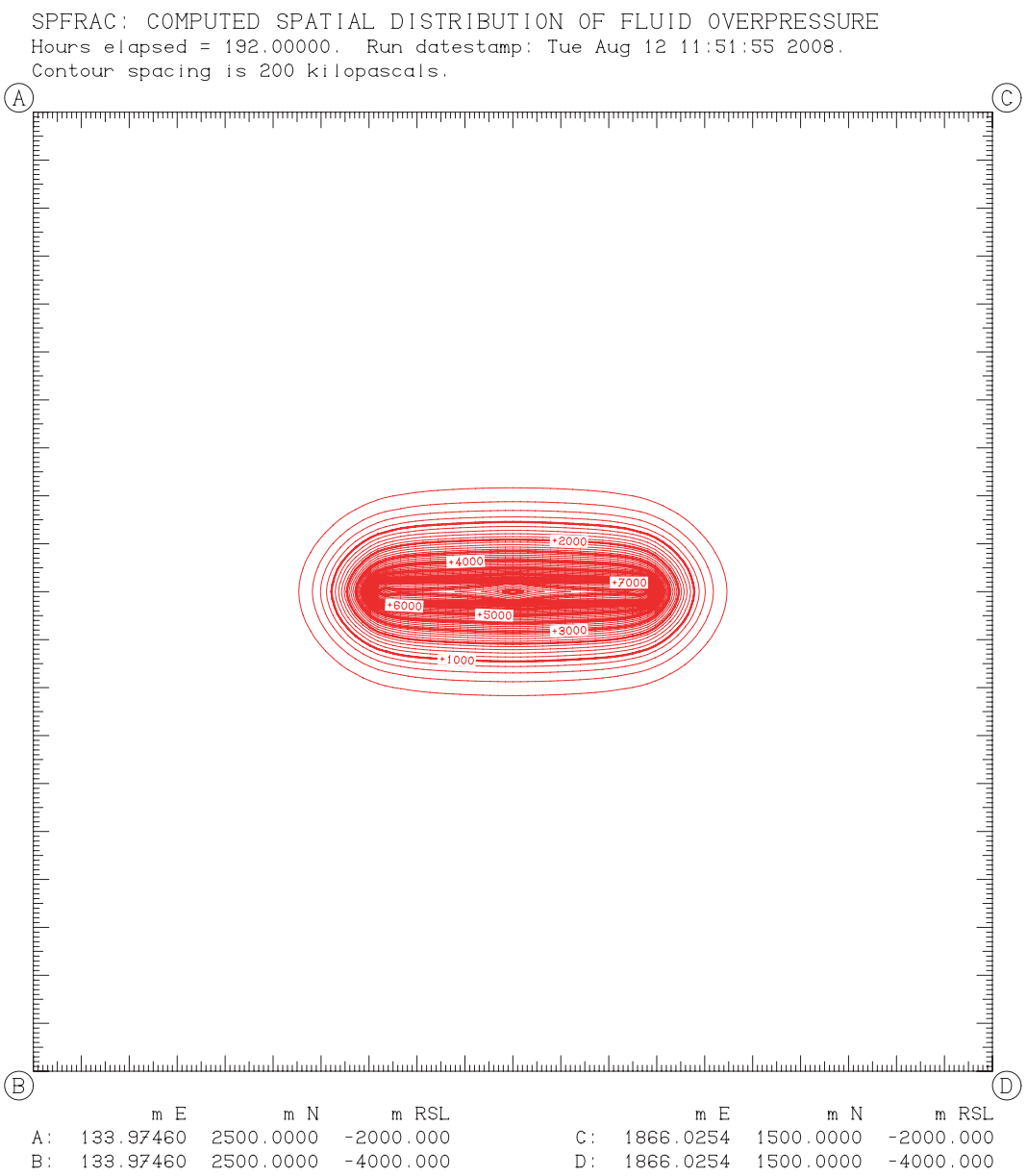

Figure C-1(a): Contour plot of the spatial distribution of fluid overpressure at t = 192 hours for sample case in vertical x-z plane at y = 0 created by running *"spspltcp.exe"* using input data shown in Appendix A, Figure A-10. Pressure data obtained from *"spfrac.exe"* output file *"rpgd0001.fil"* (similar to Appendix B, Figure B-6). Graphical output was written on file *"plpc0001.igf"* and rendered using *"Jplot."*

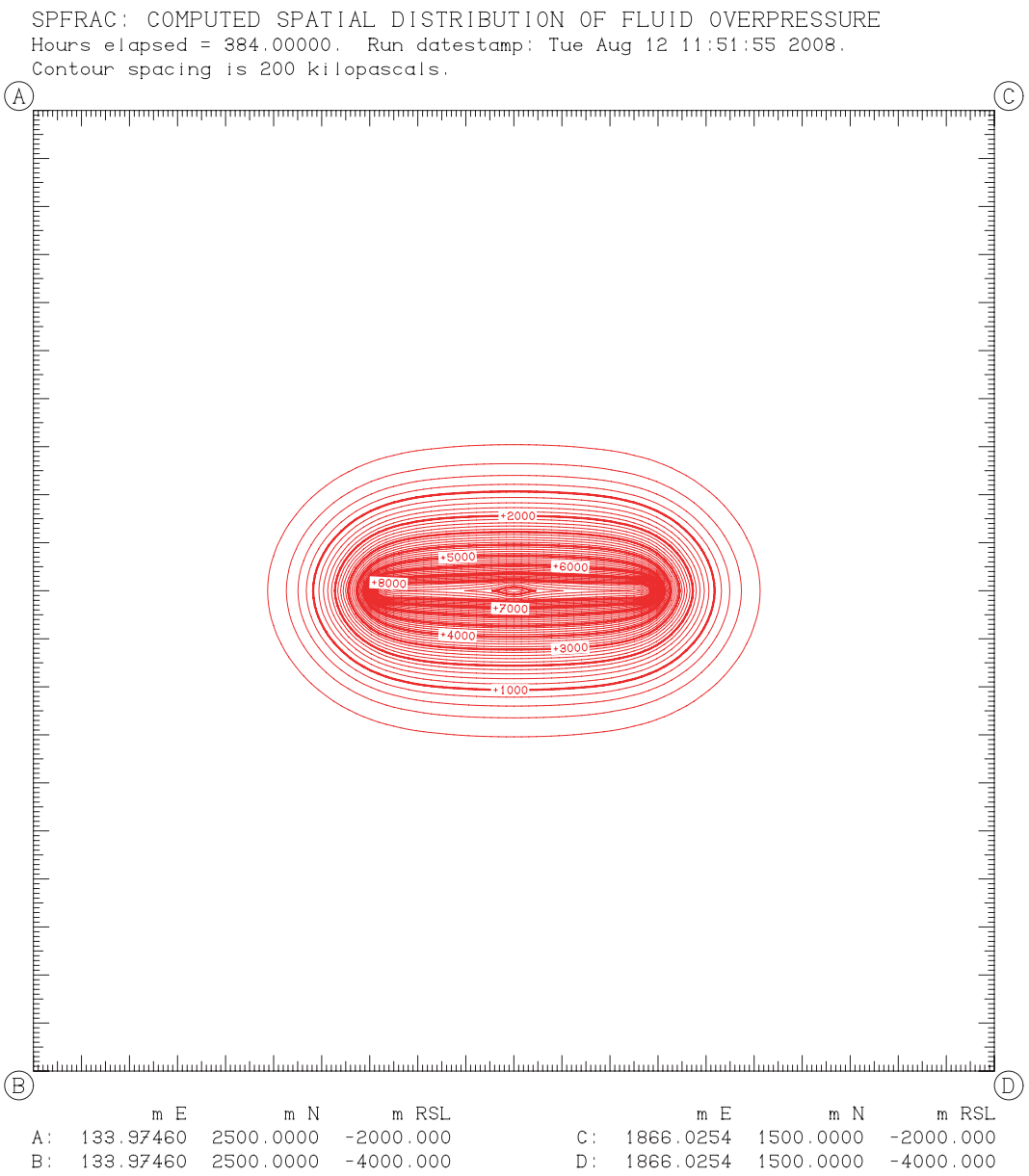

Figure C-1(b): Contour plot of the spatial distribution of fluid overpressure at t = 384 hours (end of stimulation period) for sample case in vertical x-z plane at y = 0 created by running *"spspltcp.exe"* using input data shown in Appendix A, Figure A-10. Pressure data obtained from *"spfrac.exe"* output file *"rpgd0002.fil"* (like Appendix B, Figure B-6). Graphical output was written on file *"plpc0002.igf"* and rendered using *"Jplot."*

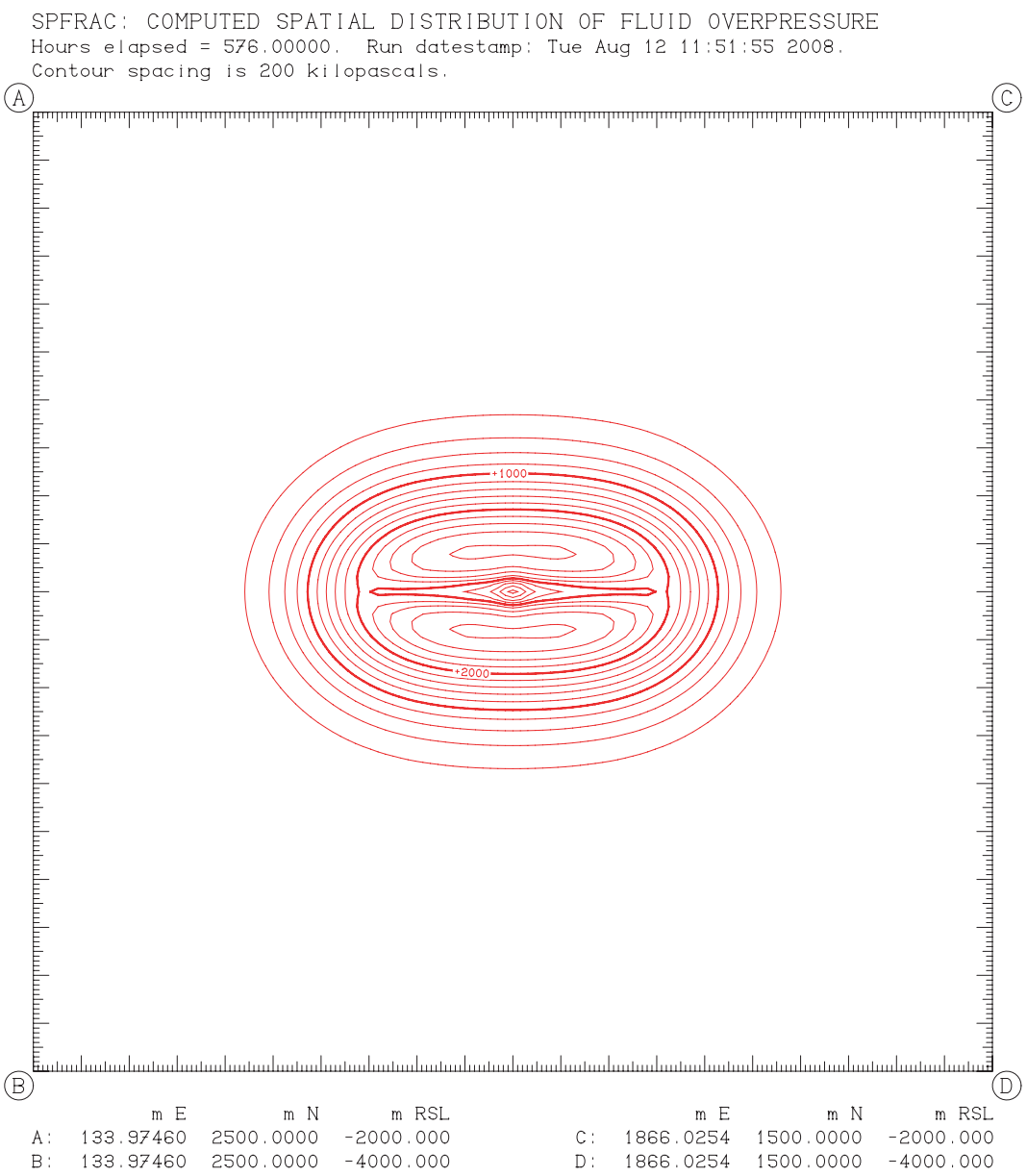

Figure C-1(c): Contour plot of the spatial distribution of fluid overpressure at t = 576 hours for sample case in vertical x-z plane at y = 0 created by running *"spspltcp.exe"* using input data shown in Appendix A, Figure A-10. Pressure data obtained from *"spfrac.exe"* output file *"rpgd0003.fil"* (Appendix B, Figure B-6). Graphical output was written on file *"plpc0003.igf"* and rendered using *"Jplot."*

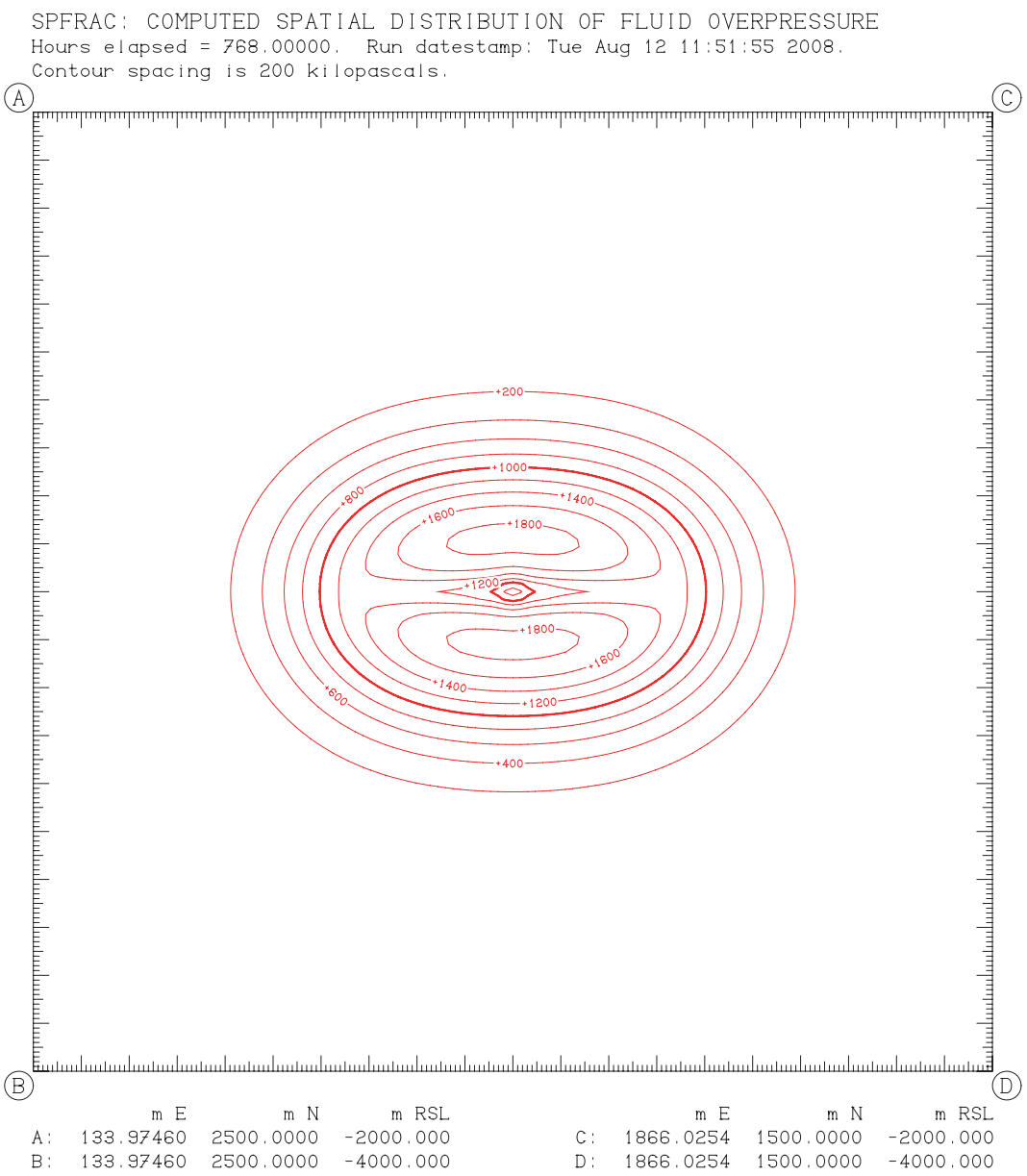

Figure C-1(d): Contour plot of the spatial distribution of fluid overpressure at t = 768 hours for sample case in vertical x-z plane at y = 0 created by running *"spspltcp.exe"* using input data shown in Appendix A, Figure A-10. Pressure data obtained from *"spfrac.exe"* output file *"rpgd0004.fil"* (similar to Appendix B, Figure B-6). Graphical output was written on file *"plpc0004.igf"* and rendered using *"Jplot."*

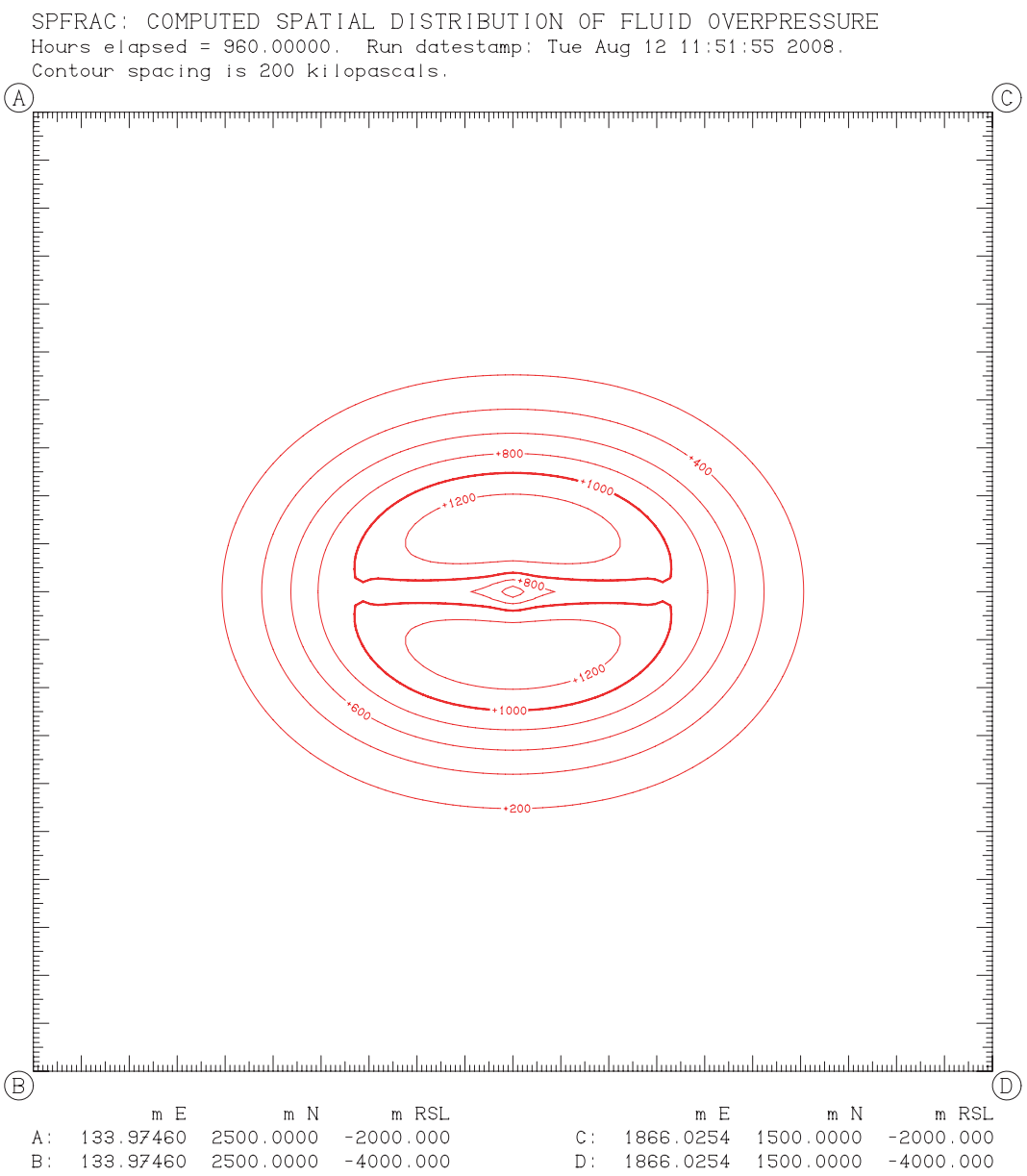

Figure C-1(e): Contour plot of the spatial distribution of fluid overpressure at t = 960 hours for sample case in vertical x-z plane at y = 0 created by running *"spspltcp.exe"* using input data shown in Appendix A, Figure A-10. Pressure data obtained from *"spfrac.exe"* output file *"rpgd0005.fil"* (similar to Appendix B, Figure B-6). Graphical output was written on file *"plpc0005.igf"* and rendered using *"Jplot."*

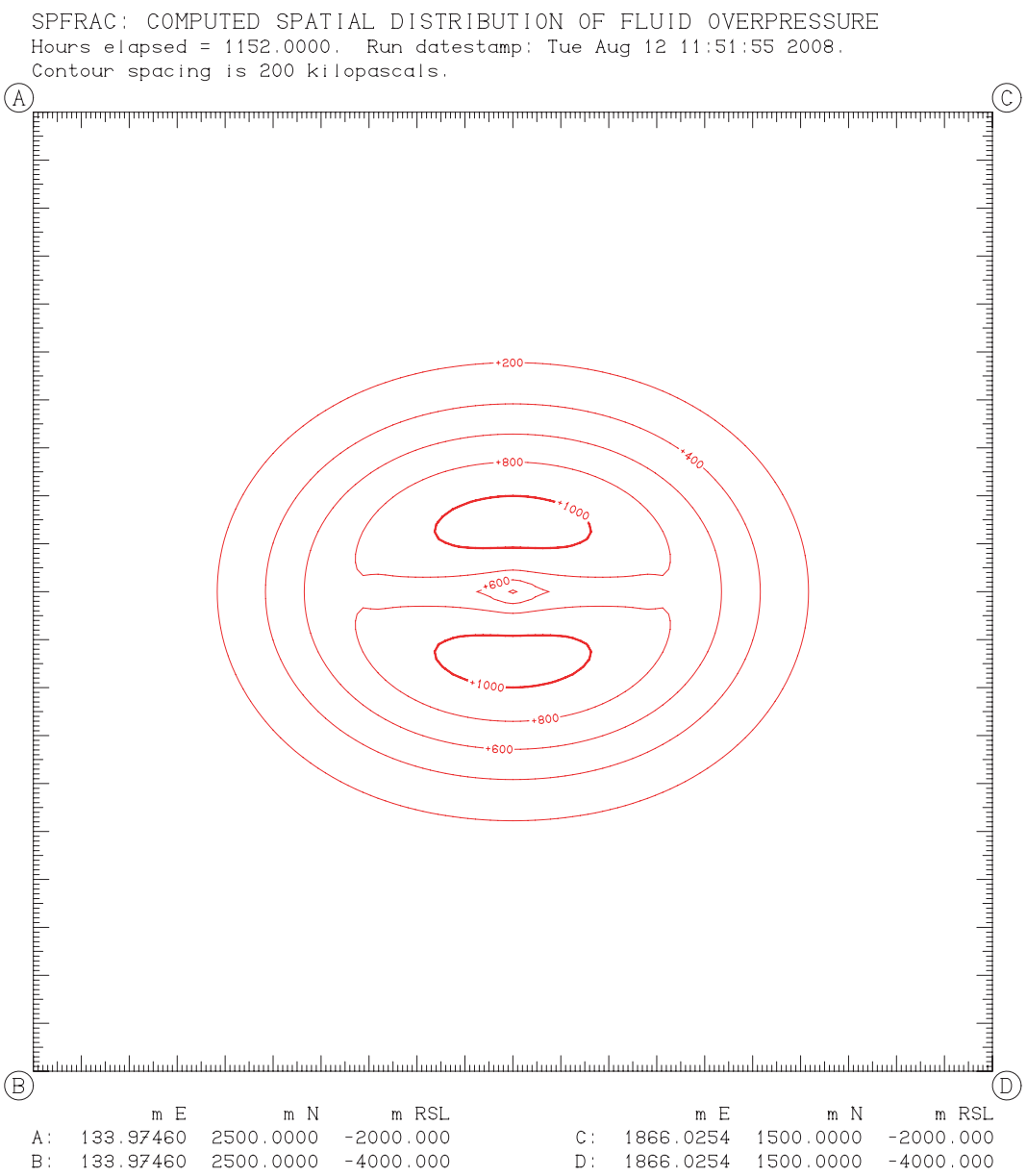

Figure C-1(f): Contour plot of the spatial distribution of fluid overpressure at t = 1152 hours for sample case in vertical x-z plane at y = 0 created by running *"spspltcp.exe"* using input data shown in Appendix A, Figure A-10. Pressure data obtained from *"spfrac.exe"* output file *"rpgd0006.fil"* (similar to Appendix B, Figure B-6). Graphical output was written on file *"plpc0006.igf"* and rendered using *"Jplot."*

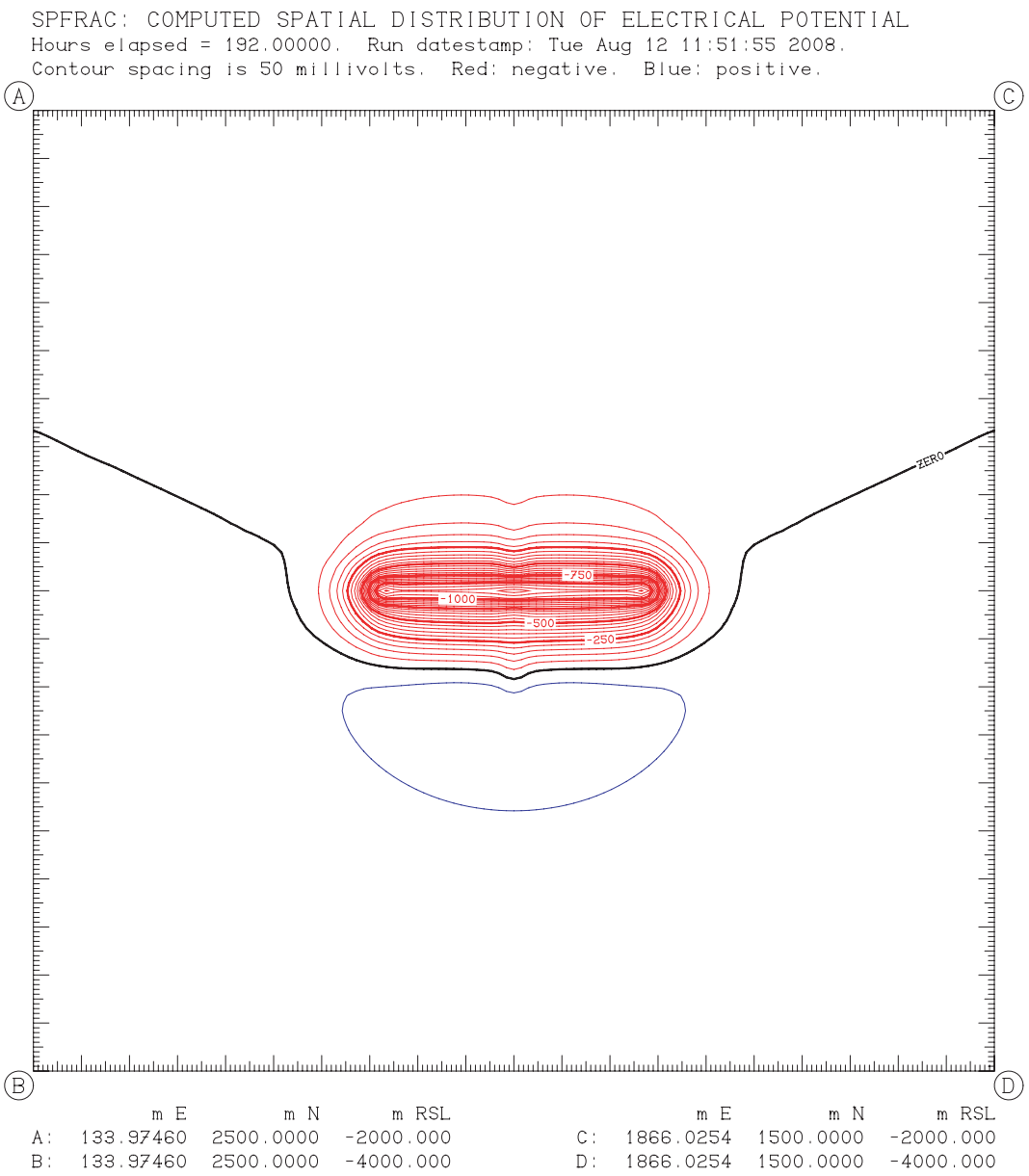

Figure C-2(a): Contour plot of the spatial distribution of electrical potential at t = 192 hours for sample case in vertical x-z plane at y = 0 created by running *"spfpltcv.exe"* using input data shown in Appendix A, Figure A-10. Potential data obtained from *"spfrac.exe"* output file *"rpgd0001.fil"* (similar to Appendix B, Figure B-6). Graphical output was written on file *"plvc0001.igf"* and rendered using *"Jplot."*

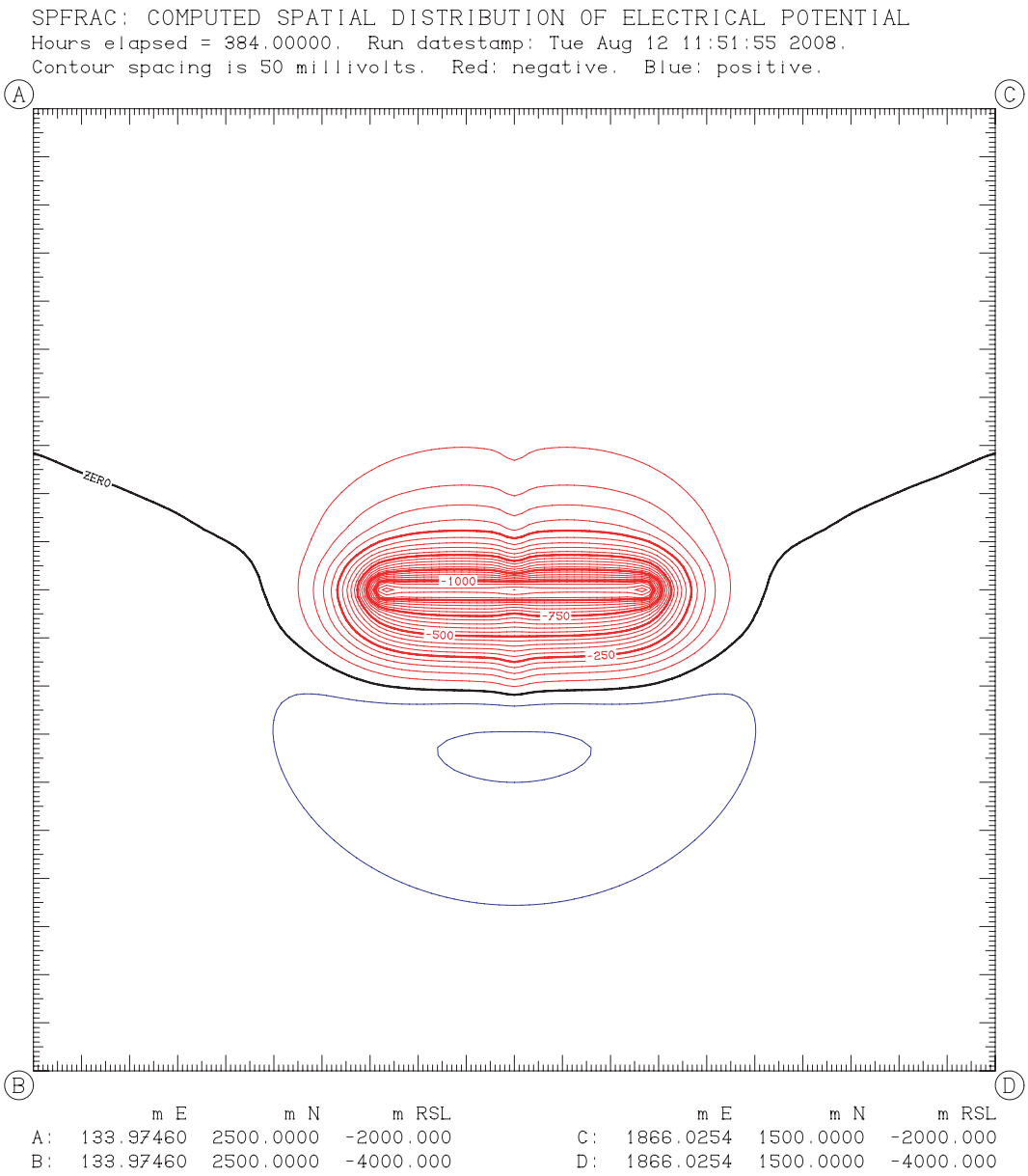

Figure C-2(b): Contour plot of the spatial distribution of electrical potential at t = 384 hours (end of stimulation) for sample case in vertical x-z plane at y = 0 created by running *"spfpltcv.exe"* using input data shown in Appendix A, Figure A-10. Potential data obtained from *"spfrac.exe"* output file *"rpgd0002.fil"* (like Appendix B, Figure B-6). Graphical output was written on file *"plvc0002.igf"* and rendered using *"Jplot."*

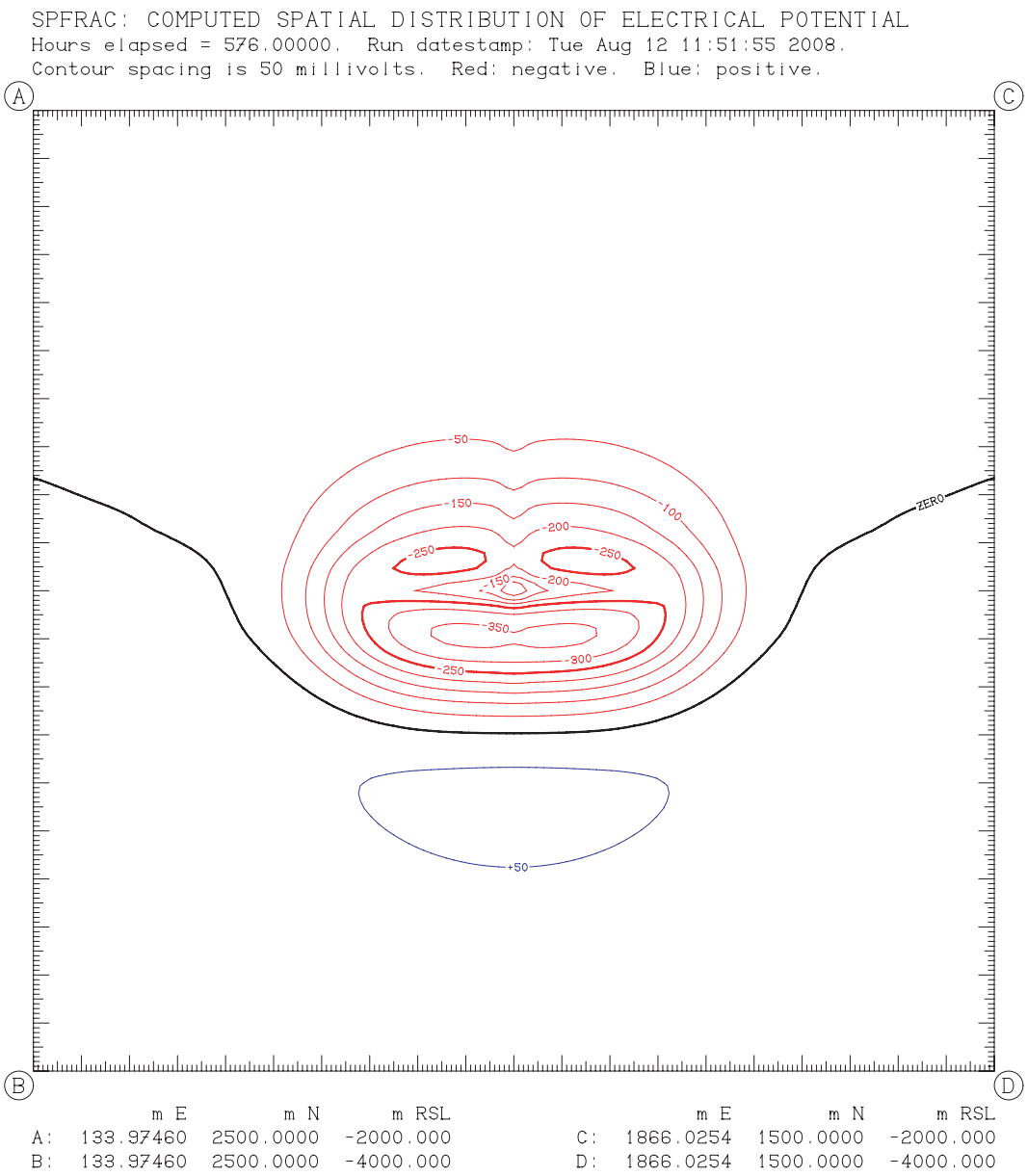

Figure C-2(c): Contour plot of the spatial distribution of electrical potential at t = 576 hours for sample case in vertical x-z plane at y = 0 created by running *"spfpltcv.exe"* using input data shown in Appendix A, Figure A-10. Potential data obtained from *"spfrac.exe"* output file *"rpgd0003.fil"* (Appendix B, Figure B-6). Graphical output was written on file *"plvc0003.igf"* and rendered using *"Jplot."*

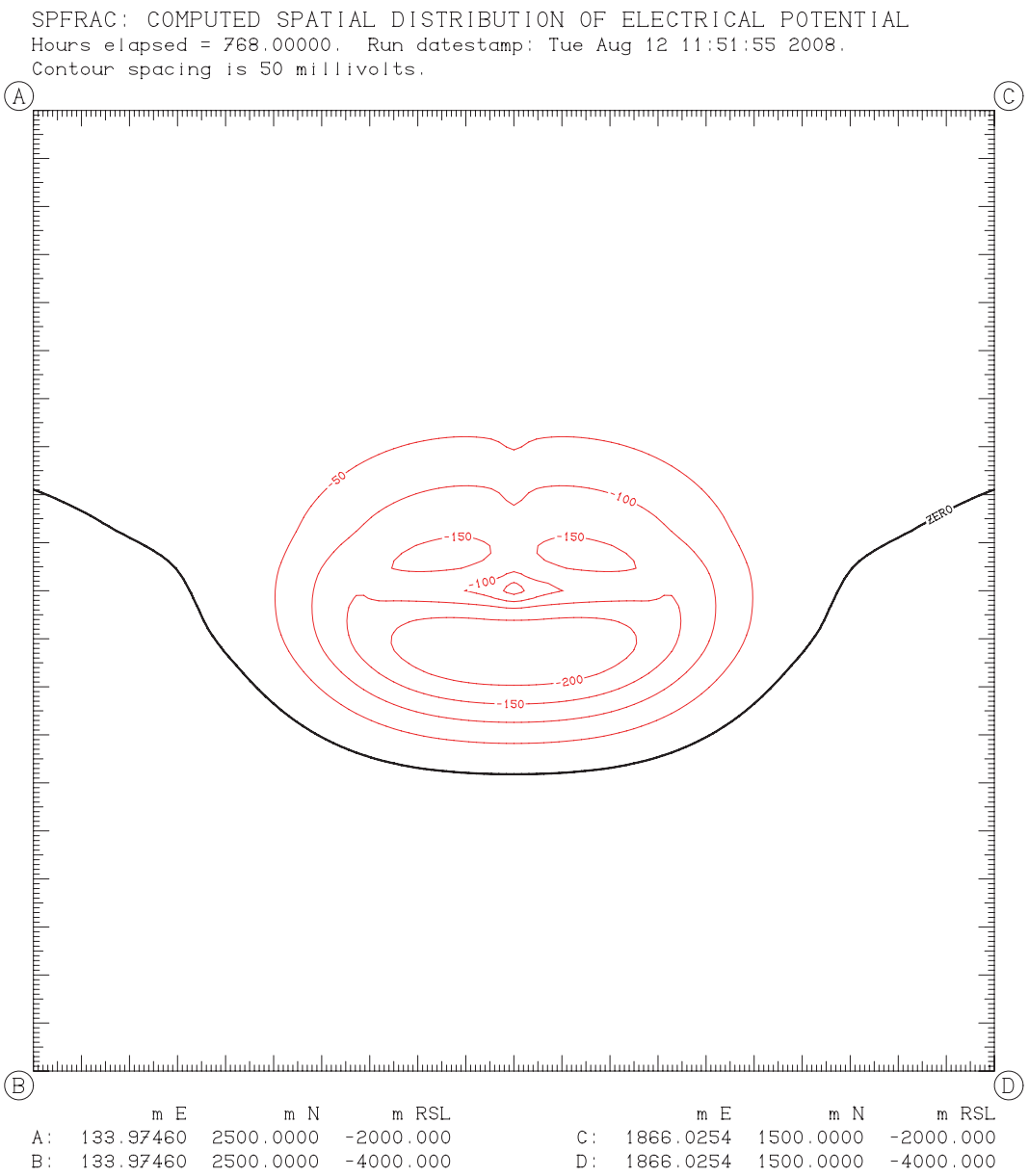

Figure C-2(d): Contour plot of the spatial distribution of electrical potential at t = 768 hours for sample case in vertical x-z plane at y = 0 created by running *"spfpltcv.exe"* using input data shown in Appendix A, Figure A-10. Potential data obtained from *"spfrac.exe"* output file *"rpgd0004.fil"* (similar to Appendix B, Figure B-6). Graphical output was written on file *"plvc0004.igf"* and rendered using *"Jplot."*

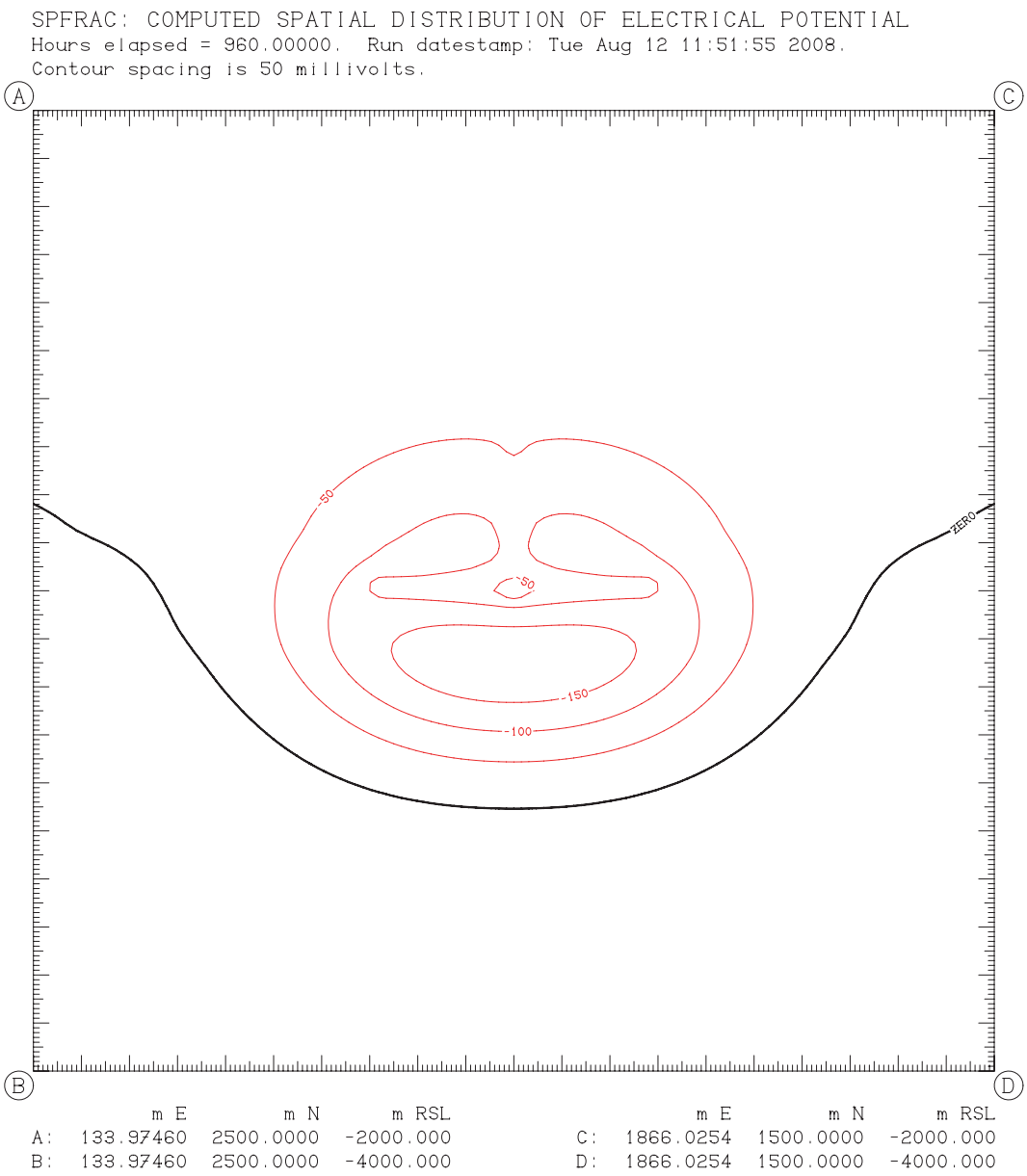

Figure C-2(e): Contour plot of the spatial distribution of electrical potential at t = 960 hours for sample case in vertical x-z plane at y = 0 created by running *"spfpltcv.exe"* using input data shown in Appendix A, Figure A-10. Potential data obtained from *"spfrac.exe"* output file *"rpgd0005.fil"* (similar to Appendix B, Figure B-6). Graphical output was written on file *"plvc0005.igf"* and rendered using *"Jplot."*

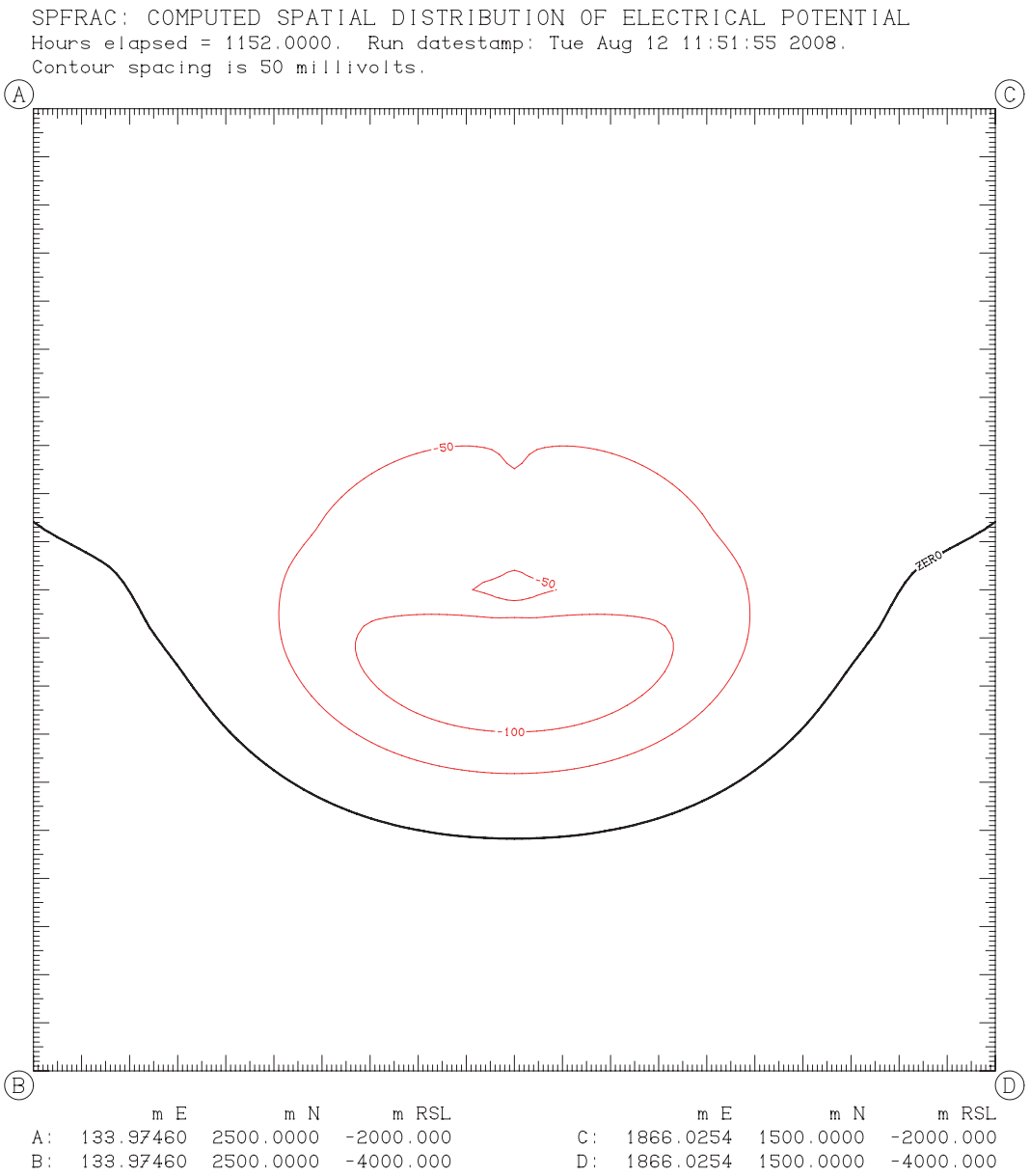

Figure C-2(f): Contour plot of the spatial distribution of electrical potential at t = 1152 hours for sample case in vertical x-z plane at y = 0 created by running *"spfpltcv.exe"* using input data shown in Appendix A, Figure A-10. Potential data obtained from *"spfrac.exe"* output file *"rpgd0006.fil"* (similar to Appendix B, Figure B-6). Graphical output was written on file *"plvc0006.igf"* and rendered using *"Jplot."*

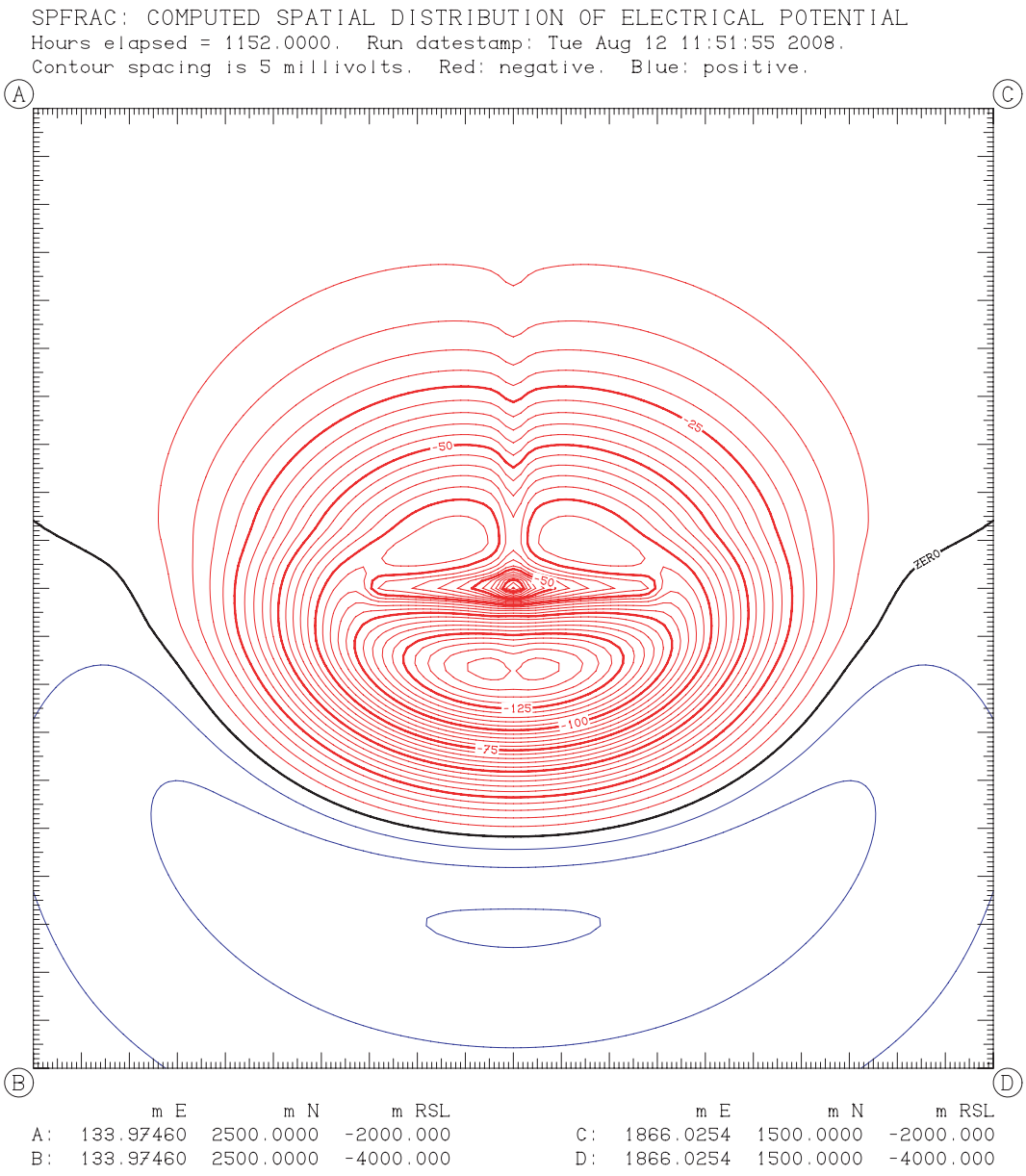

Figure C-2(g): Contour plot of the spatial distribution of electrical potential at t = 1152 hours for sample case in vertical x-z plane at y = 0 created by running *"spfpltcv.exe"* using input data shown in Appendix A, Figure A-10. Potential data obtained from *"spfrac.exe"* output file *"rpgd0006.fil"* (similar to Appendix B, Figure B-6). Data are the same as for Figure C-2(f); this plot was made by a separate run of *"spspcv.exe"* with an additional input file (*"inconttm.fil")* containing a single line with a single number ("6") entered upon it. This separate run therefore considered only the data for t = 1152 hours (instead of the entire history) in choosing contour levels, resulting in higher resolution.

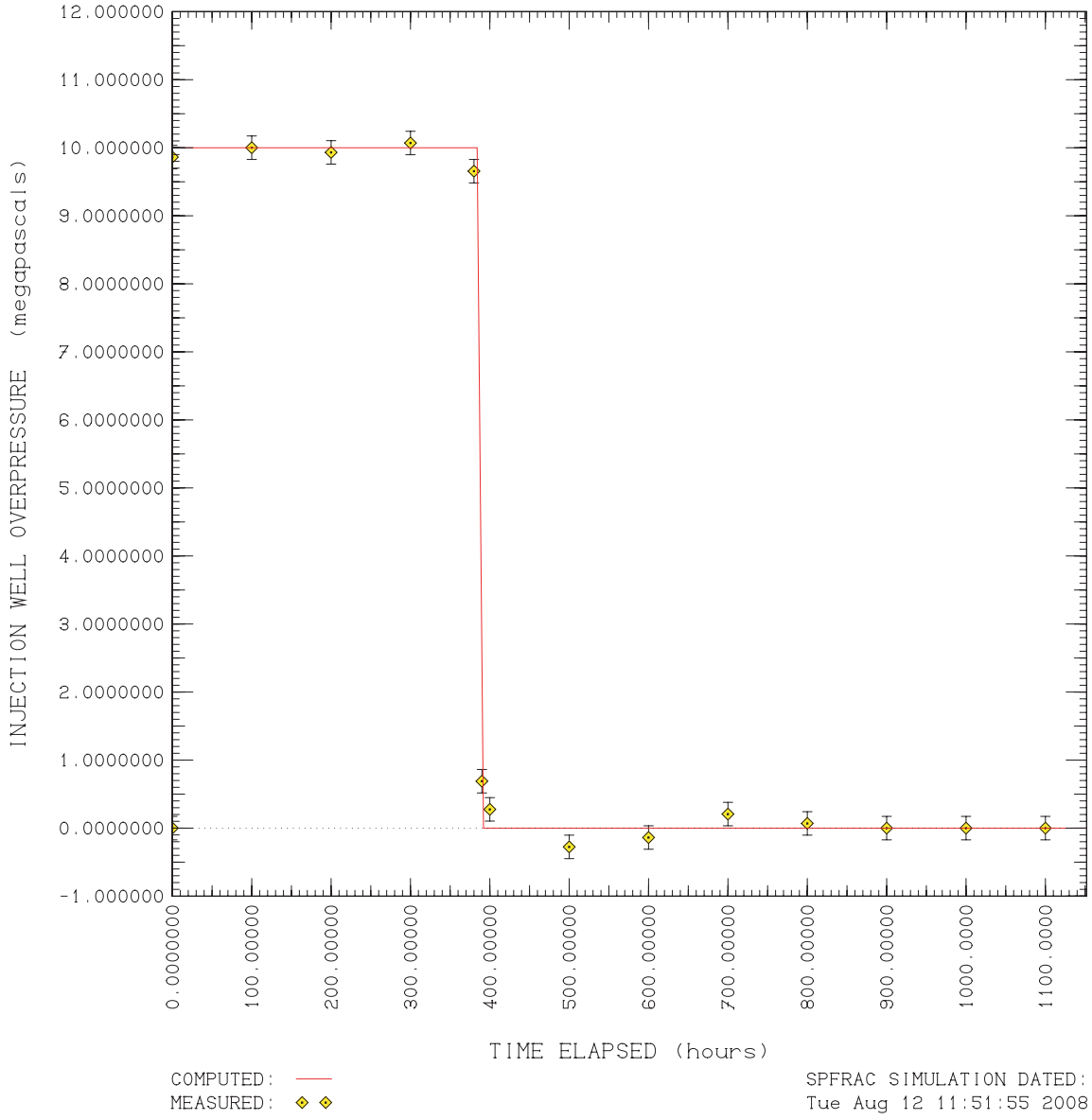

Figure C-3(a): Plot created by running *"spfpltin.exe"* graphics postprocessor of the imposed time-history of injection well overpressure as compared with "measurements" provided on input file *"dtinjprs.fil"* (see Appendix A, Figure A-11). Data for plotting was read from output file *"rpwellhs.fil"* (Appendix B, Figure B-3). Graphical output was written on file *"plinjprs.igf"* and rendered using *"Jplot."*

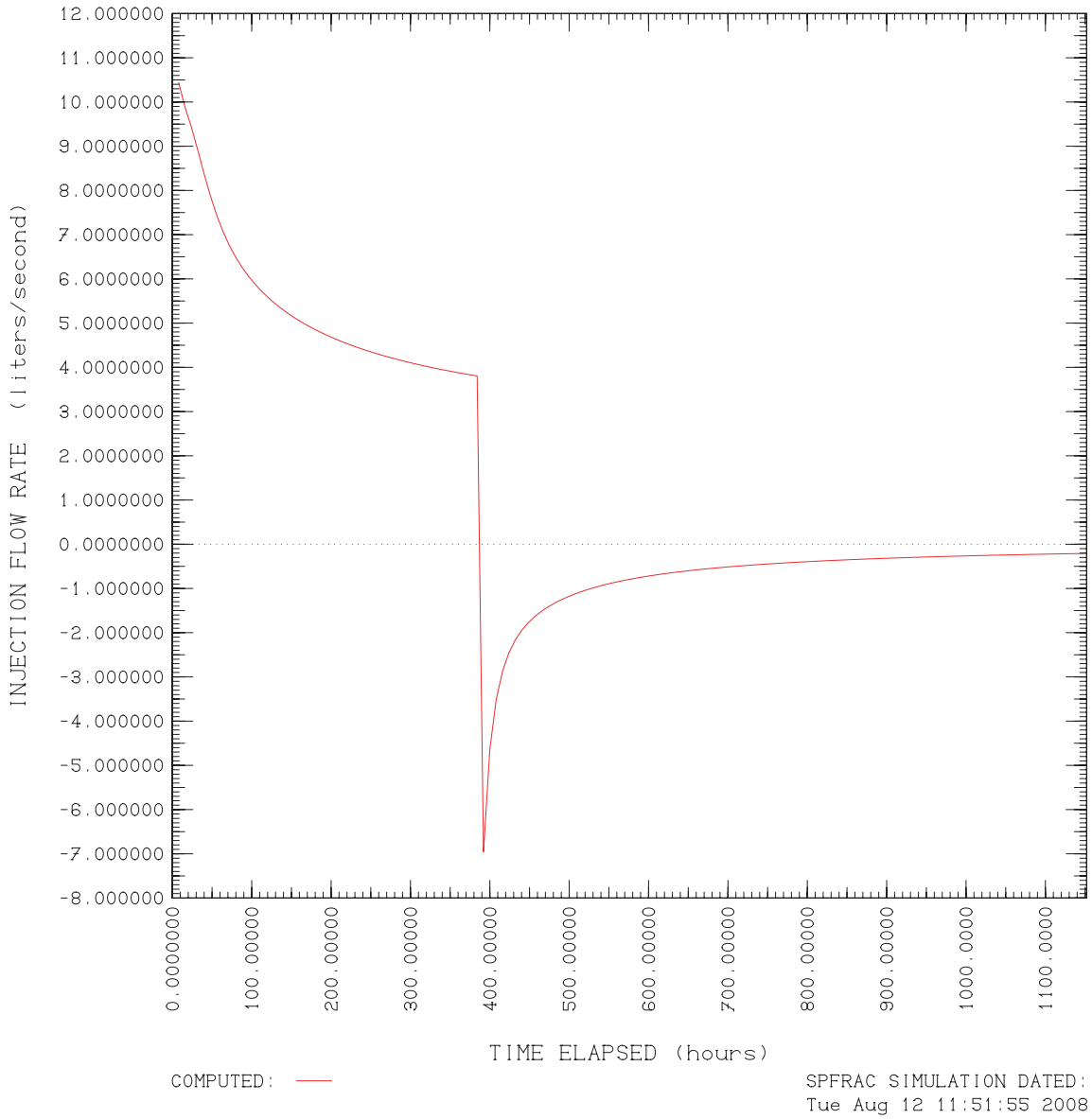

Figure C-3(b): Plot created by running *"spfpltin.exe"* graphics postprocessor of the calculated flow rate history for the injection well, obtained from output file *"rpwellhs.fil"* (Appendix B, Figure B-3). In this case, no "measured" data are available for comparison. Note that after the injection pressure is reduced from 10 MPa to zero at t = 384 hours, backflow takes place from the fractured formation into the well. Graphical output was written on file *"plinjflo.igf"* and rendered using *"Jplot."*

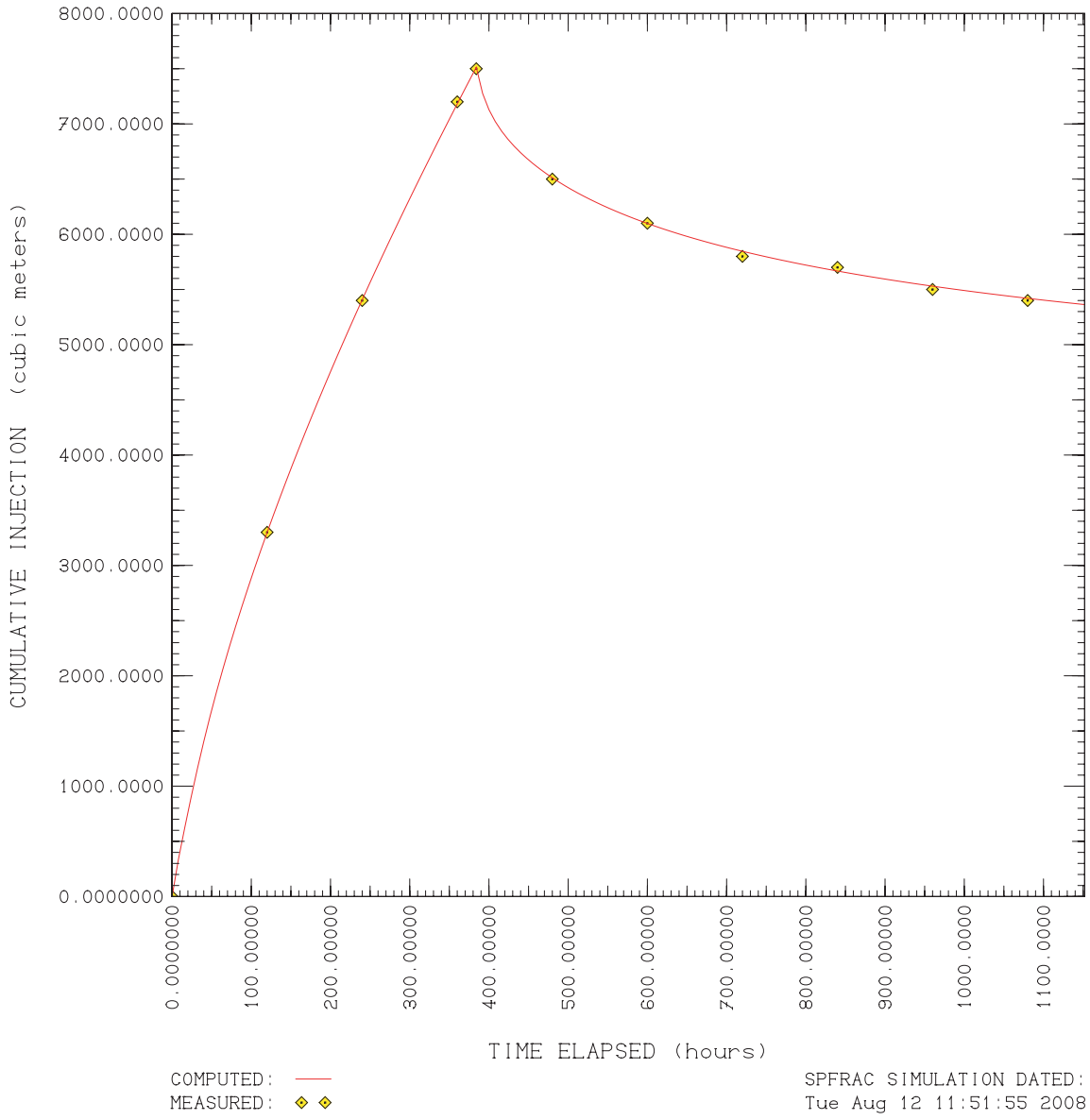

Figure C-3(c): Plot created by running *"spfpltin.exe"* graphics postprocessor of the calculated cumulative injection time-history: the time-integral of the calculated function shown in Figure C-3(b) above. Data plotted was obtained from output file *"rpwellhs.fil"* (Appendix B, Figure B-3). "Measurements" were obtained from input file *"dtinjcmi.fil"* (Appendix A, Figure A-11). Graphical output was written on file *"plinjcmi.igf"* and rendered using *"Jplot."*

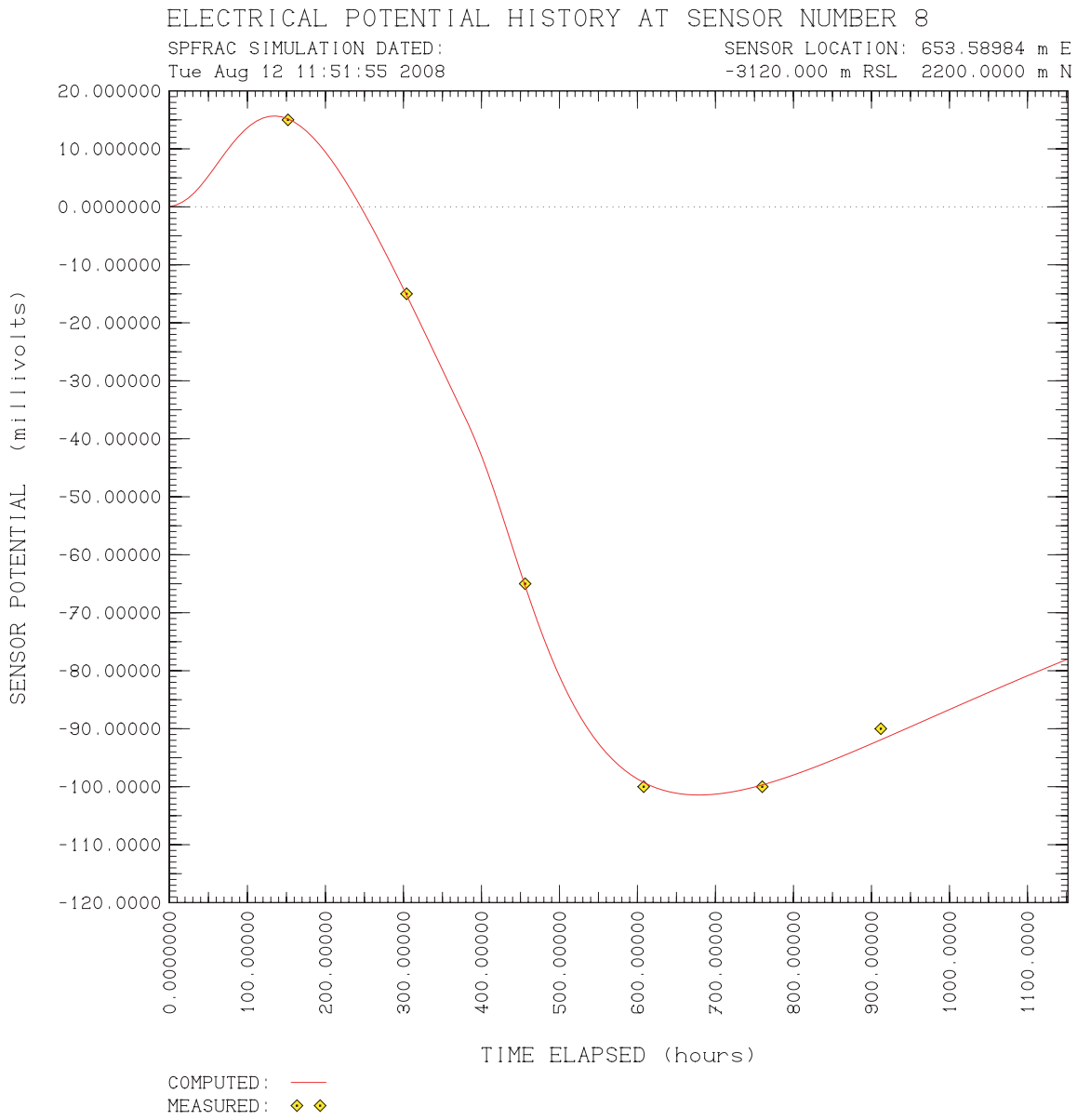

Figure C-4(a): Calculated time-history of electrical potential at "Sensor #8", located in an observation well situated at 400 meters horizontal separation from the injection well at a depth lying 120 meters below the plane of the fracture. Plot created by running *"spfpltsv.exe"* graphics postprocessor. "Measurements" obtained from input file *"dtsv0008.fil"* (Appendix A, Figure A-12). Calculated results obtained from output file *"rpsv0008.fil"* (similar to Appendix B, Figure B-5). Graphical output was written on file *"plsv0008.igf"* and rendered using *"Jplot."*

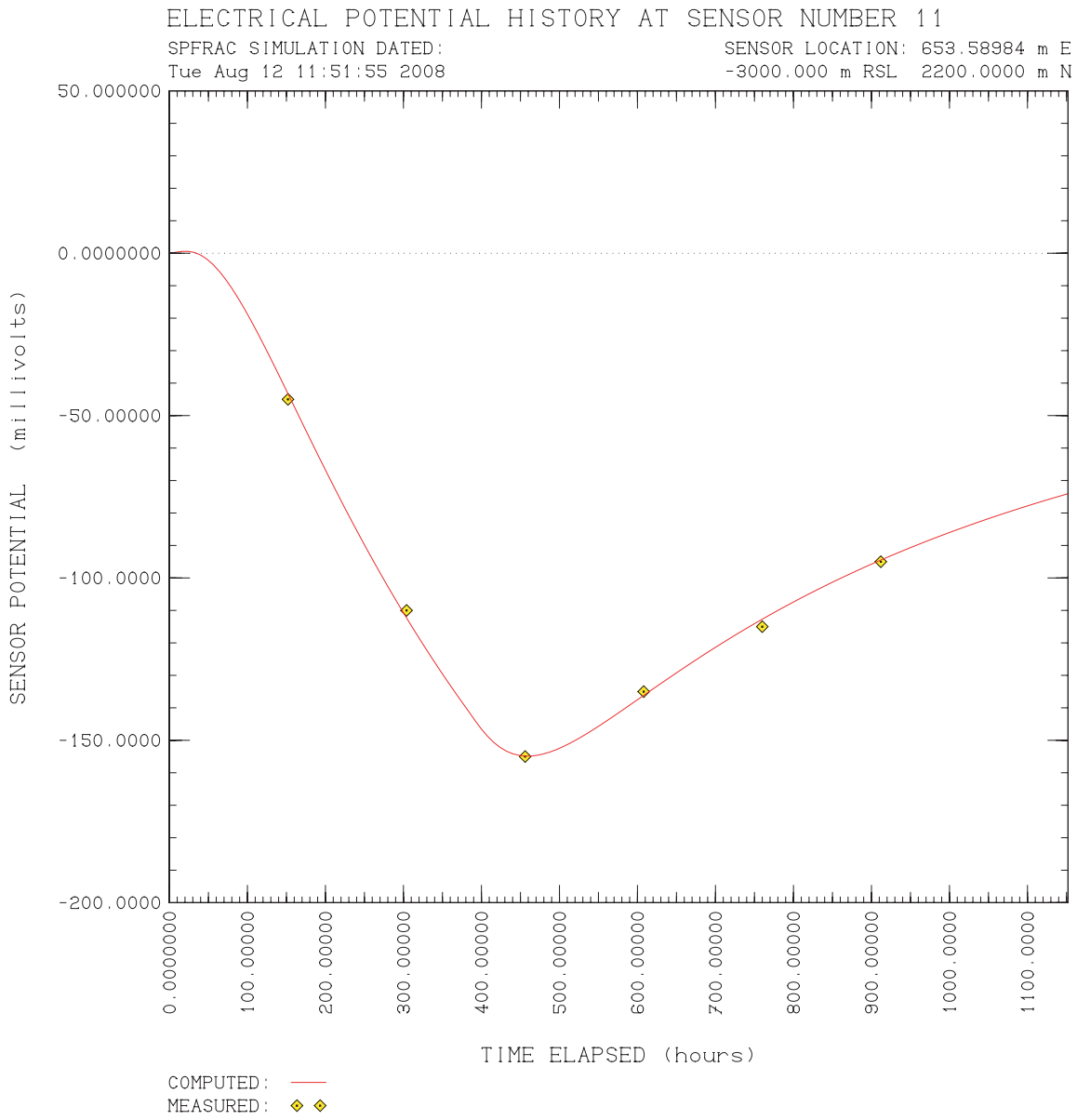

Figure C-4(b): Calculated time-history of electrical potential at "Sensor #11", located in an observation well situated at 400 meters horizontal separation from the injection well at the depth of the fracture plane. Plot created by running *"spfpltsv.exe"* graphics postprocessor. "Measurements" obtained from input file *"dtsv0011.fil"* (Appendix A, Figure A-12). Calculated results obtained from output file *"rpsv0011.fil"* (Appendix B, Figure B-5). Graphical output was written on file *"plsv0011.igf"* and rendered using *"Jplot."*

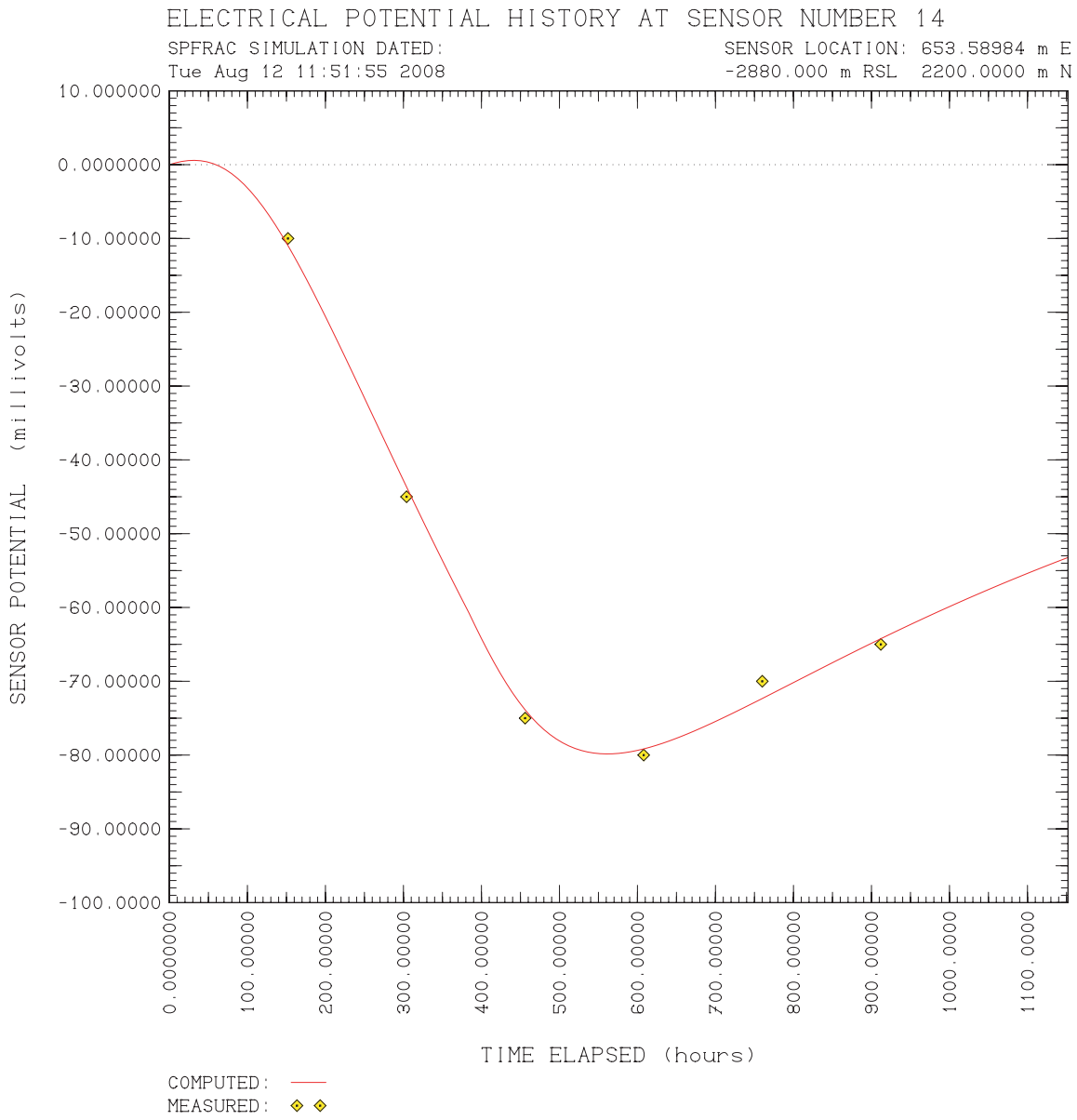

Figure C-4(c): Calculated time-history of electrical potential at "Sensor #14", located in an observation well situated at 400 meters horizontal separation from the injection well at a depth lying 120 meters above the plane of the fracture. Plot created by running *"spfpltsv.exe"* graphics postprocessor. "Measurements" obtained from input file *"dtsv0014.fil"* (Appendix A, Figure A-12). Calculated results obtained from output file *"rpsv0014.fil"* (similar to Appendix B, Figure B-5). Graphical output was written on file *"plsv0014.igf"* and rendered using *"Jplot."*

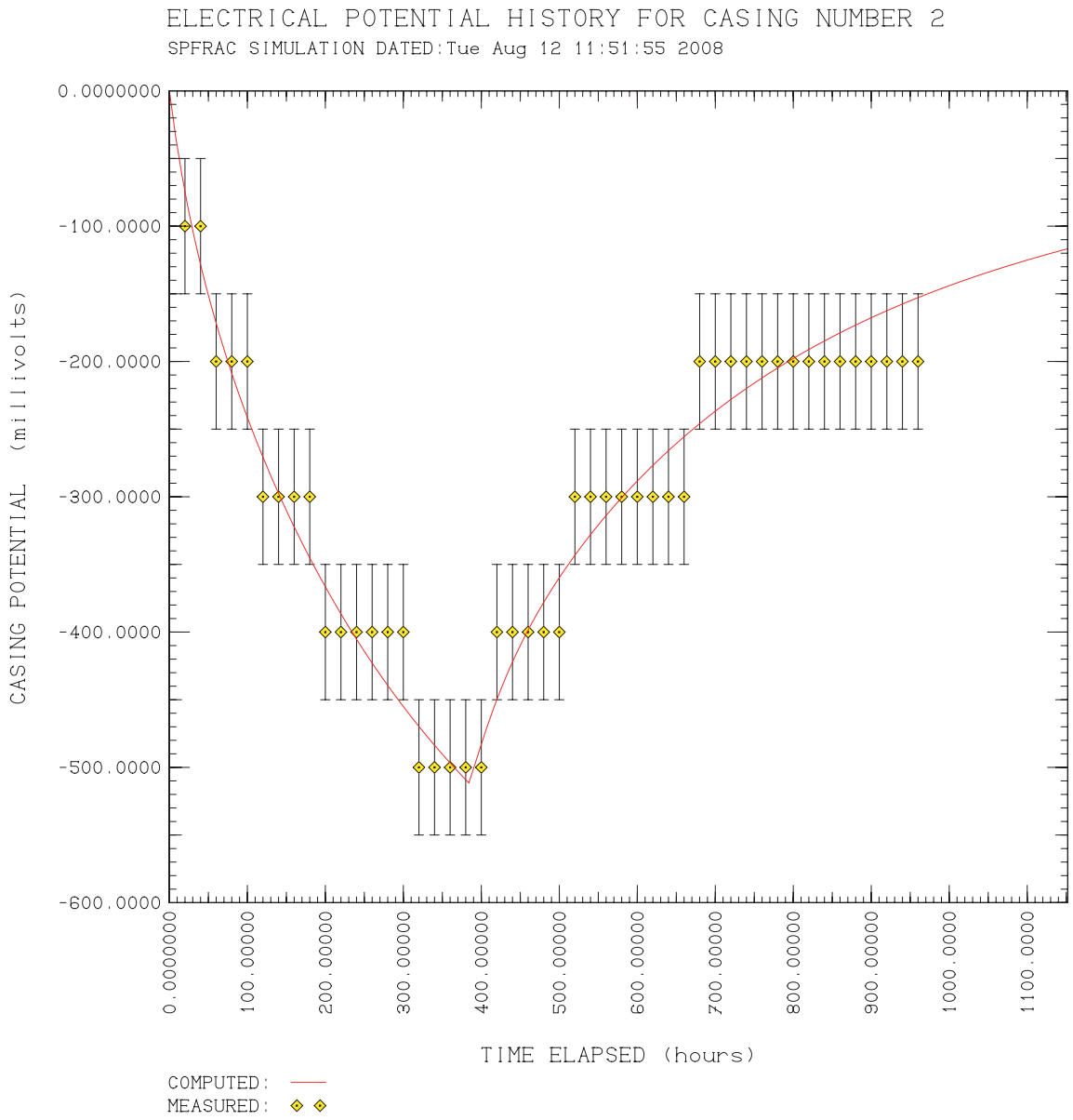

Figure C-5: Calculated time-history of electrical potential on "Casing #2", the "floating" 180-meter portion of the injection-well casing extending from –3020 m RSL to –3200 m RSL elevation below the injection horizon (see input file *"incasing.fil",* Appendix A, Figure A-7). Plot was created by running the *"spfpltwv.exe"* graphics postprocessor. "Measurements" obtained from input file *"dtwv0002.fil"* (Appendix A, Figure A-13); note the large "error bars" (±50 mV). Calculated results obtained from output file *"rpwv0002.fil"* (Appendix B, Figure B-4). Graphical output was written on file *"plwv0002.igf"* and rendered using *"Jplot."*